

Fingerprint of the mitochondrial ABC transporter Mdl1p
from *Saccharomyces cerevisiae*

Dissertation
zur Erlangung des Doktorgrades
der Naturwissenschaften

vorgelegt beim Fachbereich
Biochemie, Chemie und Pharmazie
der Johann Wolfgang Goethe-Universität Frankfurt

von
Matthias Hofacker
aus Langen/Hessen

Frankfurt am Main, 2006
(D30)

vom Fachbereich Biochemie, Chemie und Pharmazie der
Johann Wolfgang Goethe-Universität als Dissertation angenommen.

Dekan: Prof. Dr. Harald Schwalbe

1. Gutachter: Prof. Dr. Robert Tampé
2. Gutachter: Prof. Dr. Bernd Ludwig

Datum der Disputation:

Index

1	DEUTSCHE ZUSAMMENFASSUNG.....	1
2	SUMMARY.....	6
3	INTRODUCTION.....	7
3.1	FUNCTION AND ORGANISATION OF ABC PROTEINS.....	7
3.1.1	<i>Structures of nucleotide binding domains.....</i>	9
3.1.2	<i>Structures of full-length ABC transporters.....</i>	10
3.1.3	<i>Catalytic cycle and proposed transport mechanism.....</i>	12
3.2	PEPTIDE AND PROTEIN TRANSPORT OVER MEMBRANES.....	13
3.2.1	<i>Peptide import in prokaryotes driven by ABC transporters.....</i>	15
3.2.2	<i>The haemolysin system.....</i>	15
3.2.3	<i>The α-factor transporter Ste6p.....</i>	16
3.2.4	<i>The transporter associated with antigen processing like (TAPL).....</i>	16
3.2.5	<i>The transporter associated with antigen processing (TAP).....</i>	16
3.3	RELEVANCE OF MITOCHONDRIAL PROCESSES IN CELLULAR BIOLOGY.....	17
3.3.1	<i>The proteolytic system in the inner mitochondrial membrane.....</i>	18
3.4	MITOCHONDRIAL ABC TRANSPORTERS IN <i>S. CEREVISIAE</i>	19
3.4.1	<i>Mdl1p and its physiological function.....</i>	20
3.5	AIMS AND MOTIVATION.....	23
4	MATERIAL.....	24
4.1	CHEMICALS.....	24
4.2	DETERGENTS.....	26
4.3	CELLS AND MEDIA.....	27
4.4	ENZYMES, MARKERS AND KITS.....	27
4.5	VECTORS.....	27
4.6	ANTIBODIES.....	27
4.7	PEPTIDES.....	28
4.8	EQUIPMENT.....	28
4.9	CENTRIFUGES AND ROTORS.....	29
4.10	SUPPLEMENTARY MATERIAL.....	29
4.11	MEDIA, BUFFERS AND SOLUTIONS.....	30
4.11.1	<i>Cell culture media.....</i>	30
4.11.2	<i>Solutions for <i>E. coli</i> transformation.....</i>	30
4.11.3	<i>Solutions for <i>S. cerevisiae</i> transformation.....</i>	30
4.11.4	<i>Solutions for SDS-PAGE.....</i>	31
4.11.5	<i>Solutions for Tricine-PAGE.....</i>	31
4.11.6	<i>Solutions for Blue-native gel electrophoresis.....</i>	31
4.11.7	<i>Solutions for Coomassie staining.....</i>	31
4.11.8	<i>Solutions for Silver staining.....</i>	32
4.11.9	<i>Buffers for electroblotting and immunodetection.....</i>	32
4.11.10	<i>Buffers for mitochondria isolation.....</i>	32
5	METHODS.....	33
5.1	MOLECULAR BIOLOGY.....	33
5.1.1	<i>Cell culture.....</i>	33
5.1.2	<i>Competent <i>E. coli</i> cells.....</i>	33
5.1.3	<i>Transformation of competent <i>E. coli</i> cells.....</i>	34
5.1.4	<i>Transformation of <i>S. cerevisiae</i> cells.....</i>	34
5.1.5	<i>Cryostocks of yeast cells.....</i>	34
5.2	BIOCHEMICAL METHODS.....	35
5.2.1	<i>Standard SDS-PAGE.....</i>	35
5.2.2	<i>Tricine SDS-PAGE.....</i>	35
5.2.3	<i>Blue Native-PAGE.....</i>	36
5.2.4	<i>Coomassie and silver staining.....</i>	36
5.2.5	<i>Transfer of proteins to nitrocellulose membranes.....</i>	37
5.2.6	<i>Purification of the Mdl1p-NBD.....</i>	38
5.2.7	<i>Dimerisation Assay.....</i>	40
5.2.8	<i>Determination of the Nucleotide Stoichiometry.....</i>	40

5.2.9	<i>Thin layer chromatography (TLC)</i>	41
5.2.10	<i>Nucleotide binding assays</i>	41
5.2.11	<i>Isolation of yeast mitochondria</i>	42
5.2.12	<i>Tandem Affinity Purification</i>	43
5.2.13	<i>In organello translation</i>	44
5.2.14	<i>Monitoring peptide export from mitochondria</i>	44
5.2.15	<i>Detergent screening</i>	45
5.2.16	<i>Purification of full-length Mdl1p</i>	45
5.2.17	<i>ATP hydrolysis assays</i>	46
5.2.18	<i>Reconstitution of Mdl1p</i>	46
5.2.19	<i>Phospholipid concentration determination</i>	47
5.2.20	<i>Freeze-fracture electron microscopy of reconstituted Mdl1p</i>	47
5.2.21	<i>Peptide photocross-linking and detection</i>	47
5.2.22	<i>Peptide iodination</i>	48
5.2.23	<i>Peptide transport Assay</i>	49
5.2.24	<i>Single Particle electron microscopy and image analysis</i>	49
6	RESULTS	50
6.1	CHARACTERISATION OF THE NUCLEOTIDE BINDING DOMAIN OF MDL1P	50
6.1.1	<i>Purification of wild-type and E599Q mutant Mdl1p-NBDs</i>	50
6.1.2	<i>The active form of the NBD is a dimer</i>	53
6.1.3	<i>E599Q mutant NBDs</i>	54
6.1.4	<i>Nucleotide composition of the dimer</i>	54
6.1.5	<i>ATP hydrolysis cycle of Mdl1p-NBD</i>	56
6.2	CHARACTERISATION OF THE FULL-LENGTH ABC TRANSPORTER MDL1P	58
6.2.1	<i>Identification of interaction partners of Mdl1p</i>	58
6.2.2	<i>Solubilisation and purification of Mdl1p</i>	59
6.2.3	<i>Mdl1p specifically binds ATP</i>	63
6.2.4	<i>Mdl1p is active in ATP hydrolysis</i>	65
6.2.5	<i>Reconstitution of Mdl1p into lipid vesicles</i>	66
6.2.6	<i>Transport-assay</i>	69
6.2.7	<i>Single particle analysis of Mdl1p</i>	69
6.2.8	<i>In organello translation and peptide export assay</i>	71
6.2.9	<i>Occluded state in full-length Mdl1p</i>	73
6.2.10	<i>Peptide cross-linking experiments</i>	74
7	DISCUSSION	76
7.1	ATP HYDROLYSIS CYCLE OF THE MDL1P-NBD	76
7.2	FINGERPRINT OF FULL-LENGTH MDL1P	82
7.3	OUTLOOK	90
8	ABBREVIATIONS	93
9	REFERENCES	96
10	PUBLICATIONS	111

1 Deutsche Zusammenfassung

Die Ausbildung biologischer Membranen und die daraus resultierende Abgrenzung von speziellen Reaktionskompartimenten stellen einen entscheidenden Schritt in der Evolution des Lebens dar. Dabei sind Membranen allerdings keine unpassierbaren Mauern, sondern hochselektiv permeable Diffusionsbarrieren. Dies wird durch das Vorhandensein von spezifischen molekularen Kanälen und Pumpen bewerkstelligt. Der Transport von Molekülen über Membranen stellt einen vektoriellen Prozess dar, der den Stoffaustausch und die Kommunikation der einzelnen Kompartimente untereinander sowie mit der Umgebung ermöglicht.

Eine Gruppe von Membranpumpen stellt die Familie der „ATP binding cassette“ (ABC) Transporter dar, eine der größten Familien paraloger Proteine, die die aktive Beförderung unterschiedlichster Substanzen über biologische Membranen ausführt. Vertreter dieser Superfamilie finden sich in allen bekannten Organismen von Bakterien bis hin zu Säugern und nehmen an einer Vielzahl von zellulären Prozessen teil. Sie sind an der Nährstoffaufnahme, dem Lipidtransport, an der Ionen- und Osmolyt-Homöostase sowie an der Antigenprozessierung beteiligt. Unter Verbrauch von ATP transportieren sie gegen einen Konzentrationsgradienten eine Fülle von chemischen Stoffen, wie z. B. Kohlenhydrate, Peptide, Proteine, Steroide, Antibiotika, Metallionen sowie ein breites Spektrum an hydrophoben Substanzen. Neben der Transportaktivität können diese Proteine eine Funktion als Ionenkanäle, Regulatoren von Kanälen oder Rezeptoren haben.

Einige Vertreter weisen eine hohe klinische Relevanz auf. Beispielsweise ist die Mutation des ABC Transporters CFTR die molekulare Grundlage für die Entstehung der cystischen Fibrose. Andere Vertreter dieser Proteinfamilie sind an dem Phänomen der Resistenzentwicklung verschiedener Gewebe während chemotherapeutischer Behandlungen beteiligt. Ihre Überexpression stellt ein ernstzunehmendes Problem bei der Behandlung von Tumoren und AIDS dar. Demzufolge ist die Aufklärung der Struktur und Funktionsweise dieser Molekülklasse von zentraler Bedeutung.

Die Architektur von ABC Transportern ist trotz der Diversität der zu transportierenden Substrate sehr ähnlich. Typischerweise besteht ein ABC Transporter aus vier Domänen: zwei Transmembrandomänen (TMD) und zwei Nukleotidbindungsdomänen (NBD). Definiert wird die Proteinfamilie durch die Homologie innerhalb der NBDs, welche die konservierten Sequenzabschnitte Walker A und B sowie die für ABC Proteine spezifische C-Schleife beinhalten. Die NBDs gelten als die Motordomänen von ABC Transportern, die ATP hydrolysieren und dadurch die für den Transport benötigte Energie zur Verfügung stellen.

Die Anordnung der Domänen ist variabel. Bei Prokaryonten werden vornehmlich alle vier Domänen einzeln translatiert. Hier kommt häufig ein periplasmatisches Bindungsprotein mit hoher Substrataffinität vor, das mit dem jeweiligen Transporter assoziiert ist. Eukaryontische ABC Transporter existieren als „Volltransporter“ bestehend aus einer Polypeptidkette mit je

zwei TMDs und zwei NBDs oder auch als „Halbtransporter“ wie beispielsweise der ABC Transporter Mdl1p (multidrug resistance like protein 1) mit jeweils einer TMD und einer NBD pro Genprodukt.

Der Transportmechanismus, die Energetisierung sowie das strukturelle Zusammenspiel der verschiedenen Domänen innerhalb dieser Membranproteinkomplexe sind bisher größtenteils unverstanden. Auch die (physiologisch relevanten) Substrate vieler ABC Proteine sind zumeist nicht identifiziert. In dieser Arbeit wird der ABC Transportkomplex Mdl1p der inneren Mitochondrienmembran von *Saccharomyces cerevisiae* als Modellsystem funktionell und strukturell charakterisiert. Dabei soll die Tatsache nicht unerwähnt bleiben, dass die Bäckerhefe aufgrund leichter genetischer Manipulierbarkeit und schneller Produktion von Biomasse einen idealen Modellorganismus darstellt.

Mdl1p spielt eine wichtige Rolle bei der Mitochondrienbiogenese, da es für den Export von Degradationsprodukten, wie z.B. falsch assemblierter Untereinheiten der Atmungskette, verantwortlich ist. Die innere Mitochondrienmembran ist neben der inneren Chloroplastenmembran die einzige zelluläre Membran, die nicht direkt mit dem Cytosol in Kontakt tritt und folglich nicht der Qualitätskontrolle durch das Ubiquitin/Proteasomsystem unterliegt. Daher verfügen Mitochondrien über eine autonome, ATP abhängige Qualitätskontrolle, die durch einen proteolytischen Multienzymkomplex vermittelt wird. Die AAA Proteasen (ATPase associated with a variety of cellular activities) sind für den Abbau von falsch gefalteten Proteinen der inneren Mitochondrienmembran verantwortlich. Mdl1p exportiert vermutlich die dabei entstandenen Peptide aus der Matrix in den Intermembranraum des Mitochondriums.

Aufgrund seines modulartigen Aufbaus kann der ABC Transporter Mdl1p in seine N-terminale TMD und C-terminale NBD unterteilt werden. Die lösliche NBD (Aminosäuren D423 bis R695) wurde in *Escherichia coli* überexprimiert und über eine Affinitätsschleife zur Homogenität gereinigt. Die Aktivität des Proteins bezüglich ATP Bindung und Hydrolyse bleibt dabei erhalten.

Interessanterweise ist die ATP Hydrolyse nicht linear von der Proteinkonzentration abhängig wie bei Arbeiten in der Arbeitsgruppe gezeigt wurde. Diese Beobachtung lässt auf einen nicht monomeren Zwischenzustand im ATPase Zyklus schließen. Tatsächlich kann in dieser Arbeit mittels der ATPase Inhibitoren ortho-Vanadat (V_i) und Berylliumfluorid (BeF_x) ein wild-typ-NBD-Dimer in Gelfiltrationsläufen beobachtet werden. Das Gleichgewicht zwischen Monomer und Dimer ist dabei strikt abhängig von der eingesetzten Inhibitorkonzentration. Ortho-Vanadat und BeF_x stellen Analoga des anorganischen Phosphates dar. Sie arretieren einen Enzymzustand während der ATP Hydrolyse, in dem das ADP Molekül in der Bindungstasche verbleibt, während das Phosphat bereits dissoziiert ist. Eine Stöchiometriebestimmung mit radioaktiv markiertem ATP ergab, dass das Dimer mit zwei Nukleotiden beladen ist und beide hydrolysiert sind.

Die Mutation des Glutamats 599 (E599) stromabwärts des Walker B Motivs zu einem Glutamin (Q) führt zu einer NBD mit stark verringerter ATPase-Aktivität. Dieses Glutamat ist innerhalb der Familie der ABC Transporter hoch konserviert und seine Funktion während des Hydrolyseprozesses wird in der Literatur kontrovers diskutiert. In allen beschriebenen Fällen gilt diese Mutante jedoch als hydrolyse- bzw. transportdefizient. Die Mdl1p-NBD-Mutante bildet in Gegenwart von ATP ein stabiles Dimer. Stöchiometrieuntersuchungen an dem E599Q-NBD-Dimer zeigen, dass zwei Nukleotide inkorporiert sind. Nach einer Inkubation unter „Nicht-Hydrolysebedingungen“ (4 °C, ohne Mg^{2+}) bleiben zwei ATP Moleküle im Dimer erhalten. Wird die NBD jedoch bei 30 °C in Gegenwart von Mg^{2+} inkubiert, kann ein Dimer isoliert werden, in dem ein ATP und ein ADP detektierbar ist. Auch nach einer Inkubation über mehrere Stunden, kann kein Dimer mit zwei ADP Molekülen erhalten werden.

Dieses Ergebnis zeigt, dass zumindest ein ATP-Molekül zur Erhaltung des Dimers erforderlich ist. Hydrolyse beider Nukleotide führt zur Dissoziation des Komplexes. Basierend auf diesen Ergebnissen kann ein Modell für die ATP Hydrolyse erstellt werden, in dem die Bindung der Nukleotide an die monomeren Untereinheiten eine Assoziation der NBDs induziert. Zwei ATP-Moleküle werden sequentiell hydrolysiert, bevor das Dimer mit gebundenen ADP-Molekülen dissoziiert.

Bei Arbeiten in der Arbeitsgruppe wird innerhalb eines systematischen Ansatzes die Überexpression von Mdl1p als Gesamtprotein etabliert. Dazu kommen als prokaryontische Expressionssysteme das gram-negative Bakterium *Escherichia coli* und das gram-positive Bakterium *Lactococcus lactis* zum Einsatz. Weiterhin wird der homologe eukaryontische Expressionswirt *Sacharomyces cerevisiae* verwendet.

Das *MDLI*-Gen konnte durch das Einführen einer neuen und die Nutzung einer vorhandenen Restriktionschnittstelle in drei Kassetten unterteilt werden, die eine weitere genetische Manipulation und Klonierung deutlich vereinfachen. So werden Kassetten mit und ohne N-terminaler mitochondrialer Leitsequenz und verschiedenen Affinitätsschleifen konstruiert. Zu Zwecken detaillierter Untersuchung des Gesamttransporters wurde die schon von der NBD bekannte Mutante E599Q als auch die bei anderen ABC Transportern als ATP-hydrolyseinaktiv bekannte Mutation des konservierten Histidins (H631) der H-Schleife zu einem Alanin generiert (H631 → A).

Ergebnis dieser Arbeiten war, dass in *E. coli* im besten Fall 0,005 % Mdl1p (bezogen auf die Gesamtmembranproteinmenge) erzielt wurde, was deutlich unter der erwarteten und für weitere Experimente erforderlichen Expressionsausbeute lag. Dabei wurde das Protein in verschiedene „high-“ und „low-copy“ Vektoren mit unterschiedlichen Promotoren wie z. B. *T7* (IPTG-induziert), *ARA* (Arabinose-induziert) oder *TRC* (IPTG-induziert) kloniert. Weiterhin wurde die Expression in verschiedenen *E. coli*-Stämmen bei verschiedenen Wachstumstemperaturen getestet. Auch die Konzentration der Induktoren wie IPTG oder Arabinose und der Zeitpunkt sowie die Dauer der Induktion wurden systematisch variiert. Schließlich wurde Mdl1p zusammen mit der „Membraninsertionsmaschinerie“ SecY, SecE, SecG und YidC und

in Stämmen, die seltene tRNAs codieren, exprimiert. Um das Translationsprodukt möglicherweise besser vor degenerativen Prozessen innerhalb der Zelle zu schützen, werden diese mit höheren Konzentrationen Ethanol oder Sorbitol im Medium kultiviert, mit dem Ziel, auf diese Weise Chaperone zu induzieren. Die Expression wurde jeweils durch quantitativen Westerntransfer mit anschließender Immundetektion unter der Verwendung der Mdl1p-NBD als Referenz evaluiert. Ähnlich niedrige Ausbeuten von 0,01 % Mdl1p werden in *L. lactis* erzielt, wobei analoge Variationen der Expressionsbedingungen, wie für *E. coli* beschrieben, durchgeführt wurden.

In beiden Ansätzen stellen die erhaltenen Mengen keine Verbesserung der Ausbeute im Vergleich zum homologen Expressionssystem dar. Wie im Rahmen der Arbeiten zur Überexpression von Mdl1p bestimmt wurde, wird Mdl1p in *S. cerevisiae* bis zu 0,01 % des totalen mitochondrialen Membranproteingehalts exprimiert. Um die Mdl1p-Menge zu erhöhen, wurden in der Arbeitsgruppe verschiedene Ansätze getestet, wie beispielsweise die plasmidgetriebene, starke und konstitutive Expression über einen *GPD*-Promotor (Glycerolphosphatdehydrogenase). Interessanterweise wird in diesem Fall weniger Protein erhalten als bei einer wildtyp-Expression. Dies legte die Vermutung nahe, dass hohe Mengen Mdl1p von der Zelle nicht toleriert werden können. Grosse Mengen Mdl1p wurden letztlich nur über einen *GALI*-Promotor (Galaktose induzierbar) auf einem 2 μ -Plasmid erreicht.

Über die His₍₈₎-Schleife am C-Terminus des Proteins und der Verwendung der Metall-Affinitätschromatographie gelang im Rahmen dieser Arbeit die Isolierung von Mdl1p bis zu einer Homogenität von 95 %. Dabei wurde ein breites Spektrum an nicht-, einfach- und zwitterionischen Detergenzien zur Solubilisierung verwendet. Hier zeigen sich zwei wichtige Aspekte: Erstens solubilisieren unterschiedliche Detergenzien Mdl1p in sehr unterschiedlichem Ausmaß. Mit dem Detergenz Tetradecylphosphocholine (FC-14) kann beispielsweise bis zu 1 mg Protein pro Liter Hefekultur präpariert werden. Bei den Detergenzien Dodecylmaltosid (DDM) und Digitonin sind die Ausbeuten reduziert und belaufen sich auf 0,2 bzw. 0,1 mg pro Liter Zellkultur.

Zweitens wird auch die Hydrolyseaktivität des gereinigten Proteins stark durch das Detergenz beeinflusst. So zeigt Mdl1p seine höchste Geschwindigkeit in Digitonin während in DDM nur noch ein Drittel der Geschwindigkeit detektiert werden kann. In FC-14 ist keine Hydrolysetätigkeit mehr vorhanden. Daher wurden alle Experimente mit Protein durchgeführt, das in Anwesenheit von Digitonin gereinigt wurde.

Das solubilisierte Protein bindet ATP wie durch 8-azido-[α -³²P]ATP-photocross-linking-Experimente gezeigt wurde und besitzt eine Hydrolyseaktivität mit einem $K_{M(ATP)}$ von 0,85 mM und einer Wechselzahl von 2,5 ATP pro Sekunde. Die beiden Mutanten (E599Q, H631A), die in gleicher Weise und Menge exprimiert und präpariert werden können wie das Wildtyp-Protein, sind zwar in der Lage ATP zu binden, nicht jedoch es zu hydrolysieren.

Im Rahmen dieser Arbeit wird weiterhin die Existenz einer N-terminalen Leitsequenz von Mdl1p ermittelt und näher charakterisiert. In der Literatur werden spezifische Signalsequenzen diskutiert, die eine eindeutige Adressierung und einen Transport von Proteinen an ihren Einsatzort in den verschiedenen Zellorganellen gewährleisten. Für mitochondriale Proteine werden sowohl N-terminale Leitsequenzen unterschiedlicher Länge (bis zu 105 Aminosäuren) als auch interne, in der Proteinfaltung verschlüsselte, Leitstrukturen beschrieben. Auch für Mdl1p werden mittels computerbasierter Methoden („*in silico*“) verschiedene Sequenzen vorhergesagt. Daher soll die Frage nach Art und Länge der Zielsequenz für Mdl1p experimentell beantwortet werden. Dazu wird das Protein über die His₍₈₎-Schleife aus Mitochondrien präpariert und mittels N-terminalem Edman-Abbau analysiert. Da die ersten 7 Aminosäuren sequenziert werden, kann eine eindeutige Alignierung der erhaltenen Sequenz mit der Gesamt-Mdl1p-Sequenz erreicht werden. An Hand dieser Daten kann erstmals für einen mitochondrialen ABC Transporter aus Hefe experimentell eine N-terminale Leitsequenz gezeigt werden, die im Fall von Mdl1p 59 Aminosäuren beträgt.

Mdl1p kann in Liposomen rekonstituiert werden, was in Zusammenarbeit mit dem Max-Planck-Institut für Biophysik in Frankfurt durch Gefrierbruch-Elektronenmikroskopie nachgewiesen werden konnte. Hierbei blieb die ATP Hydrolysefähigkeit von Mdl1p nahezu erhalten, was den Einsatz von Proteoliposomen für Importstudien ermöglicht. Ein Peptidtransport mit radioaktiv markierten Peptidbibliotheken einer Länge von 8 bzw. 23 Aminosäuren (dabei enthalten die Peptide alle proteinogenen Aminosäuren in gleichem Verhältnis mit Ausnahme von Cystein) konnte mit diesem System allerdings nicht gezeigt werden.

Gründe für diese Ergebnisse werden in dieser Arbeit ausführlich diskutiert, was zu einer Neubewertung der Rolle von Mdl1p als Peptidtransporter führt.

Das solubilisierete Protein wurde in einer Kooperation mit dem Max-Planck-Institut für Biophysik in Frankfurt mittels Einzelpartikel-Elektronenmikroskopie untersucht, was Einsichten in den oligomeren und strukturellen Aufbau des Proteins ermöglicht. Dabei werden die Einzelpartikel zu einer dreidimensionalen Ansicht rekonstruiert und mit den Kristallstrukturen des ABC Transporters MsbA verglichen. Diese zeigen MsbA in zwei sehr unterschiedlichen Konformationen, eine offene und eine geschlossene Form. Die Dimensionen der Partikel von Mdl1p kommen hierbei der offenen Form von MsbA am nächsten. Dabei wird auch deutlich, dass Mdl1p in Detergenz sehr wahrscheinlich als Homodimer vorliegt.

Die vorliegende Arbeit mit ihren *in vitro* Studien zeigt zum ersten Mal eine Art „Fingerabdruck“ des mitochondrialen ABC Transporters Mdl1p aus *S. cerevisiae* und stellt damit eine Basis für detaillierte Untersuchungen dieses Proteins dar.

2 Summary

The multidrug resistance like protein 1 (Mdl1p) belongs to the class of ATP binding cassette (ABC) transporters which comprise a large family of membrane proteins utilising ATP hydrolysis to drive up-hill transport of a wide variety of solutes across membranes.

Mdl1p is a mitochondrial ABC transporter involved in the export of protein fragments derived from the proteolysis of non-assembled inner membrane proteins out of the mitochondrial matrix. Mdl1p forms a homodimeric complex consisting of two polytrophic transmembrane domains (TMDs) and two nucleotide binding domains (NBDs). The transport function and structural organisation of Mdl1p have not been elucidated yet.

To characterise the ATP hydrolysis cycle of Mdl1p, the His-tagged NBD (amino acids D423-R695) was over-expressed in *Escherichia coli* and purified to homogeneity. The isolated NBD was active in ATP binding and hydrolysis. The ATPase activity was non-linear regarding to the protein concentration, indicating that the functional state is a dimer. Dimeric catalytic transition states could be trapped and three different intermediate states were isolated, containing two ATPs, one ATP and one ADP, or two ADPs, which are trapped by orthovanadate or beryllium fluoride. These experiments showed that (i) ATP binding to the NBDs induces dimerisation, (ii) in all isolated dimeric states, two nucleotides are present, (iii) phosphate can dissociate from the dimer, (iv) both nucleotides are hydrolysed, and (v) hydrolysis occurs in a sequential mode.

Studies in the workgroup systematically screened for over-expression of the full-length Mdl1p and expression conditions were optimised. These studies showed that highest expression was obtained in *S. cerevisiae*, where the protein was over-expressed 100-fold. In this work over-expressed His-tagged protein was purified via immobilised metal-ion affinity chromatography that was active in ATP binding and hydrolysis with a turn-over of 2.5 ATP per second.

N-terminal amino acid sequencing of purified Mdl1p by Edman degradation confirmed experimentally a N-terminal targeting sequence of a mitochondrial ABC transporter of *S. cerevisiae* for the first time. This sequence was determined to be 59 amino acids in length.

Mdl1p was reconstituted into liposomes, which was confirmed by freeze fracture electron microscopy. The reconstituted protein showed ATP hydrolysis similar to the solubilised Mdl1p. However peptide translocation with radiolabelled $X_{(8)}$ or $X_{(23)}$ libraries as done for the transporter associated with antigen processing TAP could not be shown with this setup.

Furthermore, structural insights of the mitochondrial transport complex and its oligomeric state were obtained via single particle electron microscopy. It was shown that Mdl1p forms a homodimer in detergent.

These *in vitro* studies provide the basis for further detailed investigation of the mitochondrial ABC transporter Mdl1p.

3 Introduction

The border of a cell is formed by a biological membrane, which defines the “inside” and “outside” of a cell. This boundary prevents molecules generated inside from diffusing out and harmful molecules from invading the cell. In addition to an external cell membrane, eukaryotic cells also contain internal membranes, which form organelles such as the nucleus, the mitochondria, the chloroplasts, the endoplasmic reticulum, the Golgi apparatus, the peroxisomes, and the lysosomes. This enables a cell to separate biochemical processes into different compartments with different internal conditions and furthermore opens an elegant way of regulation and the control of biochemical processes. Specific systems have evolved to target selected proteins into or through membranes. Biological membranes have additional important functions crucial for life, such as energy storage and creation and information transduction, which are regulated by the proteins associated with them.

Solutes and proteins, which function outside the cell or in different compartments, have to pass the membrane without compromising its barrier function. This permeability is achieved by transport systems that allow molecules to be transported into or out of the cell or the different compartments. Several systems have been developed which transport solutes across membranes. One family of these transport proteins is the family of ATP binding cassette (ABC) transporters.

3.1 Function and organisation of ABC proteins

In 1982 the gene of the histidine permease was sequenced, and this gene was shown to encode the first representative of the ABC transporter superfamily, one of the largest families of paralogous transmembrane proteins (Higgins et al., 1982).

ABC transporters use the energy of the hydrolysis of ATP to drive the active transport of substrates across membrane lipid bilayers. Members of the ABC transporter superfamily are found in prokaryotes, eukaryotes and archaea. They take part in many cellular processes, and transport a wide set of substrates, like sugars and amino acids, hydrophobic drugs and lipids and even large proteins. The dysfunction of ABC transporters has been reported to play an important role in various human pathologies such as multidrug resistance (MDR/ ABCB1; MRP1/ABCC1), cystic fibrosis (CFTR/ABCC7), hypercholesterolemia (ABC1/ABCA1), adrenoleukodystrophy (ALDP/ABCD1) and Stargardt’s disease (hABCR/ABCA4). In many organisms, an additional group of ABC proteins (non-transporters) are found which do not contain a transmembrane domain (TMD) and most likely perform functions related to maintenance and repair of DNA and DNA transcription.

ABC transporters are composed of a conserved central structure with two TMDs and two nucleotide-binding domains (NBDs). The TMDs form the translocation pore, whereas the NBDs are responsible for ATP hydrolysis to energise the transport event (Higgins, 1992). All ABC transporters in eukaryotes function as exporters, but in prokaryotes and archaea, also import

systems are found which work in concert with a substrate binding protein (SBP). The amino acid sequences of the TMDs of ABC transporters are highly diverse, while the NBDs are much more conserved. This finding suggests that also in unrelated transporters the mechanism and function of the NBDs is similar whereas the diversity in the sequence of the TMDs explains the broad substrate diversity of ABC proteins.

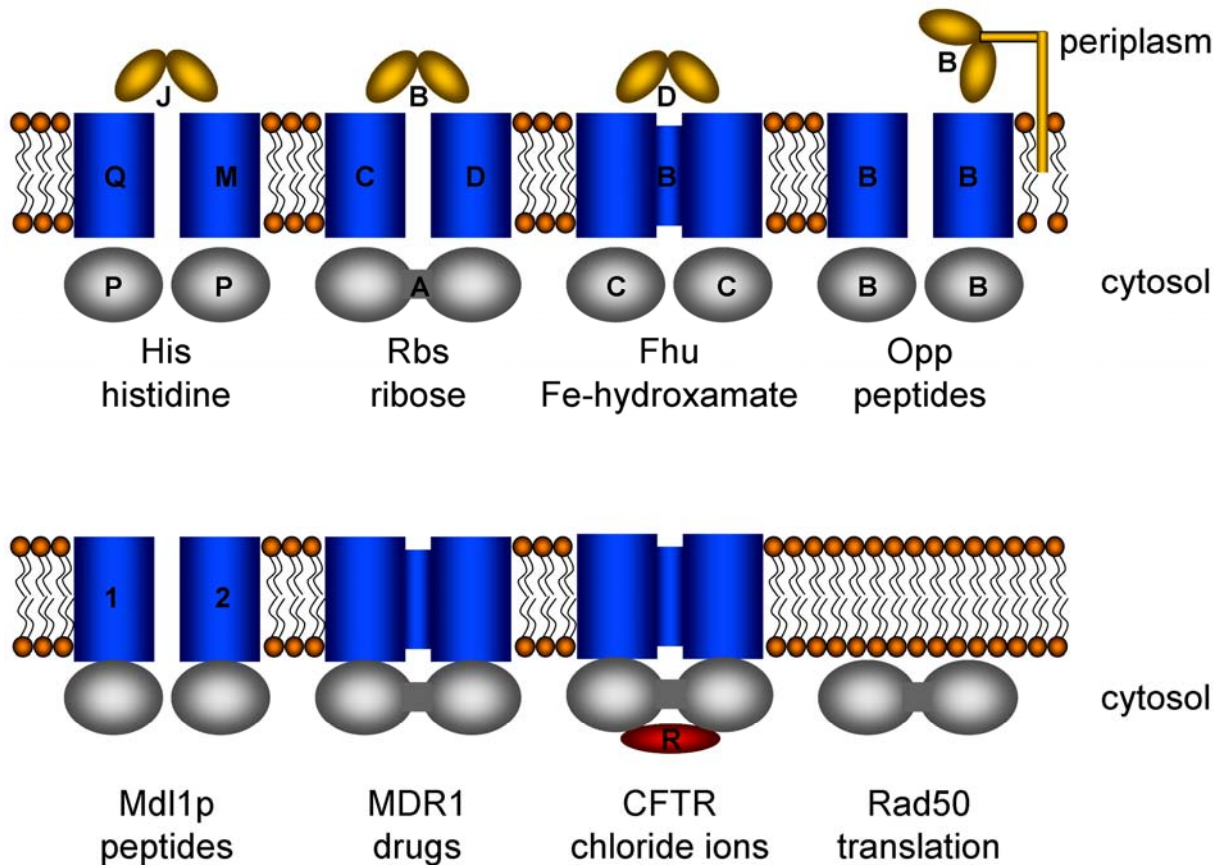


Figure 3.1: Organisation of ABC proteins (modified from (Schmitt and Tampé, 2000)). An ABC transporter consists of two transmembrane domains (blue), two nucleotide binding domains (grey) and in case of prokaryotic import systems of an additional periplasmic substrate binding protein (yellow). The domains have been found to be arranged in different ways: I) as five separate polypeptides (histidine permease), II) with fused NBDs and discrete TMDs (RbsA), III) with separated NBDs and fused TMDs (FhuCB), IV) with the SBP anchored in the membrane (Opp), V) with the NBD fused to the TMD (Mdl1p), VI) a single polypeptide (MDR1), VII) with an intercalating R domain (red; only known for CFTR). Furthermore also non-transporters, VIII) with only two fused NBDs (Rad₅₀) exist.

The TMDs and the NBDs can be found in a homo- or heterodimeric composition. The domains can be arranged in any combination e.g. as separate polypeptides like in the case of several bacterial transporters, or as a single polypeptide like in the majority of the eukaryotic ABC transporters or they are expressed as half size transporters where a TMD is fused to a NBD (Figure 3.1). Several different arrangements are also observed but they are less frequent. A canonical TMD of an ABC transporter features six transmembrane helices (TMHs), but also here exceptions can be found (Schmitt and Tampé, 2000).

3.1.1 Structures of nucleotide binding domains

The NBDs contain the highly conserved Walker A (G-X-X-G-X-G-K-S/T) and Walker B (Φ - Φ - Φ - Φ -D, where Φ is a hydrophobic residue) (Walker et al., 1982) motif. Furthermore, the D-, H-, Q- and C-loops can be found in the NBDs (Schmitt and Tampé, 2002). The latter one is the hallmark of ABC proteins and called ABC signature motif (L-S-G-G-Q).

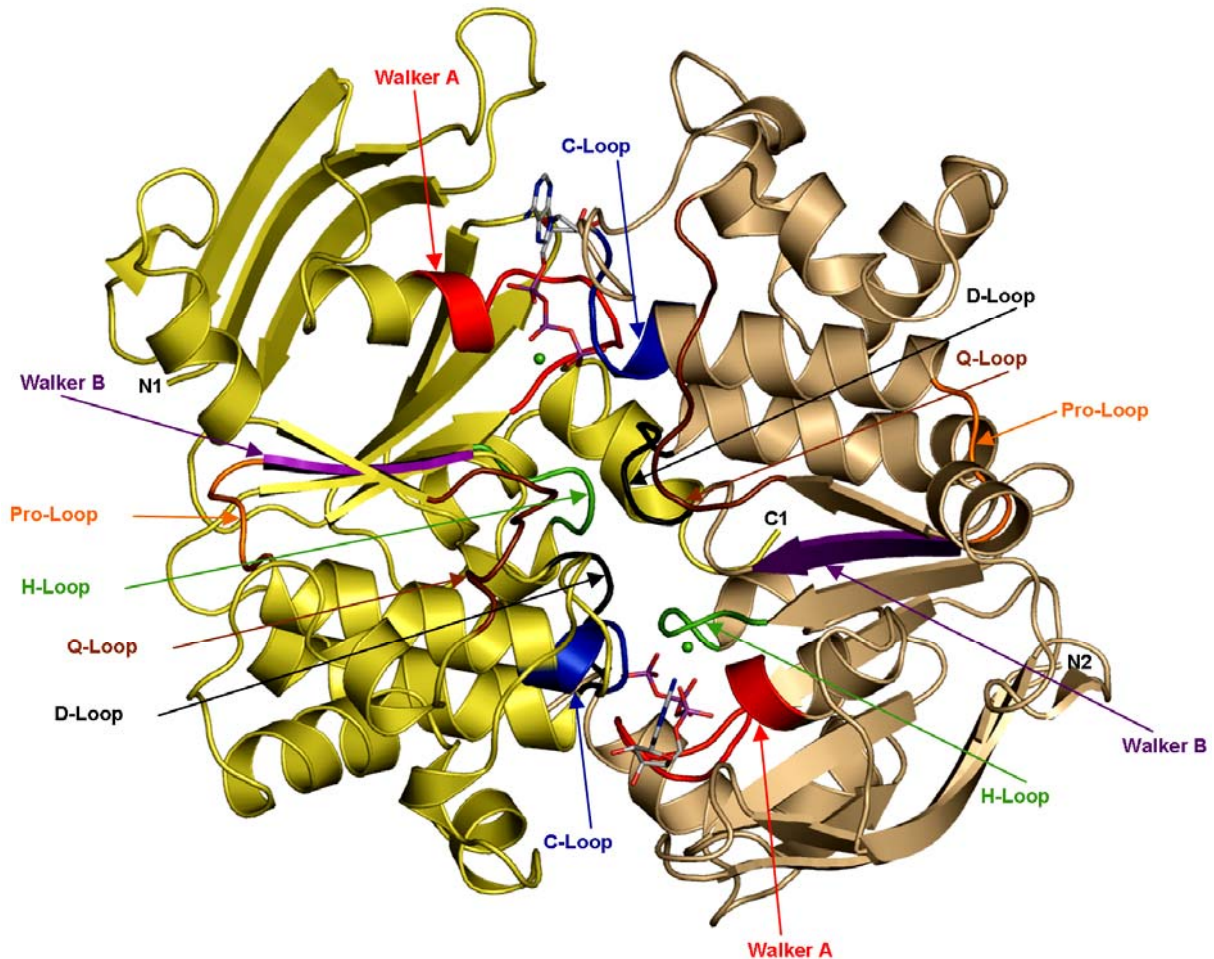


Figure 3.2: Crystal structure of a dimeric NBD. The structure shows two HlyB(H662A)-NBD monomers (light tan and light yellow), with ATP (stick representation) and Mg²⁺ (green spheres) clamped at the interface. Conserved motifs are coloured in red (Walker A motif), brown (Q-loop), blue (C-loop or ABC signature motif), magenta (Walker B), black (D-loop), and green (H-loop).

Structures of several isolated NBDs e.g. *E. coli* HisP (Hung et al., 1998), *Thermococcus litoralis* and *E. coli* MalK (Chen et al., 2003a; Diederichs et al., 2000), *Methanococcus jannaschii* MJ1276 (Karpowich et al., 2001), *M. jannaschii* MJ0796 (Yuan et al., 2001), human TAP1 (Gaudet and Wiley, 2001), *Sulfolobus solfataricus* GlcV (Verdon et al., 2003a) *E. coli* HlyB (Schmitt et al., 2003; Zaitseva et al., 2005a), human CFTR (Lewis et al., 2004) *Pyrococcus furiosus* Pfu-867808-001 (Liu et al., 2005) and *Alicyclobacillus acidocaldarius* CysA (Scheffel et al., 2005) crystallised in the absence or presence of different nucleotides have been published.

The structures of the different NBDs are remarkably similar. The monomer forms an L-shaped molecule with two arms. The highly conserved arm I includes the Walker A and B motifs as well as the H- and Q-loop, while arm II contains the C-loop (Figure 3.2). Arm II contains mainly α -helices and also comprises a structurally diverse region of about 30 residues, which is thought to interact with the TMDs to transmit signals between the “motor” and the “gate” during the transport process (Schmitt et al., 2003).

The residues of the Walker A motif interact with the ATP/ADP-phosphates (Chen et al., 2003a; Gaudet and Wiley, 2001; Hopfner et al., 2000; Hung et al., 1998; Karpowich et al., 2001; Verdon et al., 2003a; Yuan et al., 2001) and the aspartate of the Walker B motif coordinates the Mg^{2+} ion in the nucleotide binding site (Karpowich et al., 2001; Verdon et al., 2003a; Yuan et al., 2001). The γ -phosphate of the sandwiched ATPs is complexed by a conserved histidine and glutamate. The latter is one amino acid downstream of the Walker B motif and coordinates additionally via the phosphate a water molecule that was proposed to attack the γ -phosphate. Thus, this glutamate was suggested to be the catalytic base (Moody et al., 2002; Verdon et al., 2003a; Yuan et al., 2001). Based on biochemical experiments, recent data suggest that substrate assisted catalysis, rather than a general base function in ABC ATPases (Zaitseva et al., 2005c). Comparing different NBD structures with different nucleotide content, it was shown that the largest conformational changes are seen upon ATP binding within the Q-loop. ATP binding results in a rigid body movement of arm I towards arm II, while only minor differences are seen between the ADP bound and nucleotide free state. Remarkably, the dimeric structure shows a head-to-tail orientation of the two NBDs and the two ATPs are bound at the interface of the two monomers between the Walker A motif from one monomer (cis-site) and the C-loop of the other monomer (trans-site). The dimeric forms of NBD crystal structures in the ATP bound state are supported by biochemical experiments showing ATP induced dimerisation (Janas et al., 2003; Moody et al., 2002; Zaitseva et al., 2005c).

3.1.2 Structures of full-length ABC transporters

So far, X-ray structures of two different full-length ABC transporters have been solved, which was a tremendous step towards understanding the mechanism of this class of proteins.

The *E. coli* (Chang and Roth, 2001), *Vibrio cholera* (Chang, 2003) and *Salmonella typhimurium* (Reyes and Chang, 2005) MsbA proteins are homodimeric half size transporters which function as lipid flippases, and are close homolog's of the human and *Lactococcus lactis* multidrug transporters P-glycoprotein and LmrA (Reuter et al., 2003). In the first two structures MsbA was crystallised in the absence of nucleotides in an open (*E. coli*) and closed (*V. cholera*) conformation. In the open conformation, the two TMDs interact at the extra cellular ends of the membrane spanning helices to form an inverted V-shaped molecule with NBDs distant from each other and a large internal chamber accessible from the cytoplasm is formed between the interacting TMDs. In the closed conformation, both the TMDs and the NBDs are

closely packed. The two structures suggest a highly dynamic sampling of the conformational space by the protein in the absence of nucleotides. The third x-ray structure of MsbA shows a complex with magnesium, ADP, inorganic vanadate and a rough-chemotype lipopolysaccharide which is a potential substrate (Figure 3.3, A). Based on this structure together with the first two structures a model involving a rigid body torque of the two transmembrane domains during ATP hydrolysis was proposed. This suggests a mechanism by which the nucleotide-binding domain communicates with the transmembrane domain.

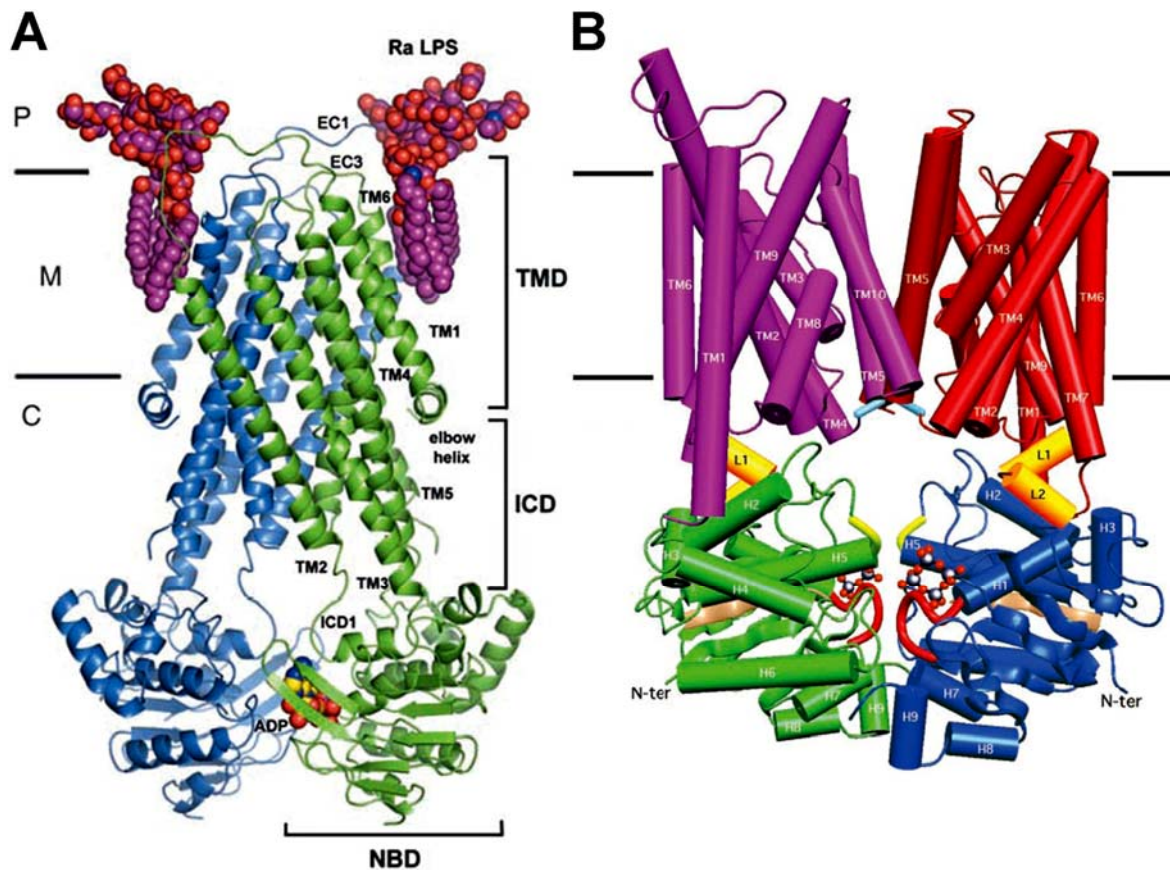


Figure 3.3: **(A)** Structure of MsbA (Reyes and Chang, 2005) trapped with Mg-ADP-V_i. The homodimer (monomers in green and blue) is shown perpendicular to the membrane (M). The two NBDs form a dimeric structure located in the cytosol (C) and enclose an ADP molecule. Two Ra lipopolysaccharide (LPS) molecules are bound on the periplasmic side (P). **(B)** Structure of the vitamin B₁₂-transporter (Locher et al., 2002). The transporter is composed of two BtuC membrane spanning subunits (purple and red), and two BtuD NBDs (green and blue). The cyclotetranadate molecules found in the ATP binding sites, are depicted in ball and stick. The membranes are indicated with straight lines.

The BtuCD structure (Locher et al., 2002) contains two copies of the TMD (BtuC) and two copies of the NBD (BtuD). In the crystal, the NBDs contain a cyclotetranadate, and are slightly apart from each other (Figure 3.3, B). They are in contact with a cytoplasmic loop located between TMH 6 and 7. This loop is suggested to be involved in interdomain communication between the TMDs. The loop interacts with the Q-loop in the NBD and is hereby linked to the γ -phosphate (Mourez et al., 1997). Apparently, this interface is responsible for a specific interaction between the NBD and the TMD. The interface “senses” the nucleotide bound state and communicates with the TMD of the transporter, which in turn signals the in-

formation of substrate binding in the other direction to the NBD. However, it remains unknown in which way the energy of ATP binding or hydrolysis is passed to the TMDs.

3.1.3 Catalytic cycle and proposed transport mechanism

Several models which suggest how a translocation event is powered and achieved by an ABC transporter are discussed presently like the “two cylinder engine” model (van Veen et al., 2000) the “alternating site” model (Senior et al., 1995) or the “flippase” model (Higgins and Gottesman, 1992). The second model was proposed because of extensive investigations of MDR1 (P-glycoprotein) and considered to be a general model for the catalytic cycle of ABC transporters. MDR1 is a full-size ABC transporter with an N- and C-terminal NBD on one polypeptide chain. Both NBDs bind MgATP, Mg-8-azido-ATP, or Mg-TNPATP (Liu and Sharom, 1997) and the two sites show approximately the same apparent nucleotide binding affinity. Experiments with the ATPase inhibitor ortho-vanadate (V_i) demonstrated that intact MDR1 in mammalian cell membranes, both NBD1 and NBD2 have the capacity to hydrolyse MgATP, and that the two nucleotide sites interact very strongly (Urbatsch et al., 1995a; Urbatsch et al., 1995b). This was apparent from the fact that trapping of ADP was sufficient to prevent turn-over. Moreover, V_i -induced trapping of ADP occurred non-selectively in either NBD, suggesting that the two sites normally alternate in catalysis. The alternating site model starts with a ATP-free NBD and a NBD which has bound ATP. ATP binding to the free site promotes ATP hydrolysis at the other site and induces a conformational change in this site, which prohibits hydrolysis at the later on loaded site. In addition, ATP hydrolysis leads to a high chemical potential state with bound ADP·P_i and relaxation of this site couples drug movement from the inside-facing, higher-affinity to outside facing, lower-affinity orientation and phosphate-release. After dissociation of the substrate also ADP leaves the NBD. The molecule is ready for another cycle, except that the NBDs have reversed their position, and the next hydrolysis event will occur in the NBD which was loaded in the cycle before (Senior and Gadsby, 1997).

In anticipation the following shema combines several results of this work with other structural and biochemical data (for review see (Higgins and Linton, 2004) and draws a picture about the putative events, which occur during a transport cycle (Figure 3.4).

- Step I. Binding of the substrate to its high affinity site on the TMDs is predicted to lower the activation energy for ATP dependent dimerisation, thus initiating the dimerisation of the NBDs and preventing futile ATP hydrolysis cycles in the absence of substrate.
- Step II & Step III. ATP binding induces NBD dimer formation. Dimerisation results in re-orientation of the high affinity-binding site to the low affinity substrate release position.
- Step IV. One ATP is hydrolysed as part of the transport cycle. Alternatively, this can be the step for reorientation of the substrate binding site.

- Step V. The second ATP is hydrolysed returning the transporter to its basal, open configuration by destabilising the NBD closed dimer. After ATP hydrolysis, the closed dimer is destabilised by electrostatic repulsion between ADP coordinated with the Walker A motif of one NBD and P_i coordinated to the signature motif of the other NBD. This leads to rigid body rotation of the subdomains of each NBD, P_i and ADP release, and restoration of the open dimer configuration.
- Step VI. P_i and ADP are released, restoring the protein to its basal state - ready to initiate another transport cycle.

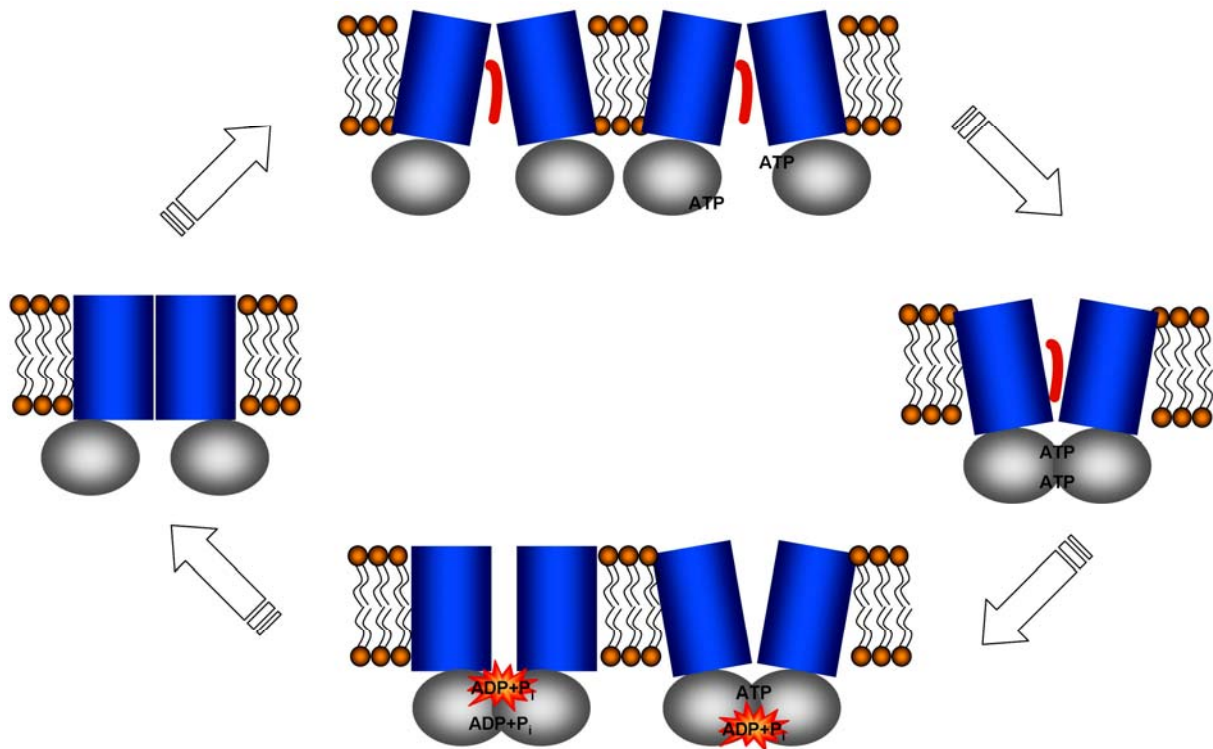


Figure 3.4: Schema for a substrate translocation cycle by an ABC export system. TMDs drawn in blue, NBDs depicted in grey. In this case “transport” means reorientation of the TMDs to a certain degree. Dimerisation upon ATP binding is represented by overlapping NBDs (see text for details).

3.2 Peptide and protein transport over membranes

Peptide and protein transport across biological membranes is essential for all kind of cells. Different ways are accomplished to fulfil this task. One way of peptide/protein transport is the use of the proton motive force by secondary active systems like DtpT (Hagting et al., 1994) or the twin arginine protein translocase (Tat) (Santini et al., 1998). The proton gradient is built and maintained by protein complexes composing the so-called respiratory chain (NADH-Q oxidoreductase, Q-cytochrome c oxido-reductase, and cytochrome c oxidase).

Alternatively, translocases use the energy of ATP hydrolysis to energise and coordinate the translocation process of their substrates. Here I would like to briefly introduce three promi-

ment representatives namely the Sec system as well as the translocase of the inner mitochondrial membrane (TIM) and the translocase of the outer mitochondrial membrane (TOM).

The Sec pathway is found in prokaryotes where it resides in the inner plasmamembrane as well as in eukaryotes where it is a key component in the endoplasmic reticulum (ER). It is the main route of protein export in most bacteria. Here I will introduce only the prokaryotic components (for reviews see (Driessen et al., 2001)). Two distinct routes can be discriminated. The signal recognition particle (SRP) mainly guides ribosome bound nascent proteins to the membrane, whereas SecB facilitates the targeting of periplasmic and outer membrane proteins. These routes converge at the translocase, a protein-conducting pore in the membrane that consists of the SecYEG complex. Membrane and secretory protein translation starts with a free cytosolic ribosome. In the SRP mediated pathway, the SRP recognises the signal sequence coming from the ribosome. The ribosome nascent chain complex (RNC) bound to SRP is then guided to FtsY – a membrane bound receptor. Binding of GTP to FtsY and SRP leads to dissociation of SRP from the RNC and releases it to the pore forming SecYEG complex. SRP is released from FtsY by GTP hydrolysis allowing it to be recycled into the cytosol. FtsY remains bound to the membrane. The polypeptide chain continues to elongate until translation is complete.

The chaperone SecB does not interact with a signal sequence but recognises longer nascent chains. SecB stabilises the translated N-terminus in denatured conformations, which most likely contain native like secondary structure elements without specific tertiary interactions. The SecB bound preproteins are guided to SecA, which is already associated with the translocon SecYEG. Targeting to the translocase requires high affinity binding of SecB to the C-terminus of SecYEG-bound SecA. The preprotein binds to SecA, which enhances the SecB-SecA interaction. That induces release of the preprotein from SecB with the simultaneous transfer to SecA. The release of SecB from the membrane is coupled to the binding of ATP to SecA.

Almost all mitochondrial proteins are synthesised by ribosomes in the cytosol and imported posttranslational. Cytosolic chaperons guide the precursor proteins to the TOM-complex forming a general import pore (GIP). Presequence carrying proteins such as matrix proteins are transported by the presequence dependent TIM23-complex in a membrane potential dependent manner. The ATP driven presequence translocase associated motor (PAM) completes the translocation process into the matrix. Non-cleavable hydrophobic inner membrane proteins, such as carrier proteins, are directed by complexes of small TIM proteins through the intermembrane space (IMS) and are introduced into the inner membrane by the proton motive force (PMF) driven TIM22-complex. The precursors of β -barrel proteins of the outer membrane are transferred from the TOM complex to the sorting and assembly machinery (SAM complex), again with the help of small TIM proteins in the IMS (for reviews see (Pfanner et al., 2004)).

In addition to these systems, ABC transporters are also used in order to move peptides/proteins over membranes. In prokaryotes, one example is the sufficient uptake of nutrients from the environment by the peptide importer families Dpp and Opp. Also very large substrates can be transported by ABC transporters e.g. *E. coli* strains can protect themselves by secreting haemolysin A, a 107 kDa protein via haemolysin B and D, which then lyses the attacked cells. The yeast α -factor, which is a dodecapeptide, is transported by the ABC transporter Ste6p and enables two haploid cells to fuse to become diploid and benefit from recombination. Another example is the adaptive immune system where peptide presentation on the cell surface enables an organism to protect itself from harmful effects. A key component of this process is the ABC transport complex TAP.

3.2.1 Peptide import in prokaryotes driven by ABC transporters

In prokaryotes, at least two families of primary active peptide importers are well known. The ABC transporter Dpp facilitates the uptake of di- and tripeptides (Foucaud et al., 1995; Sanz et al., 2001) and a second ABC transporter family the Opp system, catalyses the uptake of oligopeptides containing 4 up to 35 amino acid residues (Hagting et al., 1994; Tynkkynen et al., 1993). Peptide transport in micro-organisms is important for nutrition of the cell and various signalling processes including regulation of gene expression, sporulation, chemo taxis, competence and virulence development (Kunji et al., 1998). As a common feature for importers the peptide binding proteins DppA and OppA are responsible for substrate delivery to their cognate membrane complexes and take part in substrate selection (Doeven et al., 2004). They are anchored to the membrane via lipid modification of the N-terminal cysteine residue.

3.2.2 The haemolysin system

The toxin HlyA belongs to a protection shield of the gram-negative bacterium *E. coli*. Once released into the medium it perforates membranes of surrounding competitors. It is transported by a type I secretion complex composed of the proteins HlyB, HlyD, and TolC (Holland et al., 2005). TolC is a porin like protein in the outer membrane whereas HlyD functions as connector of the inner and outer membrane. The substrate is thereby transported in a single step process across two membranes without the release of HlyA into the periplasmic gap. HlyB exhibits all conserved sequence stretches known for ABC transporters and forms the pore in the inner membrane. HlyB with its NBD provides the energy for the process by ATP hydrolysis (Zaitseva et al., 2005b). The functional unit of HlyB is supposed to be a homodimer. HlyA with its molecular mass of 107 kDa is translocated in an unfolded manner and (re)folds after dissociation from the translocase in the outer environment. The process is initiated by a so far unknown interaction between the last 60 amino acids of HlyA, which adopt a helix-turn-helix motif, and certain areas of the HlyB-NBD (Jarchau et al., 1994; Kenny et al., 1994).

3.2.3 The a-factor transporter Ste6p

Mating in *S. cerevisiae* results from the fusion of two haploid cells of opposite mating type, a and α , to form a diploid. The mating pheromones, a-factor and α -factor, stimulate receptors on cells of the opposite mating type to initiate cell fusion (Kurjan, 1992). The ability of cells to participate in mating relies on their ability to produce and respond to mating pheromones. Screens for mutations conferring a-specific sterility identified the *STE6*-gene (Oshima and Takano, 1980; Wilson and Herskowitz, 1984; Wilson and Herskowitz, 1987). Ste6p, which belongs to the multidrug resistance (MDR/ABCB) subfamily, was the first known yeast ABC transporter and is one of the best characterised ones (Kuchler et al., 1989; McGrath and Varshavsky, 1989). Ste6p appears to be located in the Golgi apparatus and endosome like compartments, but functions at the plasma membrane where it mediates ATP dependent secretion of the yeast a-factor pheromone (Kuchler et al., 1993; Kuchler et al., 1989).

3.2.4 The transporter associated with antigen processing like (TAPL)

TAPL is a human ABC transporter highly expressed in testis and moderately expressed in brain, spinal cord, and thyroid (Zhang et al., 2000). Even though, the targeting of TAPL is under debate evidences point to a lysosomal localisation as shown for examples in double immunofluorescence staining using anti-TAPL antibody and a panel of organelle markers.

Pull-down assays with different tagged TAPL showed the homodimerisation of TAPL and in addition the ATP-dependent peptide transport was demonstrated (Wolters et al., 2005). The transport activity of TAPL strictly requires ATP hydrolysis. In contrast to TAP, which is a high-affinity transporter, no peptide-binding activity was detected for TAPL by rapid filter assays, suggesting a low-affinity transporter. The recognition principle of TAPL and TAP is similar, since both transporters recognise peptides via their backbone, including the free N- and C-termini, and by side chain interactions. The peptide specificity of TAPL is very broad, ranging from hexa- to 59-mer peptides with a slight preference for 23-mers.

TAPL seems to work as a vacuum cleaner transporting a large variety of peptides with low affinity but high efficiency. The physiological role of TAPL is currently under debate. A function as peptide transporter in cross-presentation of endogenous antigens in the MHC class II pathway is discussed (for reviews see (Zhao et al., 2006)

3.2.5 The transporter associated with antigen processing (TAP)

Most nucleated cells in vertebrates present a pool of different peptides on their surfaces via major histocompatibility complex (MHC) I molecules for recognition by T cells. The presented peptides are generated by proteasomal degradation of endogenous or viral proteins in the cytosol of a cell. The transporter associated with antigen processing (TAP) transports peptides from the cytosol across the membrane of the endoplasmic reticulum (ER) into the lumen of the ER. In the ER, these peptides are loaded on MHC I molecules – comprising a α -chain and β 2-microglobulin – in the so called peptide loading complex which further con-

sists of the chaperones tapasin, calnexin, calreticulin and ERp57. TAP is a heterodimeric half size ABC transporter composed of TAP1 (ABCB2) and TAP2 (ABCB3) and both are essential for antigen processing (Powis et al., 1991; Spies and DeMars, 1991). As predicted by hydrophobicity analysis and sequence alignments with other known ABC transporters TAP1 and TAP2 contain ten and nine TMHs, respectively. For TAP1 the predicted topology was confirmed by cysteine scanning mutagenesis recently (Schrodt et al., 2006). The domain arrangement shows an N-terminal TMD and a C-terminal NBD. Deletion of the N-terminal four (TAP1) or three (TAP2) putative TMHs does not affect peptide transport (Koch et al., 2004; Koch et al., 2005). The N-terminal helices are involved in tapasin-recruitment. The last cytosolic loop and a 15-amino acid stretch located in the last TMH of TAP1 and TAP2 were shown to be involved in peptide binding and are therefore called the peptide-binding site (Nijenhuis and Hammerling, 1996). Both NBDs of TAP1 and TAP2 are not equivalent which is mainly reflected in sequence differences of the C-loops. The C-loop in TAP2 is degenerated to L-A-A-G-Q compared to the canonical signature motif L-S-G-G-Q. Many approaches (Bouabe and Knittler, 2003; Chen et al., 2004) were undertaken to discover crucial consequences but the physiological role of these difference are still under debate (for reviews see (Abele and Tampé, 2004).

3.3 Relevance of mitochondrial processes in cellular biology

The primary function of mitochondria is to use the redox energy stored in molecules like NADH₂ and FADH₂ to convert ADP and P_i to ATP. Beside this function mitochondria play an important role in many important cellular and metabolic tasks, such as apoptosis, regulation of the cellular redox state, heme- and Fe/S-cluster synthesis, steroid synthesis and heat production. Several severe diseases are linked to aberrant biogenesis of mitochondria or abnormal function of these organelles (Abou-Sleiman et al., 2006; Chabi et al., 2005).

Mitochondria consist of two compartments, the intermembrane space and the matrix, which are separated from the cytoplasm by two membranes, the outer mitochondrial membrane (OMM) and the inner mitochondrial membrane (IMM). The outer mitochondrial membrane is permeable to most small molecules and ions because it contains many copies of mitochondrial porin, a 30–35 kDa pore forming protein. In contrast, the IMM is intrinsically impermeable to nearly all ions and polar molecules. The inner membrane has a large surface, since it is folded into a series of internal ridges called cristae, and has very high protein content. Additionally the IMM exclusively contains a special lipid called cardiolipin. Many different transporters shuttle metabolites such as ATP, pyruvate, and citrate across the IMM. The matrix also contains the mitochondrial DNA. Although these organelles enclose their own DNA, most mitochondrial proteins are encoded by the nuclear DNA. In *S. cerevisiae* only eight proteins are encoded by the mitochondrial DNA: Var1, a mitochondrial ribosomal subunit, Cox I, II, III, three subunits of the cytochrome c-oxidase, cytochrome b and subunits 6, 8 and 9 of the F₁F₀-ATP-synthase. In an approach to determine the proteome of *S. cerevisiae* mitochondria the

proteins of highly pure mitochondria were separated by several independent methods and analysed by tandem mass spectrometry (MS) (Sickmann et al., 2003). In this approach, 750 different proteins were identified. All known components of the oxidative phosphorylation machinery, the tricarboxylic acid cycle, and the stable mitochondria encoded proteins were found. Based on the mitochondrial proteins described in the literature so far, it was calculated that the identified proteins represent ~ 90 % of all mitochondrial proteins. Remarkably, the function of ~ 25 % of the identified proteins are still unknown.

3.3.1 The proteolytic system in the inner mitochondrial membrane

Maintenance of cellular functions needs constant proteolysis to degrade short-lived proteins in a regulatory process e.g. factors triggering cell cycle or those part of control systems which ensure proper assembly of multi enzyme complexes and prevent their potentially harmful accumulation. Different mechanisms, including sequence specific recognition events and tagging strategies have been developed by the cell to ensure that these proteolytic processes are highly specific. ATP dependent proteases that use energy derived from ATP hydrolysis for selective degradation of cellular proteins play a key role in these processes (Schmidt et al., 1999; Wickner et al., 1999).

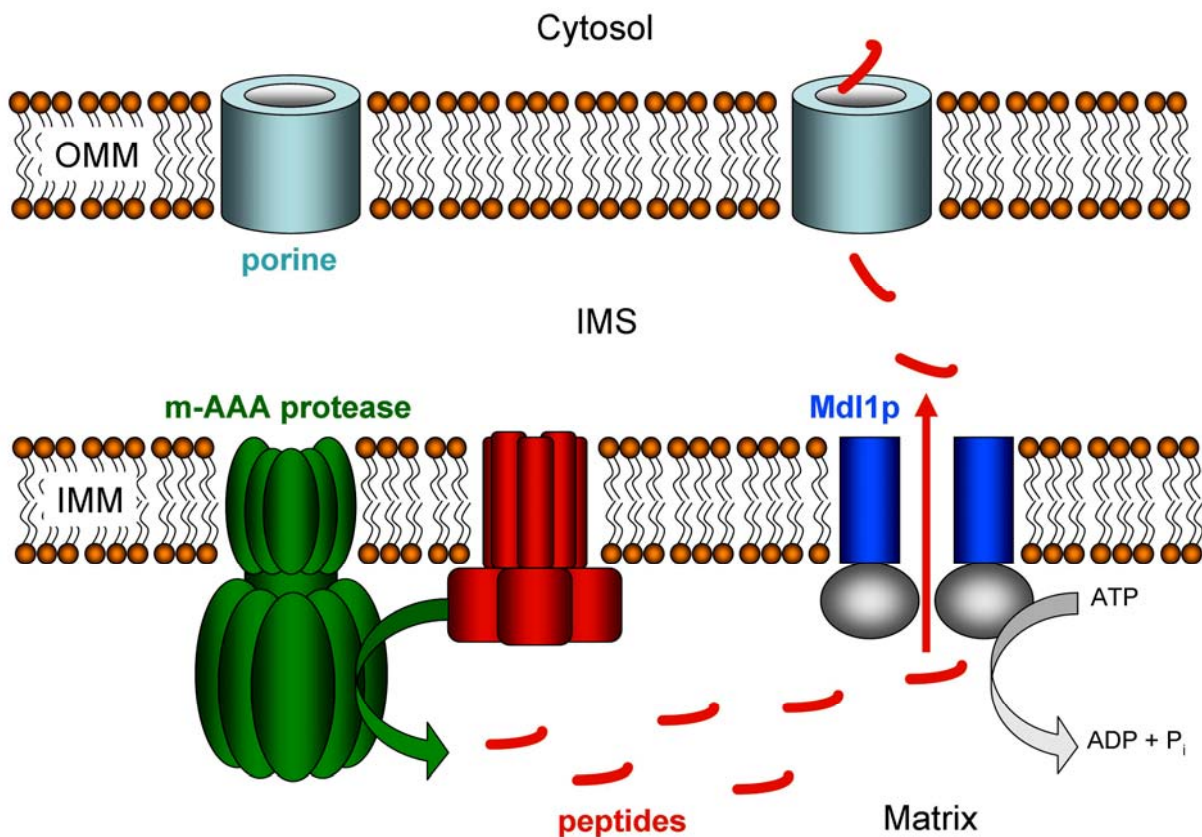


Figure 3.5: Proteolytic system of the IMM (modified from Arnold & Langer, 2002). Unfolded or non-assembled proteins embedded in the inner mitochondrial membrane (IMM) are degraded by AAA proteases. One way of peptide export is the tear down of protein complexes via the m-AAA protease which has its active centre placed in the matrix. Afterwards peptides are transferred into the inner mitochondrial space (IMS) by Mdl1p. From there they can pass the outer mitochondrial membrane (OMM) e.g. via porines.

The IMM is probably the membrane with the highest protein content. The biogenesis of the respiratory chain complexes and the ATP synthase is a complex process requiring the coordinated function of various membrane bound proteins like protein translocases and assembly factors. Therefore, a distinct quality control system is present in the membrane that selectively removes non-assembled polypeptides (Figure 3.5). The key components are two AAA proteases, membrane embedded ATP dependent proteolytic complexes, with their catalytic sites exposed at opposite membrane surfaces (for review see (Arnold and Langer, 2002).

Eukaryotic AAA proteases seem to be localised exclusively in mitochondria and chloroplasts. Three orthologues of the *E. coli* AAA ATPase FtsH have been found in human and yeast mitochondria, and at least nine homologous have been identified in the genome of *Arabidopsis thaliana* so far (Adam et al., 2001; Juhola et al., 2000; Ogura and Wilkinson, 2001). In yeast, the subunits form two AAA proteases in the inner membrane of mitochondria with a native molecular mass of roughly one MDa. The m-AAA (matrix-oriented ATPases associated with a variety of cellular activities) is a heterooligomeric complex composed of Yta10p (Afg3) and Yta12p (Rca1) and exposes its active side into the matrix, whereas the i-AAA (inter membrane space oriented ATPases associated with a variety of cellular activities) protease, forms a homooligomer of Yme1p subunits and the active side focus to the intermembrane space. The i-AAA protease subunits have one transmembrane domain, whereas two membrane spanning segments are predicted for m-AAA protease subunits (Langer, 2000). The importance of AAA proteases can be deduced from complementation studies in yeast, which revealed a functional conservation between human, *Neurospora crassa* and yeast i-AAA proteases (Klanner et al., 2001; Shah et al., 2000).

3.4 Mitochondrial ABC transporters in *S. cerevisiae*

The DNA sequence of *S. cerevisiae* was the first eukaryotic genome which was solved completely and revealed the existence of 29 (Decottignies and Goffeau, 1997) to 30 (Taglicht and Michaelis, 1998) ABC protein genes. These ABC proteins perform different functions ranging from multi drug resistance, pheromone secretion and stress response to cellular detoxification. Based on phylogenetic analysis yeast ABC proteins are classified into six subfamilies: MDR, PDR; MRP/CFTR, ALDp, YEF3, and the RLI subfamily (Decottignies and Goffeau, 1997).

The MDR family comprises four proteins: Ste6p, Atm1p, Mdl1p and Mdl2p. Except for Ste6p, which functions in the plasmamembrane (see above) the other members of the MDR family are targeted to the inner mitochondrial membrane.

Atm1p was identified in *S. cerevisiae* as the first mitochondrial ABC transporter using a PCR approach (Leighton and Schatz, 1995) and was coincidentally identified in a genetic screen designed to find new components of c-type cytochrome biogenesis (Kispal et al., 1997). The *ATM1*-gene encodes a half size transporter of 690 amino acids containing an N-terminal TMD with six putative TMHs and a C-terminal NBD. Atm1p homologous are found in lower and

higher eukaryotes. The typical sequence identity between different members of the Atm1p family is between 40 % and 50 %, and includes the TMD a region where homology between non-related ABC transporters is usually low. Remarkably, in prokaryotes and archaea no close homologs of Atm1p could be found.

Atm1p contains a mitochondrial targeting sequence and it was shown by immunofluorescence and immunostaining using a myc-epitope-tagged that Atm1p is located in the mitochondria. The membrane orientation of Atm1p was determined in protease accessibility experiments where Atm1p in mitoplasts (mitochondria lacking the outer membrane) is resistant to proteases added from the outside, while the protein is degraded after detergent lysis of the organelles (Leighton and Schatz, 1995). Therefore, the ABC domain faces the matrix and suggests that Atm1p functions as a mitochondrial exporter.

The lack of functional Atm1p leads to drastically elevated levels of free iron (non-heme, non-Fe/S clusters) inside the mitochondrial matrix. *ATMI* knock out strains grow poorly on rich media containing glucose (Kispal et al., 1997; Leighton and Schatz, 1995) and do not grow on non-fermentable carbon sources such as glycerol. These strains furthermore show a deficiency in holo-cytochromes, in the degradation of protein bound heme and increased concentrations of glutathione which can be explained by increased oxidative stress in Δ *ATMI* cells (Kispal et al., 1997). A further characteristic of the Δ *ATMI* strain is the loss of mtDNA yielding ρ^0 cells (Leighton and Schatz, 1995; Senbongi et al., 1999). Evidence against heme as a potential substrate of Atm1p was confirmed by demonstrating that over-expressed peroxisomal catalase Cta1p (a heme containing protein) displayed almost the same activity in Δ *ATMI* cells compared to wild-type cells. A trace guiding to the role of Atm1p came from the observation of a leucine auxotrophy of Δ *ATMI* cells (Kispal et al., 1999). Measurements of activities of enzymes involved in leucine biosynthesis showed a quantitative deficiency of isopropyl malate isomerase (Leu1p) even though the Leu1p polypeptide chain was present at wild-type levels. Leu1p is a cytosolic Fe/S protein that closely resembles aconitase of the mitochondrial matrix (Kohlhaw, 1988). No reduced activities as compared to wild-type cells were found for the first and third step of leucine biosynthesis. This finding suggests that Atm1p may perform a function in the maturation of cytosolic Fe/S proteins.

Little is known about Mdl2p so far except its localisation in the inner mitochondrial membrane and the fact that it does not form a heterodimeric transport complex with Mdl1p (Young et al., 2001).

3.4.1 Mdl1p and its physiological function

The *MDL1*-gene (ORF YLR188W) was discovered in an approach to identify members of the ABC transporter family (Dean et al., 1994). The *MDL1*-gene encodes a 695 amino acids long membrane protein with a N-terminal TMD and a C-terminal NBD. Hydrophobicity and sequence homology analysis suggested that Mdl1 contains six transmembrane helices with the N- and C-termini inside the mitochondrial matrix (Figure 3.6). The minimal functional unit

was suggested to be a homodimer residing in the inner mitochondrial membrane. In order to characterise the released products, high-resolution size exclusion chromatography analysis of these supernatants were performed. About 30 % of the released material resolved as a heterogeneous peptide mixture which could be divided into two areas with molecular masses of 200 to 600 daltons and 600 to 2100 daltons (Young et al., 2001). Mitochondria isolated from *AMD1* strains, showed significant differences in comparison to wild-type mitochondria. The release of long peptides (600 to 2100 Da) was reduced by 40 % in *AMD1* mitochondria. Over-expression of Mdl1p in *AMD1* cells restored this transport defect. Point mutations in the Walker A and B motifs and the L-S-G-G-Q-loop of Mdl1p which abolish ATP hydrolysis showed similar patterns in size exclusion analysis as observed in *AMD1* mitochondria (Young et al., 2001). Remarkably, peptides derived from mitochondrial encoded respiratory chain subunits have been detected in complex with class I major histocompatibility molecules at the surface of mammalian cells (Fischer Lindahl et al., 1991), suggesting that the Mdl1p homologous in higher eukaryotes are involved in the export of peptides from the mitochondrial matrix to present them on the surface of the cell.

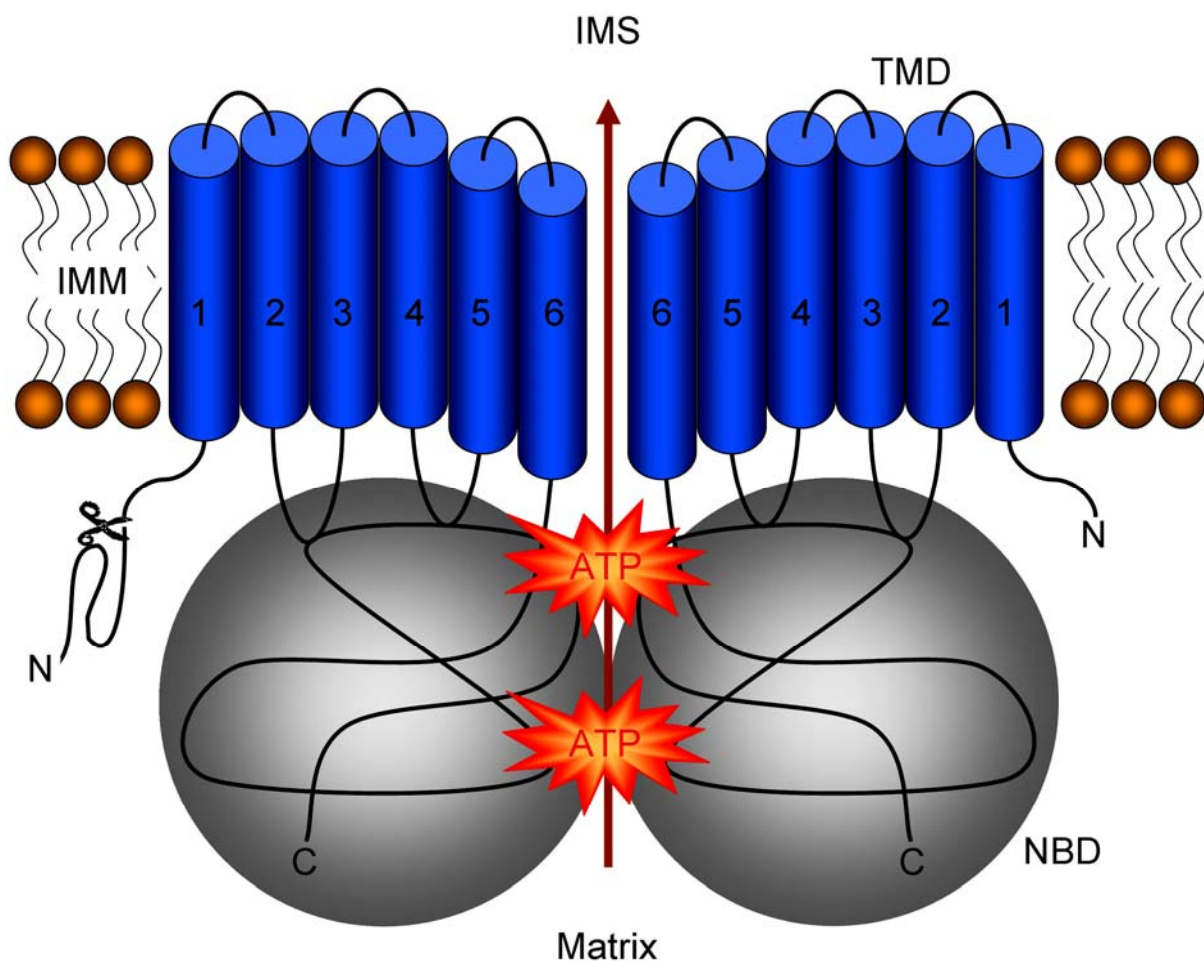


Figure 3.6. Scheme of the homodimeric ABC transporter Mdl1p. According to hydrophobicity analysis and homology comparison each Mdl1p monomer includes a N-terminal transmembrane domain (TMD) with six transmembrane helices (TMH; numbered from 1 - 6) and a C-terminal nucleotide binding domain (NBD) forming a half size transporter. The active transport complex is thought to be a homodimer with the TMDs forming the translocation pathway for the solutes through the inner mitochondrial membrane and the NBDs powering the whole process via ATP hydrolysis. The mitochondrial targeting sequence is cleaved off after import into the IMM.

Another possible role of Mdl1p was found in a screen for yeast genes capable of suppressing the abnormalities of cellular iron metabolism demonstrated by $\Delta ATMI$ cells. One of the identified genes was Mdl1p. Over-expression of Mdl1p in $\Delta ATMI$ cells results in a reduction of mitochondrial iron content decreased sensitivity to H_2O_2 and transition metal toxicity (Chloupková et al., 2003). Additionally, the study on the effect of over-expression and deletion of Mdl1p, showed a novel role for Mdl1p in the regulation of cellular resistance to oxidative stress.

A close homolog of Mdl1p in mice was discovered by searching for GATA-1 activated transcripts in G1E cells. The transcription factor GATA-1 is essential for normal erythropoiesis and GATA-1 binding sites are found in promoters or enhancers of genes expressed selectively in erythroid cells. By subtractive analysis, a new ATP binding cassette transporter was found that is strongly and rapidly induced by GATA-1 (Shirihai et al., 2000). This protein named ABC-me is localised in the inner mitochondrial membrane and expressed at high levels in erythroid tissues of embryos and adults. ABC-me is induced during erythroid maturation in cell lines and primary haematopoietic cells, and its over-expression enhances haemoglobin synthesis in erythroleikemia cells. It was therefore speculated that Mdl1p like ABC-me may mediate mitochondrial transport functions related to heme biosynthesis.

3.5 Aims and Motivation

Transport processes over membranes are essential for all cells. The membrane protects the cell from the potential destructive outside, and membrane transporters ensure the maintenance and communication of the cell. In addition, the abundance of proteins during a cell cycle has to be regulated tightly to ensure proper function of the cell even over borders from different organelles. Mdl1p is an ABC transporter in the inner mitochondrial membrane involved in peptide transport from the matrix into the cytosol and therefore it might play a role in quality control and communication.

Little is known about the physiological role of mitochondrial ABC transporters. Transporters residing in the inner mitochondrial membrane are difficult to analyse due to the complex two membrane architecture of mitochondria, the high membrane protein content with proteins with high affinity to ATP and the content of many different other transport systems.

Furthermore, since the availability of purified active protein is limited due to low yield and the stable reconstitution is difficult, obtaining basic biochemical data and structural information is challenging.

Therefore, this work sets out to address the following main research topics for the transport ATPase Mdl1p: (i) the ATP hydrolysis cycle of the motor domains of Mdl1p, (ii) expression and purification of high yields of Mdl1p in an active state, (iii) reconstitution of Mdl1p into lipid vesicles in order to examine its role in peptide transport “*in vitro*”, (iv) structural investigation of the organisation and arrangement of the transport complex and (v) the establishment of a setup to study Mdl1p “*in vivo*”.

4 Material

4.1 Chemicals

Name	Company
[³⁵ S]-Methionine	Hartmann Analytic
[α - ³² P]Adenosine-5'-triphosphate	Hartmann Analytic
[γ - ³² P]Adenosine-5'-triphosphate	Hartmann Analytic
1,4-Dithiothreitol (DTT)	Sigma-Aldrich
5-Amino-2,3-dihydro-1,4-phthalazinedione-3-aminophthalhydrazide (Luminol)	Sigma-Aldrich
8-Azido-[α - ³² P]adenosine-5'-triphosphate	MP Biomedicals
Acetic acid 99 %	Riedel de Haen
Acetonitrile (ACN)	Roth
Acrylamide	Roth
Acrylamide 30 % (Rotiphorese gel 30)	Roth
Adenine	Sigma-Aldrich
Adenosine 5'-(β,γ -imido)triphosphate (AMP-PNP)	Sigma-Aldrich
Adenosine 5'-[γ -thio]triphosphate (ATP γ S)	Sigma-Aldrich
Adenosine-5'-diphosphate (ADP)	Fluka
Adenosine-5'-monophosphate (AMP)	Fluka
Adenosine-5'-triphosphate (ATP)	Fluka
Agar	GibcoBRL
Agarose	Sigma-Aldrich
Ammonium chloride	Merck
Ammonium peroxodisulphate (APS)	Roth
Ascorbate	Sigma-Aldrich
Ascorbic acid	Roth
Beryllium chloride	Sigma-Aldrich
Biobeads SM-2	BioRad
Bisacrylamide	Roth
Bis-Tris	Roth
β -Mercapthoethanol	Roth
Bovine serum albumin (BSA)	Sigma-Aldrich
Bradford reagent	Pierce
Bromphenolblue	Merck
Calcium chloride	Merck
Calmodulin sepharose beads	GE Healthcare
Chloramine T	Riedel de Haen
Complete protease inhibitor (EDTA free)	Roche
Coomassie Blue G	Sigma-Aldrich
Cytosine-5'-triphosphate (CTP)	Fluka
Developer solutions A & B	AGFA
Dimethylsulfoxide (DMSO)	Fluka
di-Potassium hydrogen phosphate	Roth
di-Sodium hydrogen phosphate	Roth
Dowex 1 x 8 anion exchange	Sigma-Aldrich
<i>E. coli</i> lipids (total extract)	Avanti Polar Lipids

EDTA, Disodium salt	Roth
EGTA	Roth
Ethanol, abs.	Riedel de Haen
Formaldehyde, 37 % (v/v)	Roth
Formic acid	Roth
Glycerol	Roth
Glycerol 2-phosphate	Sigma-Aldrich
Glycine	Roth
HEPES	Sigma-Aldrich
Hydrochloric acid, 37 %	Merck
Hydrogen peroxide, 30 %	Merck
IgG sepharose beads	GE Healthcare
Imidazole	Fluka
Isopropanol	Roth
Isopropyl β -D-1-thiogalactopyranoside (IPTG)	PeqLab
L-Alanine	Sigma-Aldrich
L-Arginine	Sigma-Aldrich
L-Asparagine	Sigma-Aldrich
L-Aspartate	Sigma-Aldrich
L-Cysteine	Sigma-Aldrich
L-Glutamate	Sigma-Aldrich
L-Glutamine	Sigma-Aldrich
L-Glycine	Sigma-Aldrich
L-Histidine	Sigma-Aldrich
L-Isoleucine	Sigma-Aldrich
Lithium acetate	Roth
Lithium chloride	Roth
L-Leucine	Sigma-Aldrich
L-Lysine	Sigma-Aldrich
L-Methionine	Sigma-Aldrich
L-Phenylalanine	Sigma-Aldrich
L-Prolin	Sigma-Aldrich
L-Serin	Sigma-Aldrich
L-Tryptophan	Sigma-Aldrich
L-Tyrosin	Sigma-Aldrich
L-Valine	Sigma-Aldrich
Magnesium acetate	Roth
Magnesium chloride	Riedel de Haen
Magnesium sulphate	Merck
Manganese chloride	Sigma-Aldrich
Methanol	Riedel de Haen
Microsint scintillation liquid	Packard Biosciences
MOPS	Roth
N,N,N',N'-Tetramethylethylendiamin (TEMED)	Sigma-Aldrich
N,N-Dimethylformamide (DMF)	Fluka Chemie
Sodium [125]iodide	Hartmann Analytic
Nickel sulphate	Fluka
Perchloric acid	Roth
Phenylmethane sulfonyl fluoride (PMSF)	Sigma-Aldrich

Phosphate standard solution	Sigma Aldrich
Polyethyleneglycol (PEG) 4000	Sigma-Aldrich
Polyethylenimine cellulose plates	Merck
Ponceau Red S	Sigma-Aldrich
Potassium chloride	Roth
Potassium acetate	Roth
Potassium dihydrogen phosphate	Roth
Rapid Fixer Solution G354	AGFA
Salmon testes DNA	Sigma-Aldrich
Silver nitrate	Roth
Skim milk powder	Roth
Sodium acetate	Roth
Sodium azide	Roth
Sodium bisulfite	Sigma-Aldrich
Sodium carbonate	Merck
Sodium chloride	Fluka
Sodium dihydrogen phosphate	Roth
Sodium fluoride	Sigma-Aldrich
Sodium metavanadate	Sigma-Aldrich
Sodium thiosulphate	Roth
Sodium hydroxide	Riedel de Haen
<i>trans</i> -4-Hydroxycinnamic acid (p-Coumaric acid)	Sigma-Aldrich
Trichloroacetic acid (TCA)	Roth
Tricine	Roth
Trifluoroacetic acid, 98 % (v/v) (TFA)	Fluka
Tris	Roth
Uridine-5'-triphosphate (UTP)	Fluka
α -D-(+)-Galactose	Roth
α -D-(+)-Glucose	Roth
ϵ -Amino-n-caproic acid	Roth

4.2 Detergents

Name	Company
Decanoyl-n-hydroxyethylglucamide (HEGA-10)	Anatrace
Digitonin	Calbiochem
tetradecylphosphocholine (FC-14)	SynphaBase
n-Dodecyl- β -D-maltopyranoside (DDM)	Anatrace
n-Tetradecyl-n,n-dimethylamine-n-oxide (TDAO)	Anatrace
Octaethylene glycol monododecyl ether (C ₁₂ E ₁₈)	Anatrace
Octyl- β -D-glucopyranoside (OG)	Anatrace
Sodium cholate	Anatrace
Sodium dodecyl sulphate (SDS)	Roth
Triton X-100	Anatrace
Tween-20	Roth

4.3 Cells and Media

Name	Company
BL21(DE3) (<i>E. coli</i>)	Novagen
BY4743 (<i>S. cerevisiae</i>)	(Brachmann et al., 1998)
W303-1A (<i>S. cerevisiae</i>)	(Thomas and Rothstein, 1989)
Y24137 (<i>S. cerevisiae</i>)	(Brachmann et al., 1998)
YLR188W (<i>S. cerevisiae</i>)	Open Biosystems
Kanamycin	Sigma Aldrich
Lactate	Roth
Peptone/Tryptone from Casein	Roth
Yeast extract	Roth
Yeast Nitrogen Base (with $(\text{NH}_4)_2\text{SO}_4$)	Invitrogen

4.4 Enzymes, Markers and Kits

Name	Company
Apyrase	Sigma-Aldrich
Benzonase	Merck
Hexokinase	Sigma-Aldrich
Lyticase	Sigma-Aldrich
Prestained Protein Marker, Broad Range	New England Biolabs
Prestained Protein Molecular Weight Marker	MBI Fermentas
Protein Molecular Weight Marker	MBI Fermentas
TEV protease	Sigma-Aldrich
Water HPLC grade	Merck
BCA-kit	Pierce

4.5 Vectors

Vector	Relevant Characteristics	Reference
pMDL1p-NBD	pET28b carrying Mdl1p-NBD (D423-R695)	(Janas et al., 2003)
pMDL1p-NBD(E599Q)	pET28b carrying E599Q-mutant Mdl1p-NBD	(Janas et al., 2003)
pYES2.1/V5-His-TOPO-Mdl1pfl	pYES2.1/VS-His-TOPO [®] carrying full-length Mdl1p	(Hofacker et al., 2006)
pYES2.1/V5-His-TOPO-Mdl1pfl_EQ	pYES2.1/VS-His-TOPO [®] carrying full-length Mdl1p E599Q	(Hofacker et al., 2006)
pYES2.1/V5-His-TOPO-Mdl1pfl_HA	pYES2.1/VS-His-TOPO [®] carrying full-length Mdl1p H631A	(Hofacker et al., 2006)

4.6 Antibodies

Antibody	Source	Type/Dilution	Specificity	Company
R7/10	Rabbit	Polyclonal/1 : 500	C-term. of Mdl1p (KGGVIDLDNSVAREV)	Research Genetic Inc, Huntsville
Anti-Rabbit-IgG	Goat	Polyclonal/1 : 50,000	IgG (H + L)	Dianova
Peroxidase antiperoxidase	Rabbit	Polyclonal/1 : 200	Protein A	Sigma-Aldrich

4.7 Peptides

Name	Sequence/Reference
R9LQK	NH ₂ -RRYQKSTEL-COOH (9-mer)
R9LQK*	NH ₂ -RΦYQΨSTEL-COOH (9-mer)
T10	f-MYQR-Bpa [*] -LYST-COOH (9-mer)
T11	f-MYQR-Bpa [*] -LYSTNAK-COOH (12-mer)
X ₍₈₎	8-mer peptide library/(Uebel et al., 1995)
X ₍₂₃₎	23-mer peptide library/(Uebel et al., 1995)

4.8 Equipment

Apparatus	Manufacturer/Company
Abbé refractometer	Krüss Optronic
Autoclave 5075 ELVC	Tuttnauer Systec
Cary 50 Bio UV Vis spectrophotometer	Varian
Developer CP 1000	AGFA
Incubator Kelvitron	Heraeus
Infors Unitron	Infors
Ino Lab pH-meter	WTW
Kern 770 microbalance	Kern
Light microscope	Leitz
Liposofast extruder	Avestin
Liquid scintillation counter LS 6500	Beckman
Lumi imager F1	Roche
Magnetic stirrer	Ikamag
Membrane vacuum pump	Kobe
Mettler PM 460 balance	Mettler
Microwave T.D.S.	Samsung
Milli Q-Plus water system	Millipore
Multipipette	Eppendorf
EM208S electron microscope	FEI company
Phosphor-Imager 445Si	Molecular Dynamics
Polarstar Galaxy (ELISA reader)	BMG
Power supply Elite 300 plus	Polymehr systems
SDS-PAGE- BN-gel-apparatus	Institute workshop/BioRad/Hoeffer
Thermomixer	Eppendorf
Vortexer	Bender & Hobein
TVIPS 1Kx1K slow-scan CCD camera	Tietz
Freeze-fracture unit 400T	Balzers
Ikatherm HCB	IKA
Aekta Explorer	GE Healthcare
HiTrap Chelating (1 mL and 5 mL)	GE Healthcare
SMART Chromtography System	GE Healthcare
Superdex 200 HiLoad 16/60	GE Healthcare
Superdex 200 HiLoad 26/60	GE Healthcare
Superdex 200 PC 3.2/30	GE Healthcare
Superdex 75 PC 3.2/30	GE Healthcare
Superdex Peptide PC 3.2/30	GE Healthcare

4.9 Centrifuges and Rotors

Centrifuge	Rotor
Eppendorf Centrifuge 5417R	F-45-30-11
Heraeus Sepatech Megafuge 1.0 R	BS4402/A
Sorvall RC 3C Plus	H6000A
Sorvall RC 5B Plus	GSA, GS3, SS34
Beckman L-50	Ti 45, Ti 60, Ti 80, SW 27, SW 28
Beckman TLX 100	TLA-55, TLA-100, TLA-110, TLA-120.2

4.10 Supplementary material

Material	Company
Biomax MS film	Kodak
Cryotubes	Nunc
Cuvettes, plastic	Fisher Scientific
Cuvettes, quartz glass	Hellma
Douncer	Braun
Eppendorf tubes	Greiner
Filter paper	Whatman
Gloves, latex	Terumo Teruglove
Gloves, nitril	Servoprax
Microliter syringes	Hamilton
Multiwellplates	Greiner
Nitrocellulose membrane	Schleicher & Schüll
Pasteur pipettes	Merck
PCR cups	Sarstedt
Pipette tips	Greiner
Pipettes	Abimed
Polycarbonate membranes, P.D. 400 nm	Avestin
Spin columns	BioRad
Spin concentrators (Amicon)	Millipore
Sterile filters	Millipore
Syringes (plastic, div volumes)	Braun
Test tubes, sterile, 15 and 50 mL	Greiner

4.11 Media, Buffers and Solutions

4.11.1 Cell culture media

LB medium (<i>E. coli</i>)	TYM medium (<i>E. coli</i>)	YEPD medium (<i>S. cerevisiae</i>)
10 g/L peptone/tryptone	20 g/L peptone/tryptone	5 g/L yeast extract
5 g/L yeast extract	5 g/L yeast extract	10 g/L (w/v) pepton/tryptone
5 g/L NaCl	0.1 M NaCl	20 mg/mL adenine
	10 mM MgSO ₄	2 % (w/v) glucose
or culture plates 2 % (w/v) agar is supplemented		or culture plates 2 % (w/v) agar is supplemented
YEPGal medium (<i>S. cerevisiae</i>)	Lactat medium (<i>S. cerevisiae</i>)	SC medium (<i>S. cerevisiae</i>)
5 g/L yeast extract	3 g/L yeast extract	6,7 g/L yeast nitrogen base with (NH ₄) ₂ SO ₄
10 g/L (w/v) pepton/tryptone	0.5 g/L glucose	1 x amino acid mix*
20 mg/mL adenine	1 g/L KH ₂ PO ₄	
2 % (w/v) galactose	1 g/L NH ₄ Cl	
	0.5 g/L CaCl ₂	
	0.5 g/L NaCl	
	0.6 g/L MgCl ₂	
	2 % (v/v) lactic acid	
	adjust pH 5,5 with KOH	for culture plates 2 % (w/v) agar is supplemented

* amino acid mix (20 x): 224 mg/L adenine, 768 mg/L arginine, 768 mg/L histidine, 1152 mg/L isoleucine, 1152 mg/L leucine, 768 mg/L methionine, 960 mg/L phenylalanine, 1152 mg/L threonine, 768 mg/L tryptophan, 288 mg/L tyrosine, 1152 mg/L valine

4.11.2 Solutions for *E. coli* transformation

TFBI solution	TFBII solution
30 mM potassium acetate	10 mM Na-MOPS, pH 7.0
50 mM MnCl ₂	75 mM CaCl ₂
0.1 M KCl	10 mM KCl
10 mM CaCl ₂	15 % (w/v) glycerol
15 % (w/v) glycerol	

4.11.3 Solutions for *S. cerevisiae* transformation

LiAc-TE buffer	Transformation-mix	
10 mM Tris-HCl, pH 7.5	PEG 4000 (40 % w/v) in LiAc-TE buffer	350 µL
1 mM EDTA	carrier DNA	25 µL
100 mM LiAc	plasmid DNA (0.1-10 µg DNA)	3 µL

4.11.4 Solutions for SDS-PAGE

Collecting gel buffer	Separating gel buffer	SDS-Sample buffer (5 x)	Running buffer (10 x)
0.5 M Tris-HCl, pH 6.8	1.5 M Tris-HCl, pH 8.8	150 mM Tris-HCl, pH 6.8,	250 mM Tris-HCl, pH 8.3
0.4 % (w/v) SDS	0.4 % (w/v) SDS	6 % (w/v) SDS 30 % (w/v) glycerol 0.3 % (w/v) bromphenol-blue	1.92 M glycine, 1 % (w/v) SDS

4.11.5 Solutions for Tricine-PAGE

Acrylamide	Cathode buffer (10 x)	Gel buffer (3 x)	Anode buffer (10 x)
48 % (w/v) acrylamide	1 M Tris	3 M Tris-HCl, pH 8.45	2 M Tris-HCl, pH 8.9
1.5 % (w/v) bisacrylamide dissolve in dH ₂ O filtered and stored at RT in the dark	1 M Tricine 1 % (w/v) SDS	0.3 % (w/v) SDS	

4.11.6 Solutions for Blue-native gel electrophoresis

Gel buffer (3 x)	Anode buffer	Cathode buffer
150 mM Bis-Tris, pH 7.0 200 mM ϵ -amino n-caproic acid	50 mM Bis-Tris, pH 7.0	15 mM Bis-Tris pH, 7.0 50 mM Tricine +/- Coomassie blue G

Digitonin buffer	Loading dye (10 x)
20 mM Tris-HCl, pH 7.4 50 mM NaCl 10 % (v/v) glycerol 1 mM EDTA 1 mM PMSF 1 % (w/v) digitonin	100 mM Bis-Tris, pH 7.0 500 mM ϵ -amino n-caproic acid 5 % (w/v) Coomassie blue G

4.11.7 Solutions for Coomassie staining

Stain solution	Destain solution
40 % (v/v) methanol 10 % (v/v) acetic acid 0.25 % (w/v) Coomassie blue G	40 % (v/v) methanol 10 % (v/v) acetic acid

4.11.8 Solutions for Silver staining

Fixation solution	Thiosulphate buffer	Silver nitrate solution	Developing solution
30 % (v/v) ethanol	100 mM sodium-acetate pH 6.0	0.1 % (w/v) AgNO ₃	2.5 % (w/v) Na ₂ CO ₃
10 % (v/v) acetic acid	30 % (v/v) ethanol 1 mg NaS ₂ O ₃ /mL prior usage	0.025 % (v/v) formaldehyde	0.05 % (v/v) formaldehyde

4.11.9 Buffers for electroblotting and immunodetection

Blotting buffer	Blocking buffer	Wash buffer	10x TBS
25 mM Tris-HCl, pH 8.2	1x TBS	1x TBS	200 mM Tris-HCl, pH 8.0
20 % (v/v) methanol	5 % (w/v) skim milk powder	0.2 % (v/v) Tween-20	1.5 M NaCl
192 mM glycine	0.2 % (v/v) Tween-20 0.1 % (w/v) NaN ₃		

ECL solution 1	ECL solution 2
100 mM Tris-HCl, pH 8.5	100 mM Tris-HCl, pH 8.5
2.5 mM luminol sodium salt	0.02 % H ₂ O ₂
0.4 mM coumaric acid	

4.11.10 Buffers for mitochondria isolation

DTT buffer	Lyticase buffer	Homogenisation buffer	SEM buffer
100 mM Tris-SO ₄ , pH 9.4	20 mM KP _i , pH 7.4	10 mM Tris-HCl, pH 7.4	20 mM MOPS, pH 7.2
10 mM DTT	1.2 M sorbitol	600 mM sorbitol	250 mM sucrose
		1 mM EDTA	1 mM EDTA
		0.2 % BSA	

5 Methods

5.1 Molecular Biology

5.1.1 Cell culture

For expression of the Mdl1p-NBD the *E. coli* strain BL21(DE3) was transformed with the plasmids pMDL1p-NBD or pMDL1p-NBD(E599Q). LB medium was supplemented with 50 µg/mL kanamycin after sterilisation and a 50 mL culture was inoculated with the transformants from an agarose plate and grown overnight at 37 °C and vigorous agitation. One litre of culture was inoculated 50 : 1 (v/v) with the overnight culture. The expression culture was grown at 37 °C to the midlogarithmic phase ($OD_{600} = 0.5$) for induction of protein expression with 0.2 mM IPTG. After 3 hours at 30 °C, cells were harvested (4,000 x g; 15 min; 4 °C) and the cell pellet was washed with water and recentrifuged (4,000 x g; 5 min; 4 °C). The pellet was frozen in liquid nitrogen and stored at -80 °C.

For expression of full-length Mdl1p in *S. cerevisiae* the strain BY4743 (chapter 4.3) was transformed with the plasmid pYES2.1/V5-His-TOPO-Mdl1pfl, pYES2.1/V5-His-TOPO-Mdl1pfl_EQ or pYES2.1/V5-His-TOPO-Mdl1pfl_HA and grown overnight in SC minimal medium (Sherman, 1991) supplemented with an amino acid mix without uracil and with 2 % glucose. Cells were harvested and resuspended to an OD_{600} of 0.4 in SC minimal medium supplemented with an amino acid mix without uracil and with 2 % galactose. Growth was continued at 30 °C and cells were harvested after 8 to 12 hours by centrifugation (5,000 x g; 12 min; 4 °C).

In order to test the influence of culture media in respect of the efficiency of the *in organello* synthesis and peptide export from mitochondria cells were grown in YEPD, YEPGal or Lactat medium. In all cases, a 5 mL starter culture was grown for at least 24 hours at 30 °C and used for inoculation of a 50 mL preculture (1 : 10) which was grown overnight at 30 °C. The main culture was inoculated with the preculture 40 : 1 and grown until an OD_{600} between 1 and 2 was reached.

5.1.2 Competent *E. coli* cells

An overnight culture of *E. coli* DH5 α cells was diluted 1 : 100 in 100 mL TYM-medium and grown at 37 °C to an OD_{600} of 0.6. The culture was cooled on ice and the cells were harvested (1,000 x g; 10 min; 4 °C).

The cell pellet was carefully resuspended in 10 mL sterile, ice-cold 0.1 M CaCl₂ and incubated on ice for 1.5 hours. After centrifugation the pellet was washed in 50 mL ice-cold TFBII solution and harvested again. The resulting pellet was resuspended in 5 – 10 mL TFBII solution. Cell aliquots of 100 µL were snap-frozen in liquid nitrogen and stored at -80 °C.

5.1.3 Transformation of competent *E. coli* cells

Competent *E. coli* cells were thawed strictly on ice. Plasmid DNA (10 ng to 1 µg) was mixed with 100 µL of competent cells and incubated on ice for 30 minutes. The suspension was transferred to 42 °C for 45 seconds (heat shock). The cells were regenerated in 1 mL LB-medium for 1 hour at 37 °C with vigorous agitation. The cell suspension was centrifuged (1,000 x g; 1 min; 25 °C) and plated on pre-warmed LB-agar plates supplemented with kanamycin (50 µg/mL) and incubated overnight at 37 °C.

5.1.4 Transformation of *S. cerevisiae* cells

The following stock solutions were prepared: 10 x TE buffer (100 mM Tris-HCl, pH 7.5; 10 mM EDTA), 10 x lithium acetate (1M LiAc) and 50 % (w/v) PEG 4000. All solutions were autoclaved before use. Cryostocks of the designated cells were cultured for at least 24 hours at 30 °C in 5 mL of the appropriate medium. Cells were washed with water and LiAc-TE buffer and finally resuspended in 50 µL LiAc-TE buffer. The carrier DNA (10 mg/mL Salmon testis DNA dissolved in TE buffer overnight at 4 °C, aliquoted and stored at -20 °C) was denatured at 95 °C for 20 minutes and placed on ice immediately. The LiAc-treated cell suspension was added to the transformation mix and incubated at 30 °C for an hour. Subsequently, cells were placed at 42 °C for 10 minutes to trigger a heat shock response of the cells.

The cells were sedimented (1,000 x g, 1 min, 4 °C) and the supernatant was discarded. For regeneration the cells were incubated for 1 hour in complex medium without selection pressure. After harvesting, the cells were resuspended in a maximum of 100 µL of water, plated onto selective medium plates and incubated at 30 °C for 2 - 3 days. An additional selection step was performed by plating five to seven colonies onto a fresh selection agar-plate and incubated for one day at 30 °C.

5.1.5 Cryostocks of yeast cells

5 ml YEPD medium was inoculated with a preexisting cryostock or started from an agarose-plate and grown for two days at 30 °C. Subsequently cells were adjusted to 20 % (v/v) glycerol (sterile), aliquoted to 500 µL, frozen in liquid nitrogen and stored at -80 °C.

5.2 Biochemical Methods

5.2.1 Standard SDS-PAGE

Sodium dodecyl sulphate polyacrylamid gel electrophoresis (SDS-PAGE) is used to separate proteins according to their size. SDS treatment of the samples dissociates non-covalent protein complexes into single subunits. Reducing agents like DTT are necessary to break disulphide bonds. Hence the structure of the protein is destroyed and polypeptide chains are unwound to filaments. As proteins associate with anionic SDS, the intrinsic charge of the protein is overcome producing identical mass/charge ratios and uniform ellipsoidal forms. In the electrical field, polyanions are separated according to their molecular mass by the meshes of the polyacrylamide gel.

After assembling the gel block the ingredients are mixed in a ration shown in the table below. The polymerisation reaction is started with 10 % (w/v) ammonium peroxidsulphate (APS; radical initialiser) and TEMED (radical stabiliser).

	5 %	10 %	15 %
30 % acrylamid	7 mL	24 mL	29 mL
collecting gel buffer	5 mL	-	-
separating gel buffer	-	18 mL	18 mL
dH ₂ O	28 mL	30 mL	25 mL
APS	320 µL	470 µL	470 µL
TEMED	32 µL	40 µL	40 µL

After pouring the separation gel a layer of isopropanol is applied onto the surface, to get a sharp clear boundary between the separation and collecting gel. After 10 minutes of polymerisation, the isopropanol is removed and the collecting gel is poured in the same manner. One comb per gel for the sample application was inserted before polymerisation. Wetted minigels can be stored for up to two weeks at 4 °C without effects on the resolution. Before electrophoresis the proteins were dissolved in 5 x sample buffer supplemented with 40 mM DTT prior to usage. The soluble Mdl1p-NBD was incubated for 5 minutes at 95 °C and full-length Mdl1p as well as membrane protein fractions were incubated for 15 minutes at room temperature. SDS electrophoresis was performed at 120 V in the collecting gel and for 45 - 60 minutes at 200 V in the separation gel at room temperature in a vertical flat bed apparatus with a plate size of 120 mm x 80 mm and a gel thickness of 0.75 mm. For molecular mass calibration 5 – 8 µL of protein standard (s. chapter 4.4) was used.

5.2.2 Tricine SDS-PAGE

After the assembling of a mid-size gel (16 x 8 cm², e.g. from BioRad), the stacking, spacer and separation gel solution are prepared according to the table below except for APS and TEMED which are only added directly before usage. After the separation gel is poured, it is directly overlaid with ~ 2.5 cm of the spacer gel. To ensure that the separation gel polymerises before the spacer gel a excess of APS and TEMED is added. The spacer gel is covered by

isopropanol during the polymerisation process. After termination of the polymerisation and the removal of the isopropanol, the stacking gel (~ 1.5 cm) is poured. The samples run overnight at either 80 V or 18 mA as limiting parameters.

	4 % stacking gel	10 % spacer gel	16.5 % separation gel
acrylamide	2.5 mL	6 mL	10 mL
3 x gel buffer	7.5 mL	10 mL	10 mL
glycerol			4 mL
dH ₂ O	20 mL	14 mL	6 mL
10 % (w/v) APS	250 µL	100 µL	150 µL
TEMED	25 µL	10 µL	15 µL

5.2.3 Blue Native-PAGE

A gradient maker with a pump is used to pour a 16.5 % to 6 % gradient gel and a Hoeffer gel system is employed. Gels are poured the day prior to use and stored at 4 °C. Before loading the gel, samples are centrifuged (20.400 x g; 15 min; 4 °C) and 5 µL loading dye is added to 45 µL sample. Cathode buffer (with Coomassie blue G) is gently overlaid on top of the samples and electrophoresis is as follows:

The run was performed at 100 V in the stacking gel and 500 V in the gradient gel (total electrophoresis time about 5 hours). The gel temperature was kept at 4 °C using a cooling water pump and magnetic stirrer. The cathode buffer is replaced by fresh cathode buffer without dye after the running front with Coomassie blue G has made its way through the gel. The electrophoresis run is complete just prior to exit of the blue front from the gel into the anode buffer. After documentation the proteins are transferred from the gel to a nitrocellulose membrane (s. chapter 5.2.5).

6 % running gel	16.5 % running gel	Stacking gel
3 mL gel buffer (3 x)	3 mL gel buffer (3 x)	2.5 mL gel buffer (3 x)
1.07 mL acrylamide (49.5 % T, 3 % C)	3.05 mL acrylamide (49.5 % T, 3 % C)	0.6 mL acrylamide (49.5 % T, 3 % C)
	1.8 mL glycerol	
38 µL APS (10 % (w/v))	30 µL APS (10 % (w/v))	30 µL APS (10 % (w/v))
3.8 µL TEMED	3 µL TEMED	3 µL TEMED
add dH ₂ O to 9 mL	add dH ₂ O to 9 mL	add dH ₂ O to 7.5 mL

5.2.4 Coomassie and silver staining

After electrophoretic separation of proteins via SDS-PAGE, the bands were fixed with acetic acid and stained by incubating the gel for 15 minutes in a solution of Coomassie brilliant blue. Excessive dye was removed with a mixture of acetic acid and methanol until distinct protein bands were visible.

Silver staining is up to 100-fold more sensitive than Coomassie staining and can detect less than 10 ng protein. After fixation of the protein bands with acetic acid, contaminations are reduced with Na₂S₂O₃. Rinsing the gel with water removes excess of Na₂S₂O₃ which would

otherwise react with the silver reagent to form black silver sulphide. In the next step, the protein (functional groups and peptide bonds) reduces silver ions to silver nuclei. Harsh reductive agents like formaldehyde initiate reduction of all silver ions in the gel, but the silver nuclei dominate in growth and stain the protein bands black. The reaction is terminated by shifting the pH with acetic acid.

For silver staining, the gel is incubated for 15 minutes in 50 mL fixation solution. In the next step the gel is shaken for 15 minutes in 50 mL thiosulphate buffer. Afterwards the gel is rinsed with water (4 x 5 min). For staining it is incubated for 30 minutes in 50 mL silver nitrate solution. After rinsing the gel with water the developing solution (100 mL) is added stepwise (2 x 20 mL, 1 x 60 mL) to enhance the contrast. The development of the gel is stopped with 1 mL acetic acid. Prior to scanning the gel is incubated for 5 minutes in water.

5.2.5 Transfer of proteins to nitrocellulose membranes

The transfer of proteins from a SDS gel to a nitrocellulose membrane with subsequent immunodetection is termed “Western Blotting”. The principles were described by (Renart et al., 1979; Towbin et al., 1979). After separation of proteins by SDS-PAGE, they are blotted onto a membrane via electrotransfer. During electroblotting (Tankblotting, Semidry-Blotting) the SDS is removed from the protein due to different migration behaviour. The protein adheres to the membrane through hydrophobic interactions.

Finally, the immunodetection is carried out by adding the first antibody against the blotted protein (antigen) followed by an antibody coupled to a reporter system like HRP. The enzyme catalyses the oxidation of luminol and the emitted chemiluminescence is enhanced by coumaric acid.

The principle setup of the apparatus is depicted in Figure 5.1. The gel is placed on a nitrocellulose membrane with dimensions of 10 cm x 7 cm and sandwiched by Whatmann paper soaked in blotting buffer. The sandwich is transferred to a Semidry apparatus from Bio-RAD with the nitrocellulose membrane facing the anode. The transfer runs for 1 hour with a current of 1,43 mA/cm².

Alternatively, the blotting buffer soaked sandwich is placed in a tank blot apparatus (Bio-Rad) in which the transfer of proteins takes place overnight at 18 V. To determine whether the proteins were transferred to the same extend, the membrane was stained with Ponceau Red (0.1 % Ponceau Red S (w/v), 5 % (v/v) acetic acid) for 5 minutes, and washed with water until defined bands become visible.

For immunodetection the membrane was incubated with blocking buffer for at least 30 minutes at room temperature or overnight at 4 °C. After blocking the membrane was incubated at room temperature for at least 1 hour with the primary antibody against Mdl1p which was diluted 1 : 500 in TBS-T (1 x TBS supplemented with 2 % Tween-20) completed with 2 % (w/v) skim milk powder. After three times washing with wash buffer for 5 minutes, the

membrane was incubated with horseradish peroxidase conjugated second antibodies in an appropriate dilution for an hour.

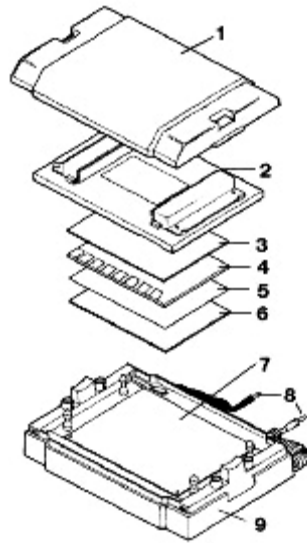


Figure 5.1: View of a Trans-Blot SD cell. 1: lid; 2: cathode; 3, 6: filter paper; 4: gel; 5: membrane; 7: anode; 8: power cables; 9: base.

Subsequently, the membrane was washed again three times and incubated with 10 mL ECL solution 1 for 5 minutes followed by 10 mL ECL solution 2 for 30 seconds. The chemiluminescent signal was detected by a LumImager. Alternatively, the ECL-system from GE Healthcare was used and the light reaction was detected by a photographic film.

5.2.6 Purification of the Mdl1p-NBD

The cloning of the NBD was done by Dr. Eva Janas, Institute of Biochemistry Goethe-University Frankfurt and is described in (Janas et al., 2003). Briefly, the NBD-fragment was amplified by PCR on genomic DNA of *S. cerevisiae*. The resulting PCR fragment was purified and cloned into the *Bam*HI and *Hind*III sites of pET28b resulting in plasmid pMDL1p-NBD (chapter 4.5). Expression was controlled by the vector derived *T7* promoter. The recombinant plasmid includes the expression cassette with an N-terminal His₍₆₎-tag, a thrombin cleavage site and a T7-tag encoded by the vector (Figure 5.2).

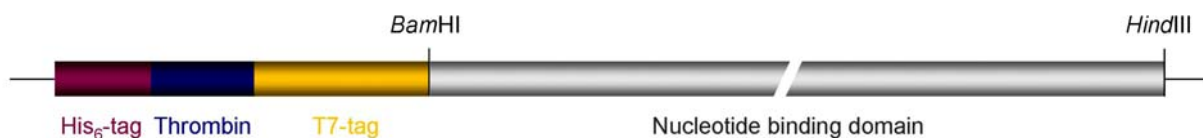


Figure 5.2: Schematic representation of the Mdl1p-NBD expression cassette. The cassette includes the vector derived His₍₆₎-tag (purple), a thrombin cleavage site (blue) and a T7-tag (yellow) on the N-terminus of the NBD (grey).

A conserved glutamate (E599, GAA) located one amino acid downstream of the Walker B motif was changed to glutamine (\rightarrow CAA) resulting in the plasmid pMDL1p-NBD(E599Q).

E. coli strain BL21(DE3) was transformed with the plasmids and grown in LB medium with 50 µg/mL kanamycin at 30 °C. At an OD₆₀₀ of 0.5 the cells were induced with 0.2 mM IPTG, and after 3 hours the cells were harvested by centrifugation.

To purify the NBD with the His₍₆₎-tag ‘immobilised metal-ion affinity chromatography’ (IMAC) was applied. This method is used to separate His-tagged biomolecules via complex formation from the rest of low affine or non-binders. The column material consists of agarose modified with iminodiacetate. After loading with Ni²⁺, a complex is formed with molecules, e.g. proteins, bearing a five or more times histidine repeat. The binding specificity is enhanced in the presence of low concentrations of imidazole, which competes with histidines for metal binding sites. His-tagged proteins are eluted in the order of increasing complex stability with an imidazole gradient.

All buffers for chromatographic purposes were sterile filtered and degassed before use. Cells were pelleted and resuspended in lysis buffer (10 mM Na₂HPO₄/NaH₂PO₄, pH 7.6, 150 mM NaCl, 5 mM KCl, 20 mM imidazole, 1 mM PMSF) containing 1 % lysozyme, and 5 - 10 U benzonase and disrupted by French press treatment at 1,000 p.s.i. After centrifugation (100,000 x g; 1 h; 4 °C) the supernatant was applied via an Äkta explorer on a 5 mL HiTrap Chelating HP Ni-IDA column loaded with a Nickel sulphate solution (100 mM) and preequilibrated with running buffer (10 mM Na₂HPO₄/NaH₂PO₄, pH 7.6, 150 mM NaCl, 5 mM KCl, 20 mM imidazole). The chromatographic process was monitored by recording protein absorption at 280, 260 and 216 nm. After washing the column with a step gradient of 80 mM and 100 mM imidazole, the protein is eluted with elution buffer (10 mM Na₂HPO₄/NaH₂PO₄, pH 7.6, 150 mM NaCl, 5 mM KCl, 250 mM imidazole).

Further purification of the protein was achieved by a size exclusion chromatography (SEC) step to separate the NBD from contaminating proteins and high molecular aggregates. Selected fractions from the IMAC containing the NBD were combined, concentrated via Amicon Ultra centrifugal filter device (MWCO 10,000 Da) and applied to a superdex 200 16/60 HiLoad size exclusion chromatography column preequilibrated in size exclusion buffer (20 mM Tris-HCl, pH 8; 100 mM NaCl).

The size exclusion chromatography separates molecules according to their molecular mass due to different permeation of analytes in a porous matrix. High molecular weight compounds are hindered from entering the matrix and elute in the void volume with the solvent. Low molecular weight substances move according to their size in the internal pore volume. Thus they are retained on the column and eluted within a characteristic elution volume.

For column calibration a solution containing 0.5 % (w/v) each of aldolase (158 kDa), catalase (232 kDa) and thyroglobulin (669 kDa) in phosphate buffer were analysed after filtration. For each standard substance the logarithm of its molecular mass was plotted against the elution volume.

The NBD eluted with an apparent molecular weight of 33 kDa corresponding to the size of the monomer. Peak fractions of monomeric NBD were combined and concentrated up to 10 mg/mL in an Amicon Ultra centrifugal filter device (MWCO 10,000 Da) and stored in the presence or absence of 5 mM ATP at 4 °C. The addition of ATP was figured out to have a positive effect on the stability of the NBD since almost no precipitation after several days of storage was observable. Wild-type and mutant proteins were purified to greater than 99 % homogeneity as assessed by Coomassie stained protein on SDS-PAGE and MALDI-TOF.

5.2.7 Dimerisation Assay

For several mutants of ABC transporter NBDs e.g. MJ0796(E171Q), MJ1267(E179Q) (Moody et al., 2002) or GlcV(E166Q) (Verdon et al., 2003b) it was reported that a specific dimerisation occurs upon addition of ATP. This effect was used to examine the oligomeric state of the Mdl1p-NBD in more detail.

Before use, ortho-vanadate stock solution adjusted to pH 8.0 was boiled for five minutes to break polymeric species. Before use, beryllium fluoride solution was prepared by mixing BeCl₂ and NaF in a ratio of 1 : 100 (mol/mol). For non-radioactive assays, purified wild-type NBD (30 µM) was incubated with different concentrations of beryllium fluoride (BeF_x) or ortho-vanadate in the presence or absence of nucleotides and nucleotide analogues for five minutes at 30 °C in binding buffer. The mutant NBD (E599Q, 30 µM) was incubated for 5 minutes in the absence of Mg²⁺ and on ice (non-hydrolysing conditions) or in the presence of 5 mM Mg²⁺ and at 30 °C (hydrolysing conditions) with different concentrations of nucleotides and nucleotide analogues. The samples were applied to a Superdex 75 PC 3.2 size exclusion chromatography column at a flow rate of 50 µL per minute at 4 °C in 20 mM, Tris pH 8.0, 150 mM NaCl, and 5 mM MgCl₂ as indicated.

5.2.8 Determination of the Nucleotide Stoichiometry

In this method, ATP is hydrolysed and the resulting ADP is captured *in situ*, via interaction with beryllium-fluoride or ortho-vanadate, that mimic different stages in hydrolysis, the pre hydrolysis state (BeF_x) and the transition state (VO₄) (Fisher et al., 1995; Smith and Rayment, 1996).

Radioactive trapping experiments were performed in the same buffer as non-radioactive trapping experiments and separated by size exclusion chromatography. Fractions were analysed by β-counting, thin layer chromatography and for protein concentration by the BCA assay. Over the range of protein concentrations used, the absorption at 280 nm measured with the UV detector of the SMART system was linearly related to the protein concentration determined by the BCA assay. In particular, wild-type NBD (250 µM) was incubated with 500 µM MgATP supplemented with 0.1 µM of either [α-³²P]ATP or [γ-³²P]ATP (4,500 Ci/mmol) in the presence of BeF_x (500 µM) for 5 minutes at 30 °C. The E599Q mutant (250 µM) was incubated for 5 minutes in the absence of Mg²⁺ and on ice. To follow one to two turn-overs of

the E599Q mutant, 250 μM NBD were incubated for prolonged time periods (0 – 500 min) at 30 °C with limiting concentration of MgATP (250 – 500 μM) and tracer amounts of radioactive ATP. To test whether ADP is incorporated in the dimer at a high ADP concentration, the E599Q mutant was incubated with 500 μM ADP and 0.1 μM [α - ^{32}P]ADP in the presence of various concentration of unlabeled ATP (0, 5, 50, 100 and 500 μM) for 10 minutes at 30 °C. Alternatively, incorporation of ADP under limiting concentrations of MgATP was tested by incubation of the E599Q mutant (250 μM) with MgATP (250 – 500 μM) supplemented with tracer amounts of [α - ^{32}P]ADP at 30 °C for 400 minutes. The [α - ^{32}P]ADP was formed by incubation of [α - ^{32}P]ATP with hexokinase according to the manufacturers instructions and separated from hexokinase by Centricon 10 centrifugation. Full conversion to [α - ^{32}P]ADP was confirmed by thin layer chromatography.

In a similar approach, the nucleotide content in full-length Mdl1p was assayed. H631A-mutant Mdl1p (50 $\mu\text{g}/\text{mL}$) was incubated with 4.82 mM ATP supplemented with 0.062 μM [γ - ^{32}P]ATP for 5 minutes at 4 °C. The sample was applied to a Superdex 200 size exclusion chromatography column and fractions were analysed in respect of their nucleotide by β -counting and protein content using the Bradford assay.

5.2.9 Thin layer chromatography (TLC)

The nucleotide composition of the dimer was analysed by TLC according to (Scheffers et al., 2000). Immediately after size exclusion chromatography the fraction containing the NBD-dimer was incubated with 15 mM EDTA for 30 minutes and precipitated with trichloroacetic acid (10 % w/v) for 30 minutes at 4 °C. After centrifugation at 20,400 x g for 5 minutes, the sample was neutralised with 0.5 M KHCO_3 , pH 8.3 and applied onto polyethylenimine (PEI) cellulose plates in 2 M formate and 250 mM LiCl. [α - ^{32}P]ATP and [γ - ^{32}P]ATP treated with hexokinase were used as references.

5.2.10 Nucleotide binding assays

Nucleotide binding was measured by 8-azido-[α - ^{32}P]ATP photocross-linking experiments as described in (Wolters et al., 2005). Purified Mdl1p (0.5 μM) was incubated with increasing concentrations of 8-azido-[α - ^{32}P]ATP for 5 minutes on ice and then irradiated with UV light for 5 minutes. For concentrations of 10 μM and above, 8-azido-[α - ^{32}P]ATP was supplemented 1:5 (mol/mol) with non-radioactive 8-azido-ATP. Subsequently, samples were analysed by SDS-PAGE (10 %). Gels were dried and exposed to a Kodak SO230 phosphor screen. Photocross-linked protein was quantified by phosphor-imaging. The intensities (I) were plotted against the 8-azido-ATP concentration and fitted with a 1:1 Langmuir binding isotherm. To determine the half maximal inhibitory concentration (IC_{50}) for ATP, equation 5.1 was used (where bg displays background intensity).

$$I = \frac{I_{\max}}{I + \left(\frac{[N_3 - ATP]}{IC_{50}} \right)^{\text{slope}}} + bg \quad (\text{eq 5.1})$$

Applying the Cheng-Prusoff equation (Cheng and Prusoff, 1973), the dissociation constant K_D for ATP was derived from the IC_{50} value for ATP and the K_D value for 8-azido-ATP as shown in equation 5.2.

$$K_{D(ATP)} = \frac{IC_{50}}{I + \frac{[N_3 - ATP]}{K_{D(N_3 - ATP)}}} \quad (\text{eq 5.2})$$

5.2.11 Isolation of yeast mitochondria

The mitochondria were isolated according to (Meisinger et al., 2000). Cells were harvested by centrifugation (5,800 x g; 12 min; RT), washed once with distilled water, resuspended with 2 mL/g of wet weight cells in DTT buffer and incubated for 20 minutes at 30 °C under gentle shaking. The preincubation with DDT facilitates the break of disulphide bonds preparing the subsequent digestion of the cell wall by lyticase. After centrifugation (1,600 x g; 8 min; RT) the cell pellet was washed once with 1.2 M sorbitol in order to remove DTT traces. The cell pellet is resuspended in lyticase buffer at 7 mL/g wet weight cells. 4 mg lyticase per g wet weight of cells were added and the suspension was incubated at 30 °C with gentle shaking for 45 minutes. Conversion of spheroplasts was checked measuring the OD₆₀₀ of a 1 : 100 dilution (in dH₂O) which decreases over time. Spheroplasts were harvested by centrifugation (1,600 x g; 8 min; 4°C) and washed very carefully in lyticase buffer without lyticase. Afterwards the spheroplasts were resuspended in 7 mL/g wet weight of cells in homogenisation buffer and lysed by homogenisation with a tight fitting douncer (15 strokes) at 4 °C. The homogenate was centrifuged (700 x g; 10 min; 4 °C) to remove non-lysed spheroplasts and cell debris. An additional clearing step is made (1,250 x g; 8 min; 4 °C) and the mitochondria were harvested with a high speed centrifugation step (11,250 x g; 15 min; 4 °C). The pellet was carefully washed with 5 mL SEM buffer and centrifuged (11,250 x g; 15 min; 4 °C) again. The crude mitochondria pellet was resuspend in SEM buffer to a final protein concentration of 10 mg/mL, aliquoted, shock frozen with liquid nitrogen and stored at -80°C.

The protocol described above provides a crude mitochondria preparation that contains significant amounts of non-mitochondrial proteins, especially derived from the endoplasmic reticulum. Many applications, however, require a clear separation of mitochondria from microsomes. Therefore, a purification protocol using a sucrose density gradient was applied. The crude mitochondria fraction was loaded onto a three step sucrose gradient (1.5 mL 60 %, 4 mL 32 %, 1.5 mL 23 %, 1.5 mL 15 % sucrose in 20 mM HEPES, pH 7.2). After centrifugation (76,000 x g, 3 h, 4 °C) in a SW 28 swinging-out rotor the purified mitochondria were recovered from the 60 %/32 % interface.

5.2.12 Tandem Affinity Purification

The tandem affinity purification (TAP) tag consists of a calmodulin binding peptide, a TEV cleavage site and two IgG binding domains of *Staphylococcus aureus* protein A (Figure 5.3).

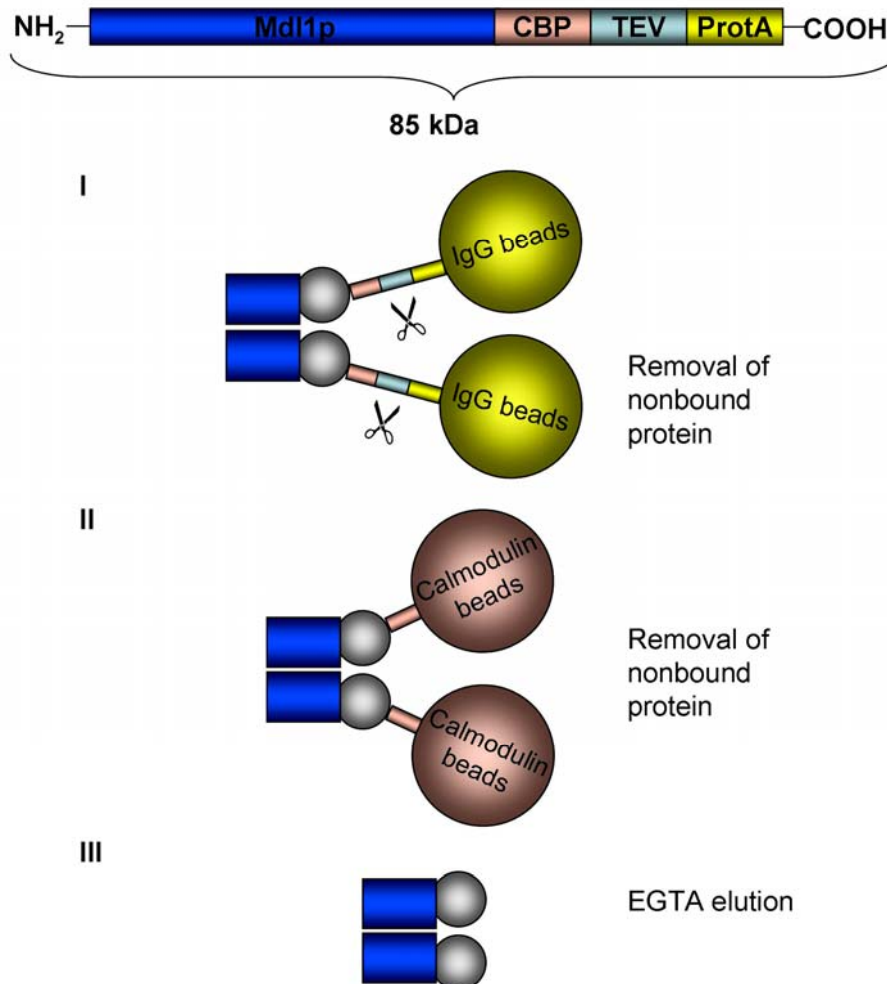


Bild 5.3: Schematic representation of Mdl1p with a C-terminal TAP tag. Overview of the TAP purification strategy: After solubilisation the TAP tagged protein binds to IgG-sepharose beads via its protein A portion and is specifically eluted by TEV cleavage. The second purification step uses the high affinity of a calmodulin binding peptide to calmodulin sepharose beads. After the binding step and stringent washing the protein is eluted by addition of EGTA.

S. cerevisiae strain YLR188W where Mdl1p is fused to a C-terminal TAP-tag was grown in YEPD medium to an OD₆₀₀ of 1.5 and mitochondria were prepared. For tandem affinity purification of Mdl1p a modified protocol according to (Rigaut et al., 1999) was used. 750 µg mitochondria were pelleted (20,400 x g; 5 min; 4 °C) and resuspended in solubilisation buffer (20 mM Tris-HCl, pH 8; 150 mM NaCl; 20 % glycerol (w/v)) supplemented with 1.6 % (v/v) Triton X-100 and complete protease inhibitor and solubilised for 30 minutes on ice. Soluble and insoluble fractions were separated (190,000 x g; 20 min; 4 °C) and the supernatant was diluted 1 : 2 with solubilisation buffer in order to lower the Triton X-100 concentration. 50 µL of IgG-beads were washed 3 x with solubilisation buffer and the diluted sample was added to allow binding for 2 hours at 4 °C under gentle rotation. Beads were sedimented by gravity and

washed 3 x with 175 μ L solubilisation buffer supplemented with 0.2 % (v/v) Triton X-100, 1mM DTT and 0.5 mM EDTA. Protein was eluted by TEV cleavage.

Therefore, the beads with bound protein were incubated with 20 units TEV protease for 1 to 4 hours. Afterwards the supernatant was separated from the beads and used for electrophoretic analysis and immunodetection.

In an alternative approach the supernatant was adjusted to 10 mM β -mercaptoethanol, 1 mM Mg-acetate, 1 mM imidazole and 2 mM CaCl_2 after ultracentrifugation and added to 50 μ L prewashed calmodulin beads. Binding was performed for 1 hours at 4°C. Beads were sedimented by gravity and washed 3 x with buffer C. Protein was eluted 3 x with 50 μ L of buffer E (10 mM β -mercaptoethanol; 10 mM Tris-HCl, pH 8.0; 150 mM NaCl; 1 mM Mg-acetate; 1 mM imidazole; 2 mM EGTA; 0.2 % Triton X-100).

5.2.13 *In organello* translation

The translation of mitochondrial encoded proteins was modified according to a protocol from (McKee et al., 1984) with isolated mitochondria. 100 μ L of 1.5 x translation buffer (0.9 M sorbitol; 22.5 mM KP_i buffer pH 7.2; 30 mM Tris-HCl, pH 7.4; 225 mM KCl; 19 mM MgSO_4 ; 6 mM ATP; 0.75 mM GTP; 2 mM NADH; 7.5 mM α -ketoglutarate; 7.5 mM phosphoenolpyruvate; 150 μ M of all amino acids except methionine; 4.5 mg/mL BSA (fatty acid free)) was mixed with 33 μ L H_2O and 2 μ L pyruvate kinase (2 mg/mL) and 10 μ L mitochondrial suspension (10 μ g/ μ L). The whole mix was incubated for 3 minutes at 30 °C. Subsequently 5 μ L [^{35}S]-methionine was added and the mixture was incubated for an additional 20 minutes. The chase was stopped upon addition of 38 μ L 0,2 M unlabeled methionine. The sample was centrifuged for 5 minutes at 9,000 x g (4 °C) and the pellet was washed two times with 500 μ L SHKCL buffer (50 mM HEPES-KOH, pH 7.4; 0.6 M sorbitol; 80 mM KCl) plus 5 mM methionine.

5.2.14 Monitoring peptide export from mitochondria

The assay was basically performed as described by (Augustin et al., 2005). Purified mitochondria were resuspended in translation buffer (0.6 M sorbitol; 15 mM KP_i buffer pH 7,2; 20 mM Tris-HCl, pH 7.4; 150 mM KCl; 12.5 mM MgSO_4 ; 4 mM ATP; 0.5 mM GTP; 1.25 mM NADH; 5 mM α -ketoglutarate; 5 mM phosphoenolpyruvate; 100 μ M of all amino acids except methionine; 3 mg/mL BSA (fatty acid free). After two additional washing steps using 1 mL of SHKCl buffer, mitochondria were incubated in translation buffer lacking pyruvate kinase at a concentration of 10 mg/mL for 30 minutes at 37 °C to allow proteolysis to occur. Samples were separated into supernatant and pellet fractions by centrifugation (16,100 x g; 4 min; 4 °C). Mitochondrial supernatants (50 μ L) were subjected to size exclusion chromatography at 12 °C using a Superdex peptide column (PC 3.2/30) (equilibrated in 40 % (v/v) acetonitrile, 0.1 % (v/v) trifluoroacetic acid).

5.2.15 Detergent screening

To test the solubilisation efficiencies of different detergents, mitochondria (5 mg/mL) were solubilised for 30 minutes in buffer S (50 mM Tris-HCl, pH 8.0; 150 mM NaCl; 15 % (v/v) glycerol; 2 mM imidazole) with DDM, FC-14 and digitonin in concentrations defined by a ρ -value of 15 and 50 respectively (eq. 5.3; where [lipid] is 0.1 times the protein concentration and the average molecular weight of a lipid was taken as 875 Da).

$$\rho = \frac{[\text{detergent}] - \text{CMC}}{[\text{lipid}]} \quad (\text{eq. 5.3})$$

Fractions were separated by centrifugation (100,000 x g, 4 °C, 30 min) and soluble/insoluble Mdl1p was compared by Western blotting using an anti-Mdl1p antibody.

5.2.16 Purification of full-length Mdl1p

Cloning of the full-length *MDL1* expression vectors pYES2.1/V5-His-TOPO-Mdl1fl, pYES2.1/V5-His-TOPO-Mdl1fl_EQ and pYES2.1/V5-His-TOPO-Mdl1fl_HA was done by S. Gompf, C. Presenti and C. van der Does, Institute of Biochemistry, University Frankfurt and described in (Hofacker et al., 2006). By introducing several new restriction sites, the *MDL1*-gene was systematically divided into three cassettes, thus facilitating later exchange between different constructs. *MDL1* cassettes were amplified by PCR on genomic DNA of *S. cerevisiae*. Cassette I includes the N-terminus of Mdl1p until a silent *ClaI* site introduced between amino acid A220 and S221. Cassette II includes the middle domain of Mdl1p from the introduced *ClaI* site, to an intrinsic and unique *BamHI* site comprising amino acids S221 to D423. Cassette III includes the C-terminal NBD from amino acid P424 to V695.

To generate the yeast over-expression vector, the *MDL1*-gene was amplified by PCR and cloned into pYES2.1/V5-His-TOPO via the TOPO TA Expression cloning kit. This resulted in a construct expressing Mdl1p with a C-terminal Gly₍₄₎-spacer, a factor X_a cleavage site and a His₍₈₎-tag via the galactose inducible promoter of pYES2.1 (Figure 5.4).

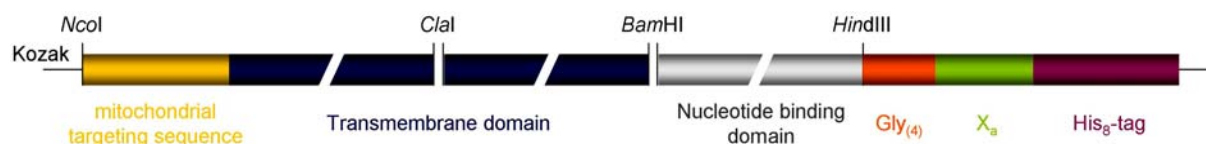


Figure 5.4. Schematic representation of the Mdl1p full-length expression cassette. The cassette includes a newly introduced Kozak sequence, the mitochondrial targeting sequence (yellow), the transmembrane domain (blue) which is split up into two parts, the nucleotide binding domain (grey), a glycine spacer (orange) and a factor X_a-cleavage site (green). The His₍₈₎-tag (purple) lies on the 3'-end of the construct.

Mitochondria (5 mg/mL) were solubilised in buffer S supplemented with 1 % (w/v) - corresponding to a ρ -value of 15 - digitonin and complete protease inhibitor cocktail (EDTA free) for 30 minutes at 4 °C under gentle shaking. Soluble and insoluble fractions were separated by centrifugation (100,000 x g, 4 °C, 30 min) and the supernatant was applied to a HiTrap chelating IDA-column loaded with Ni²⁺ and equilibrated with IMAC buffer (50 mM Tris-

HCl, pH 8.0; 150 mM NaCl; 15 % (v/v) glycerol; 2 mM imidazole; 0.1 % digitonin). The column was washed with 60 and 120 mM imidazole and finally Mdl1p was eluted in IMAC buffer containing 200 mM imidazole. The identity of the purified protein was confirmed by western blotting and MALDI-TOF peptide mass fingerprint (PMF) analysis of the trypsin digested protein using Mascot (database NCBI nr 20040521) as reference.

For N-terminal amino acid sequencing (Edman degradation) the protein was subjected to a 10 % SDS-PAGE and subsequently transferred to a PVDF membrane. The membrane was Coomassie stained, welded in an autoclave bag and submitted for external sequencing (Biotechnology Laboratory University of British Columbia, Canada)

5.2.17 ATP hydrolysis assays

The ATPase activity of the full-length Mdl1p was determined essentially as described in (Gorbulev et al., 2001). 25 μ L of ATP buffer A (50 mM Tris-HCl, pH 8; 150 mM NaCl; 10 mM DTT; 20 mM MgCl₂) with varying concentrations of ATP supplemented with [γ -³²P]ATP (4 μ Ci) and 0.02 % (w/v) FC-14, 0.02 % (w/v) DDM or 0.1 % (w/v) digitonin was mixed with 25 μ L of detergent solubilised protein and incubated for 10 minutes at 30 °C. The reaction was stopped by addition of 1 mL of reagent A (2.5 M H₂SO₄, 1 % (w/v) ammonium molybdate, 15 μ L of 20 mM H₃PO₄). 2 mL of reagent B (isobutanol, cyclohexane, acetone and reagent A in a ratio of 5:5:1:0.1) were added and the sample was vortexed vigorously for 30 seconds. After phase separation, 1 mL of the organic phase was mixed with scintillation fluid and the release of inorganic phosphate was determined by β -counting. Maximal velocity of the reaction v_{max} and the Michaelis constant K_M were derived by fitting the data to the Michaelis-Menten equation (eq. 5.4; where [S] reflects the substrate concentration):

$$v = \frac{v_{max} \cdot [S]}{K_M + [S]} \quad (\text{eq 5.4})$$

To see whether ATP hydrolysis shows a cooperative behaviour in respect of the ATP concentration the Hill coefficient was determined using equation 5.5.

$$y = \frac{ax^n}{(b^n + x^n)} \quad (\text{eq 5.5})$$

A similar protocol, using 25 μ L of 0.4 mg/mL proteoliposomes was used to determine the ATPase activity of reconstituted Mdl1p.

5.2.18 Reconstitution of Mdl1p

E. coli lipids were suspended in buffer R (50 mM Tris-HCl, pH 7; 25 mM KCl) at a concentration of 4 mg/mL. The lipid suspension was extruded 11 times through a 400 nm polycarbonate filter. The liposome suspension was then titrated to a final DDM concentration of 4.2 mM and mixed in a lipid to protein ratio of 200 : 1 (mol/mol) with detergent solubilised

Mdl1p. Polystyrene beads (Bio-beads SM-2) were washed three times with methanol, five times with buffer R and incubated in a suspension of *E. coli* lipids. After incubation for 30 minutes at room temperature, polystyrene beads were added to a final concentration of 80 mg/mL, and the mixture was incubated overnight at 4 °C. Fresh Bio-beads (80 mg/mL) were added and an additional incubation was performed for 60 minutes at 4 °C. After removal of Bio-beads, proteoliposomes were pelleted by centrifugation (190,000 x g, 1 h, 4 °C), resuspended in buffer R, applied to a sucrose step gradient (10, 20, and 30 % (w/v)); centrifuged (100,000 x g; 18 h; 4 °C) and different fractions were collected. The sucrose concentration of each fraction was determined by an Abbé refractometer while the protein concentrations were determined by quantitative immunodetection using solubilised Mdl1p as reference.

5.2.19 Phospholipid concentration determination

The lipid concentration was determined essentially as described (Chen et al., 1956). Samples of 10-100 µL were mixed with an equal volume of 70 % (v/v) perchloric acid and after drying the samples for 2 hours at 200 °C, 700 µL reagent C (2.5 % (w/v) ammonium molybdate, 12.5 % perchloric acid) and 700 µL 3 % (w/v) ascorbic acid was added. Finally, the samples were incubated for 5 minutes at 100 °C and absorbance at 820 nm was measured and compared to a phosphate standard.

5.2.20 Freeze-fracture electron microscopy of reconstituted Mdl1p

Freeze-fracture electron microscopy of reconstituted Mdl1p was done in collaboration with Dr. Winfried Haase in the department of Prof. Dr. Werner Kühlbrandt from the Max-Planck-Institute of Biophysics Frankfurt. A drop from a suspension of reconstituted membrane vesicles was placed between two small copper blades and rapidly frozen in ethane cooled to -180 °C. Samples were fractured in a freeze-fracture unit 400T and shadowed with platinum/carbon at an angle of 45°. Replicas reinforced by pure carbon shadowing at an angle of 90° were cleaned from organic material in chromo-sulphuric acid and analyzed by electron microscopy in an EM208S electron microscope. Images were taken with a TVIPS 1Kx1K slow-scan CCD camera.

5.2.21 Peptide photocross-linking and detection

To elucidate the role of Mdl1p in peptide transport peptide cross-linking experiments were performed. As control samples microsomes prepared from Sf9 insect cells containing the TAP peptide transporter were used (kindly provided by Dr. Min Chen).

An approach according to (Uebel et al., 1997) was chosen and the following peptides were selected: R9* (NH₂-RΦYQΨSTEL-COOH, Figure 5.5) with the cross-linker function trifluoromethyl-diazirine-phenylalanine on position 2 and the peptide T10 (f-MYQR-Bpa-LYST-COOH) with the cross-linker 4-benzoyl-L-phenylalanyl (Bpa) in position 5.

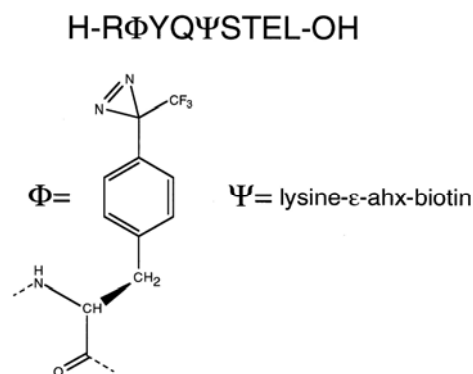


Figure 5.5: The photoactivatable peptide R9* which was used for cross-linking experiments to elucidate the role of Mdl1p in peptide transport (Uebel et al., 1997).

T10 was designed according to findings that formylated peptides were found in complex with class I major histocompatibility molecules at the surface of mammalian cells as so called minor antigens derived from mitochondrial encoded respiratory chain subunits e. g. subunit I of cytochrome c oxidase. The original sequence of Cox1p from *S. cerevisiae* (MVQRWLYS TNAK) was modified to meet the requirements of photocross-linking hence tryptophane in position 5 was exchanged for Bpa and valine in position 3 was interchanged with tyrosine in order to label the peptide with Na¹²⁵I.

The photocross-linker peptides were labelled with Na¹²⁵I (see 5.2.22) and added to 12.5 μ g microsomes to reach a final concentration of 4 μ M. The same peptide concentration was used for experiments using mitochondria prepared from *S. cerevisiae* strains expressing either no Mdl1p or Mdl1p under different conditions. 75 μ g mitochondria were solubilised in SEM buffer containing 0.8 % Triton X-100 for 10 minutes. Peptide binding was allowed for 3 minutes in ice-cooled aluminium devices and UV irradiation was performed for 10 minutes at 350 nm with a UV lamp. In a second set cross-linker peptides were competed out by using a 100-fold excess of non-labelled R9 (without the cross-linker function) or T10. Samples were incubated with 1 x loading buffer for 10 minutes at 65 °C and subjected to a 10 % SDS-PAGE. The gel was exposed to a Biomax x-ray film after drying and the autoradiography was developed after 48 hours using an automated film developer machine.

5.2.22 Peptide iodination

Iodination of peptide libraries and peptide transport was performed essentially as described in (Chen et al., 2003b) and (Hunter and Greenwood, 1964). Chloramine T solution (1 mg/mL) and sodium bisulfite (0.17 mg/mL) were freshly prepared in PBS, pH 7.0. The reaction was routinely performed with 1.5 nmol peptide in a total volume of 50 μ L and 1 μ L (100 μ Ci) Na¹²⁵I. The reaction was started by addition of 10 μ L chloramine T. After 5 minutes incubation at room temperature, the reaction was stopped by addition of 120 μ L Na₂S₂O₅ (sodium bisulphite). Free iodine was removed by anion exchange chromatography using Dowex 1 x 8 material. Dowex (10 mg) was equilibrated in PBS, pH7.0 containing 0.2 % dialysed BSA and was washed two times with PBS buffer without BSA. The Dowex suspension (220 μ L) was

added to the radiolabeled reaction mix, vortexed and incubated for 5 minutes at room temperature. The suspension was applied to an empty spin column and centrifuged for 2 minutes at 20,400 x g. The eluate contained the radiolabelled peptide in a concentration of approximately 3.75 μM .

5.2.23 Peptide transport Assay

Proteoliposomes (0.5 μg of Mdl1p) were preincubated with 4.8 mM ATP and 10 mM MgCl_2 in 50 μL of transport buffer (50 mM Tris-HCl, pH 7; 25 mM KCl; 0.1 mM DTT) for 1 minute at 30 °C. The transport reaction was started by adding ^{125}I -labeled $X_{(8)}$ and $X_{(23)}$ peptide libraries (Uebel et al., 1995) to a final concentration of 2 μM . The reaction was stopped after 6 minutes at 30 °C by addition of 500 μL ice-cold transport buffer supplemented with 10 mM EDTA and stored on ice. After centrifugation, the pellets were washed once and radioactivity was quantified by γ -counting. To determine background levels of radioactivity samples were treated with apyrase (1 unit) instead of MgATP.

5.2.24 Single Particle electron microscopy and image analysis

After IMAC preparation purified Mdl1p was concentrated (Amicon Ultra-4, MWCO 100,000 Da) to 1 mg/mL and subjected to a Superdex 200 PC 3.2 size exclusion chromatography column equilibrated with SEC-buffer (50 mM Tris-HCl, pH 8; 150 mM NaCl; 0.1 % digitonin). Peak fractions corresponding to a molecular weight of about 440 kDa (based on the soluble marker proteins β -amylase (200 kDa), apoferritin (443 kDa) and thyroglobulin (669 kDa) in 20 mM HEPES pH 7, 100 mM NaCl, 10 % (v/v) glycerol) containing Mdl1p were pooled and analysed by negative staining in an electron microscope using 2 % uranyl acetate.

Single Particle Electron Microscopy of Mdl1p was done in collaboration with Dr. Kirstin Model in the department of Prof. Dr. Werner Kühlbrandt from the Max-Planck-Institute of Biophysics Frankfurt.

EM images were recorded on film under low-dose conditions in a CM120 electron microscope. For three-dimensional reconstruction, tilt pairs were collected at 0° and 48° tilt and corresponding micrographs digitised on a Zeiss SCAI Scanner with 7 μm pixel size. Particle images were analysed using the SPIDER package (Frank et al., 1996). XMIPP software (Sorzano et al., 2004) was used for classification of untilted images based on the Kohonen neural network. The first maps were obtained from a total data set of 2 x 1404 projections by the random conical tilt method (Radermacher et al., 1987). The known pseudo two-fold symmetry of the complex was imposed. After refinement of all three Euler angles the final volume was computed.

A low-pass filtered volume of a closed MsbA form was calculated from the pdb-file with Accession number 1PF4 and the atomic structures of the PDB files 1Z2R, 1JSQ and 1PF4 were overlaid using Chimera software (Pettersen et al., 2004).

6 Results

6.1 Characterisation of the nucleotide binding domain of Mdl1p

Today's picture of how ABC transporters translocate their substrates over a membrane includes the idea of a series of conformational changes in response to ATP binding and hydrolysis of the NBDs, and binding, reorientation and release of substrate at the TMDs. Despite extensive research to obtain structural information, only little is known about intermediate states during a transport process. This work addresses the question how ATP binding and hydrolysis might influence the translocation of substrates mediated by Mdl1p. It is proposed that this half-size transporter forms a homodimer in its minimal active form. Various aspects of the mechanism how the motor domains of ABC transporters cooperate can be learned from the isolated NBDs. Therefore, the Mdl1p-NBD was cloned, purified and investigated. Different intermediate states of the NBD during an ATP binding and hydrolysis cycle are studied in detail.

6.1.1 Purification of wild-type and E599Q mutant Mdl1p-NBDs

Based on sequence alignments (Figure 6.1) in which Mdl1p was compared to other characterised ABC transporters (eukaryotic) or NBDs of ABC transporters (prokaryotic) the *MDLI*-gene was cut behind an intrinsic and unique *Bam*HI restriction site producing the C-terminal domain (amino acids D423 to R695) of Mdl1p.

To gain insight into the ATP hydrolysis cycle, a mutant of Mdl1p-NBD was created based on mutations in different ABC transporters, which affected ATPase activity (Moody et al., 2002; Urbatsch et al., 2000b). The mutations in the NBDs of P-glycoprotein (E552Q; E1197Q) were reported to result in a highly impaired ATPase activity (Urbatsch et al., 2000b). A comparable mutation of the archaeal NBDs of MJ0796 and MJ1267 (E171Q/E179Q) induced an ATP-dependent dimerisation of the NBDs (Moody et al., 2002). Hence, an equivalent mutation of the conserved glutamate (E599Q) of Mdl1p-NBD was introduced by site-directed mutagenesis.

Both constructs were over-expressed in *E. coli* BL21(DE3) and purified by immobilised metal affinity chromatography (IMAC) followed by size exclusion chromatography. Both the wild-type protein as well as the E599Q mutant was purified to homogeneity as shown by coomassie stained SDS-PAGE (Figure 6.2) and the identity of the protein band was confirmed by MALDI-TOF MS. About 50 mg purified protein at a concentration of 10 mg/mL was obtained from one litre culture.

```

                                     *
Mdl1-NBD (S. cerevisiae)  -----DPVSLAQKPIVFNKVSFTYPTRP--KHQIFKDLNITIKPGEHVCAV 466
MsbA-NBD (E. coli)      KDEGKRVIERATGDVEFRNVTFTYFGR--DVPALRNINLKIIPAGKTVALV 375
MsbA-NBD (V. cholerae)  RDNGKYEAERVNGEVDVKDVTFTYQGK--EKPALSHVVSFSIPQGKTVALV 375
TAP1-NBD (H. sapiens)  PPSGLLTPHLHLEGLVQFQDVVSFAYPNRP--DVLVLQGLTFTLRPGEVTALV 537
TAP2-NBD (H. sapiens)  PSPGTLAPTTLQGVVKEQDVVSFAYPNRP--DRPVLKGLTFTLRPGEVTALV 502
HlyB-NBD (E. coli)     -----DITFRNIRFRYKPD--SPVILDNINLSIKQGEVIGIV 501
MJ0796 (M. janaschii)  -----MIKLNVTKTYKMGEIIYALKNVNINIKEGEFVSIIM 37
GlcV (S. solfataricus) -----MVRIIVKKNVSKVFKKGGK--VVALDNNVNIINENGERFGIL 37
MalK (E. coli)         -----MASVQLQNVTKAWG----EVVVSKDINLDIHEGEFVVFV 35
HisP (E. coli)        -----MMSENKLVIDLHKRYG----GHEVLKGVSLQARAGDVISII 38
BtuD (E. coli)        -----MSIVMQLQDVAESTRLGP-----LSGEVRAGEIILHLV 32

                                     π
*****
Mdl1-NBD (S. cerevisiae)  GPSSGSGKSTIASLLRYYDVNSGSIIEFGDEDIRNFNLRK----- 505
MsbA-NBD (E. coli)      GRSSGSGKSTIASLITRFYDIDEGEILMDGHDLDREYTLAS----- 414
MsbA-NBD (V. cholerae)  GRSSGSGKSTIANLFTRFYDVS DSGSICLDGHDVDRDYKLTN----- 414
TAP1-NBD (H. sapiens)  GPNGSGKSTVAALLQNLVYQPTGGQQLLDGKPLPQYEHRY----- 576
TAP2-NBD (H. sapiens)  GPNGSGKSTVAALLQNLVYQPTGGQVLLDEKPI SQYEHY----- 541
HlyB-NBD (E. coli)     GRSSGSGKSTLTKLIQRFYIPENGQVLDGHDLDLADPNW----- 540
MJ0796 (M. janaschii)  GPSSGSGKSTMLNIIIGCLDKPTEGEVYIDNIKTNDLDDDE-----LT 78
GlcV (S. solfataricus)  GPSSGAGKTTFMRIIAGLDVPTGELYFDRLVASNGKLI-----VP 78
MalK (E. coli)         GPSSGCGKSTLLRMIAGLETITSGDLFI GEKRMNDT-----P 71
HisP (E. coli)        GSSGSGKSTFLRCINFLEKPSGAIIVNGQINLVRDKDGQLKVDKQNL 88
BtuD (E. coli)        GPNGAGKSTLLARMAGMTS--GKGSIQFAGQPLEAWSATK----- 70
WALKER A

                                     *
Mdl1-NBD (S. cerevisiae)  --YRRLIGYVQQEPLLFN--GTILDNIIYCIPEEIAEQDDIRRAIGKANC 552
MsbA-NBD (E. coli)      --LRNQVALVSNVHLLFN--DTVANNIAYARTEQYSR--EQIEEAARMAYA 440
MsbA-NBD (V. cholerae)  --LRRHFALVSNVHLLFN--DTIANNIAYAAEGEYTR--EQIEQAARQAHA 440
TAP1-NBD (H. sapiens)  --LHRQVAAVGQEPQVFG--RSLQENIAYGLTQKPTM--EEITAAAVKSGA 621
TAP2-NBD (H. sapiens)  --LHSQVVSVQGEPVLFV--GSVRNNIAYGL--QSCED--DKVMAAAQAHA 585
HlyB-NBD (E. coli)     --LRRQVGVVLDQDNVLLN--RSIIDNISLAN--FGMSV--EKVIYAACKLAGA 584
MJ0796 (M. janaschii)  KIRRDKIGFVQGFNLIPLLTALLENVLP LIFKYRG----AMSGEERRKR 124
GlcV (S. solfataricus)  PEDR-KIGMVFQTWALYPNLTA FENIAFP LTNMK-----MSKEEIRKR 120
MalK (E. coli)         PAER--GVMVFQSYALYPHLSVAENMSFG LKPAG-----AKKEVINQR 113
HisP (E. coli)        RLLRTRLTMVQHFNLWSHMTVLENVMEAP IQVLG-----LSKHDARER 132
BtuD (E. coli)        --LALHRAYLSQQQTPPFATPVVH YLTLHQ-----HDKTRTE 105
Q-loop

                                     ***** *
Mdl1-NBD (S. cerevisiae)  TKFLANFPDGLQTMVGARGAQLSGGQQR IALARAFLLD-P-----A-- 593
MsbA-NBD (E. coli)      MDFINKNMNGLDTVI GENGVLSSGGQRQR IARALLRDS P----- 500
MsbA-NBD (V. cholerae)  MEF IENMPQGLD TVI GENG TSLSGGQRQRVA IARALLRDAP----- 500
TAP1-NBD (H. sapiens)  HSFISGLPQGYDTEVGEAGS QLSGGQRQAVALARALIRK-P-----C-- 662
TAP2-NBD (H. sapiens)  DDFIQEMEHGIYTDVGEKGSQ LAAGQKQRLA IARALVRD-P-----R-- 626
HlyB-NBD (E. coli)     HDFISELREGYNTIVGEGAGLSGGQRQR IARALVNN-P-----K-- 625
MJ0796 (M. janaschii)  ALECLKMAELEEERFANHKPNQLSGGQQQRVA IARALANN-P-----P-- 167
GlcV (S. solfataricus)  VEEVAKILDIHH--VLNVHFPRELSGAQQQRVALARALVKD-P-----S-- 162
MalK (E. coli)         VNQVAEVLQLAH--LLDRKPKALSGGQRQRVA IGRTLVAE-P-----S-- 155
HisP (E. coli)        ALKYLAKVGIDERAQGYKYPVHLSGGQQQRVS IARALAME-P-----D-- 175
BtuD (E. coli)        LLNDVAGALALDDKLG RSTNQLSGGEWQRVRLA AVVLQITPQANPAGQ-- 155
C-loop                               Pro-loop

**   ****                               * *
Mdl1-NBD (S. cerevisiae)  VLILDEATSA L D S Q S E E I V A K - N L Q R R V E R - G F T T I S I A H R L S T I K H S T R 641
MsbA-NBD (E. coli)      ILILDEATSA L D T E S E R A I Q A A L D E L Q K - - - N R T S L V I A H R L S T I E K A D E 547
MsbA-NBD (V. cholerae)  VLILDEATSA L D T E S E R A I Q A A L D E L Q K - - - N K T V L V I A H R L S T I E Q A D E 547
TAP1-NBD (H. sapiens)  VLILDDATSA L D A N S Q L Q V E Q - L L Y E S P E R Y S R S V L L I T Q H L S L V E Q A D H 711
TAP2-NBD (H. sapiens)  IIIILDEATSA L D V - - - Q C E Q - A L Q D W N S R G D R T V L V I A H R L Q T V Q R A H Q 671
HlyB-NBD (E. coli)     ILIFDEATSA L D Y E S E H V I M R - N M H K I C K - - G R T V I I I A H R L S T V K N A D R 672
MJ0796 (M. janaschii)  IILADEPTGA L D S K T G E K I M Q - L L K K L N E E D G K T V V V V T H D E R I I Y L K D G 203
GlcV (S. solfataricus)  LLLLDEPFSNL D A R M R D S A R A - L V K E V Q S R L G V T L L V V S H D P A D I F A I A D 210
MalK (E. coli)        VFLLEDEP L S N L D A A L R V Q M R I - E I S R L H K R L G R T M I Y V T H D Q V E A M T L A D 203
HisP (E. coli)        VLLFDEPTSA L D P E L V G E V L R - I M Q Q L A E E - G K T M V V V T H E M G F A R H V S S 212
BtuD (E. coli)        LLLLDEP M N S L D V A Q S A L D K I L S A L C Q Q - - G L A I V M S S H D L N H T L R H A H 202
Walker B   D-loop                               H-loop

```

Figure 6.1. CLUSTAL W (1.83) multiple sequence alignment of different ABC transporter NBDs. Conserved motifs are marked and coloured separately. ATP contact sites from the protein are labelled by red stars, interactions within the NBD monomer are marked with green stars and black stars indicate contacts in the dimer interface.

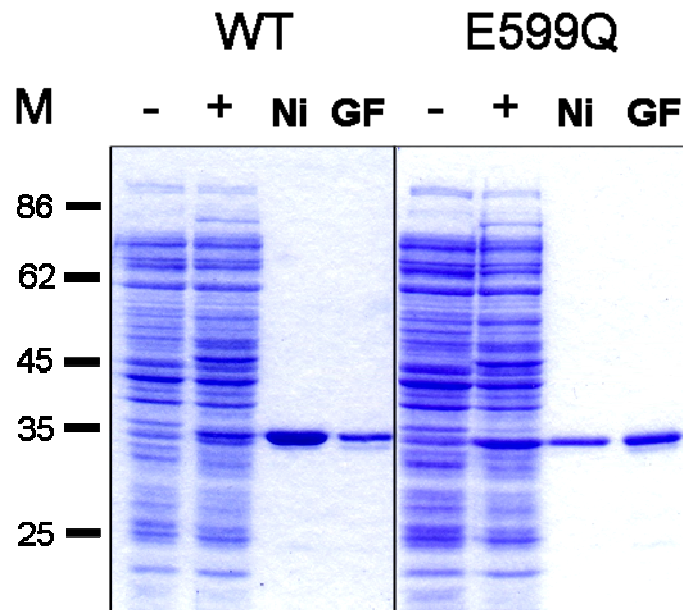


Figure 6.2. Expression and purification of wild-type (WT) and mutant (E599Q) NBD of Mdl1p. Coomassie stained 15 % SDS-PAGE containing crude extract of non-induced (-) and induced (+) cells, purified NBD after Ni²⁺-chelating affinity purification (Ni) and gel filtration (GF). M indicates protein marker in kDa.

The activity of the isolated wild-type NBD was analysed with respect of ATP and ADP binding using 8-azido-[α -³²P]ATP photolabeling experiments. Photolabeling with 8-azido-[α -³²P]ATP was specifically competed by excess of unlabeled nucleoside di/triphosphates (Janas et al., 2003).

The IC₅₀, roughly reflecting the $K_{D(ATP)}$ value, was determined to be 2 μ M for MgATP and 64 μ M for MgADP. The absence of Mg²⁺ dramatically reduced the affinity of nucleotides to the NBD. The affinity for MgCTP, MgGTP and MgUTP was roughly 30-fold lower compared to MgATP (Janas et al., 2003).

The isolated NBD was active in ATP hydrolysis with a $K_{M(ATP)}$ of 0.6 mM and showed no cooperativity with increasing ATP concentration (Hill coefficient of 1.0; (Janas et al., 2003). The ATPase activity was observed to be non-linearly dependent on the protein concentration. The specific ATPase activity increased over two orders of magnitude at higher protein concentrations. At concentrations above 250 μ M the NBD precipitated. Based on a V_{max} of 25 ATP per NBD and minute, a $K_{0.5(NBD)}$ of 75 μ M and a Hill coefficient of 1.7 were determined, suggesting that the active form of the enzyme is a dimer. Also at low (5 μ M) and high (150 μ M) NBD concentrations, the $K_{M(ATP)}$ was 0.6 mM and showed no cooperativity with increasing ATP concentration. The NBD had a maximal ATPase activity at a pH of 8 – 9, comparable to the pH of the mitochondrial matrix (Janas et al., 2003).

6.1.2 The active form of the NBD is a dimer

It is postulated that the interaction of both NBDs plays a central role in the catalytic cycle of ABC transporters (Nikaido, 2002). So far, size exclusion chromatography experiments with isolated NBDs (e.g. HisP and P-gp) did not demonstrate ATP-dependent dimerisation, independent of the presence of nucleotides or non-hydrolysable analogues like AMP-PNP (Kerr, 2002; Nikaido et al., 1997). The wild-type Mdl1p-NBD appeared as a monomer in size exclusion chromatography studies independent of the presence of different nucleotides.

To analyse intermediate states of the ATPase cycle, the NBD was trapped using ortho-vanadate (V_i) or beryllium fluoride (BeF_x). As shown by myosin x-ray structures the vanadate-inhibited complex resembles a post-hydrolysis state while the complex trapped by BeF_x represents a pre-hydrolysis state (Fisher et al., 1995). After 5 minutes of pre-incubation of the NBD with BeF_x in the presence of MgATP at 30 °C, a stable dimer corresponding to a molecular mass of 66 kDa was observed by size exclusion chromatography even in the absence of MgATP and BeF_x in the mobile phase (Figure 6.3 A.). The formation of the dimer was dependent on the concentration of BeF_x . At a concentration of 1 mM BeF_x , almost 80 % of the protein was detected as a dimer. The same result was observed with ortho-vanadate (Figure 6.3 B). Importantly, neither pre-incubation of the NBD with MgADP or MgAMP-PNP in the presence of BeF_x/V_i at 30 °C, nor incubation with MgATP and BeF_x/V_i at 4 °C induced dimerisation of the NBDs. Omission of Mg^{2+} from the reaction inhibited the formation of the dimer. This demonstrated that ATP hydrolysis is essential for the formation of the BeF_x/V_i -stabilised dimer.

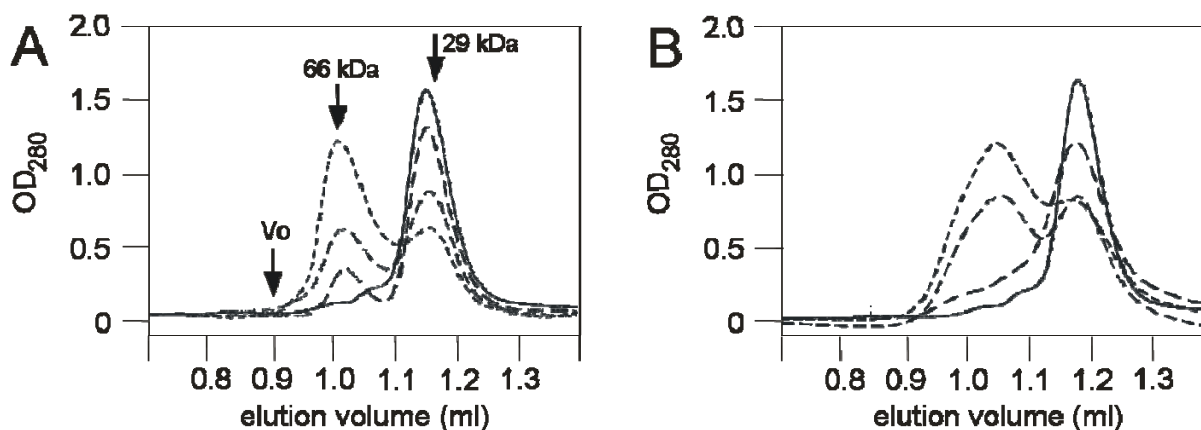


Figure 6.3. Formation of the ATP-induced dimer. After pre-incubation of the wild-type NBD (30 μ M) with increasing concentrations of different ATP hydrolysis inhibitors for 5 minutes at 30 °C in the presence of MgATP (500 μ M), the formation of the dimer was monitored by size exclusion chromatography. Arrows indicate the void volume (V_o), and column calibration standards bovine serum albumin (66 kDa) and carbonic anhydrase (29 kDa). (A) Trapping with BeF_x (0 mM, straight line; 0.25 mM, long dashes; 0.5 mM, intermediate dashes; and 1 mM, short dashes). (B) Trapping using ortho-vanadate (0 mM, straight line; 0.5 mM, long dashes; 2.5 mM, intermediate dashes; and 5 mM, short dashes).

To test dimer stability fractions corresponding to the dimer were combined after size exclusion chromatography and immediately re-injected to a subsequent size exclusion chromatography run. It was observed that a peak at the position of the monomer appeared while the

dimer peak almost disappeared, demonstrating that trapping of the dimer by BeF_x is not irreversible (Janas et al., 2003).

6.1.3 E599Q mutant NBDs

The mutant NBD bound ATP to the same extent as the wild-type NBD as analysed by 8-azido-ATP photolabeling experiments (Janas et al., 2003). No steady-state ATP hydrolysis was observed by measuring the release of P_i using the malachite green assay. To assay the ability of the mutant to form nucleotide-dependent dimers, the mutant NBD was incubated with MgATP on ice for 5 minutes. Size exclusion chromatography showed that MgATP induced dimerisation in a concentration-dependent manner (Figure 6.4). The E599Q NBD dimer was stable during size exclusion chromatography even without nucleotides in the mobile phase, indicating that the ATP-induced dimer only slowly dissociates. Importantly, ADP did not induce dimerisation, and the addition of ADP to the monomers impaired ATP-dependent dimer formation. Furthermore, dimerisation was independent of the Mg^{2+} -concentration (0 – 5 mM). MgAMP-PNP or MgATP γ S could bind to the wild-type and mutant NBD of Mdl1p to the same extent as MgATP, but did not induce dimerisation (Janas et al., 2003). Based on these results it was concluded that presence of ATP is required for the formation of both wild-type and mutant dimer.

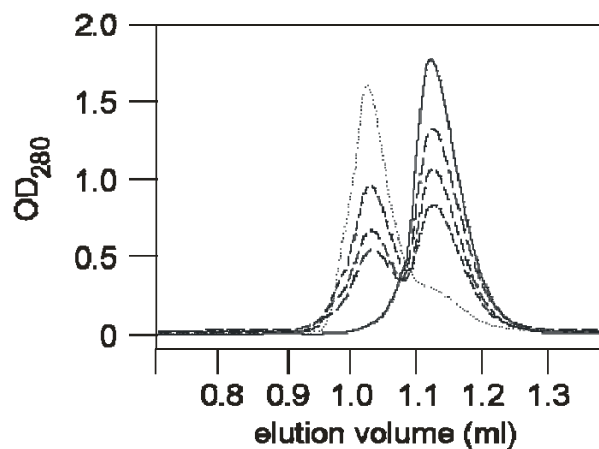


Figure 6.4. ATP dependent dimerisation of the E599Q mutant. After pre-incubation of the E599Q mutant (30 μM) with increasing concentrations of MgATP (0 μM , straight line; 20 μM ; long dashes; 200 μM , intermediate dashes; and 500 μM short dashes) for 5 minutes on ice, the formation of the dimer was monitored by size exclusion chromatography.

6.1.4 Nucleotide composition of the dimer

In order to see changes of the nucleotide composition in the occluded state (the NBD dimer with two trapped nucleotides) the ATP hydrolysis cycle of the NBDs was followed. Therefore, the wild-type NBD was incubated with tracer amounts of either $[\alpha\text{-}^{32}\text{P}]\text{ATP}$ or $[\gamma\text{-}^{32}\text{P}]\text{ATP}$ under BeF_x -trapping conditions and applied to the size exclusion chromatography column. Radioactive nucleotides exclusively coeluted with the dimer, whereas no nucleotides were observed in fractions corresponding to the monomer (Figure 6.5). The amount of $[\alpha\text{-}^{32}\text{P}]\text{ATP}$ bound per wild-type dimer was determined and a stoichiometry of two nucleotides

per dimer was obtained (Figure 6.5 A, open circles). Incubation of the NBD with ATP/BeF_x in the presence of [γ -³²P]ATP resulted in a dimer with almost no radioactive nucleotides incorporated (Figure 6.5 A, filled circles, Table 6.1).

Nucleotide/dimer, (mol/mol)	Wild-type 30 °C, BeF _x -trapped	E599Q 4 °C, no Mg ²⁺ , ATP	E599Q 30 °C, Mg ²⁺ , limiting ATP
[γ - ³² P]ATP	0.01 ± 0.01	2.50 ± 0.18	1.16 ± 0.06
[α - ³² P]ATP	1.76 ± 0.06	2.27 ± 0.15	2.18 ± 0.14
[α - ³² P]ADP	-	-	0.02 ± 0.0

Table 6.1. Nucleotide composition of the dimer (average of 5 experiments).

These results demonstrate that two ATP molecules are hydrolysed in the BeF_x-trapped wild-type dimer and the [γ -³²P]_i is released from the complex. This was confirmed by TLC analysis (Figure 6.5 A).

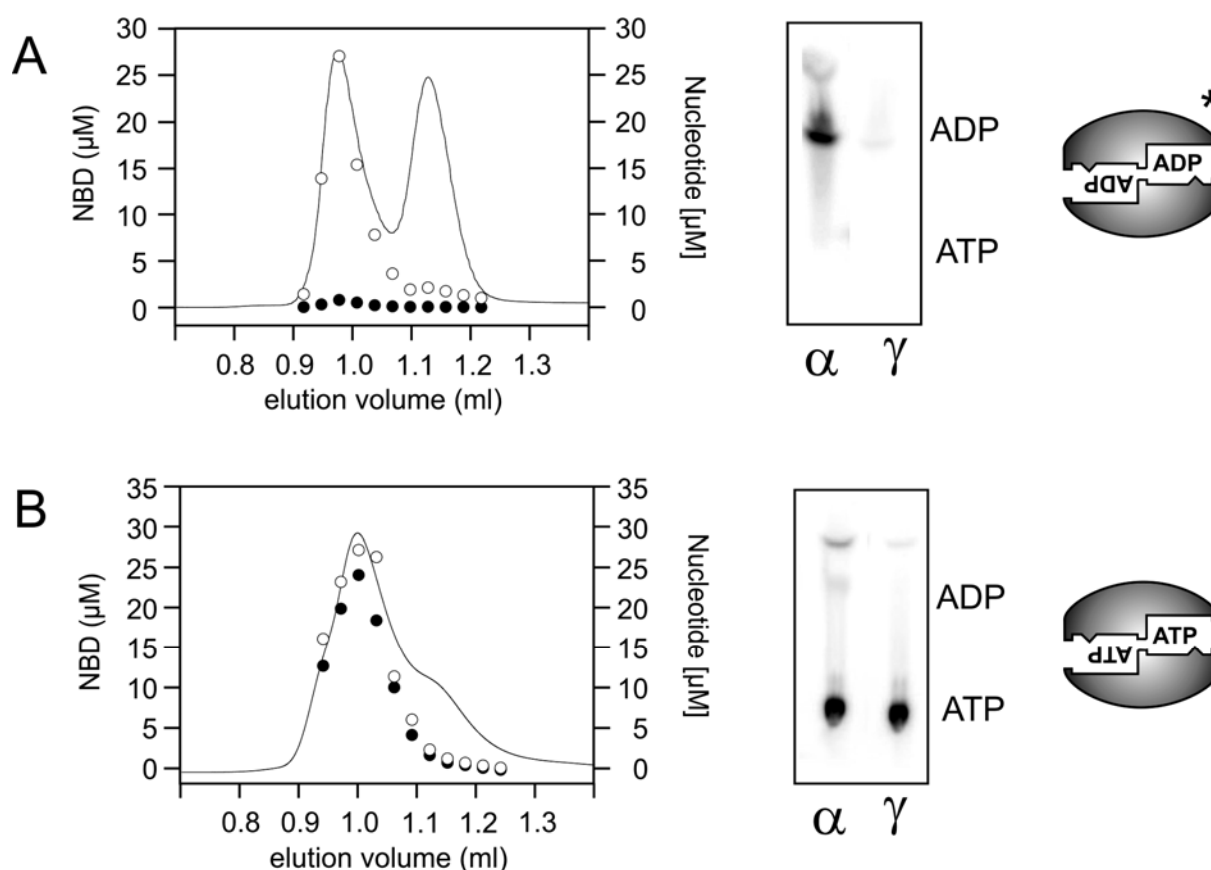


Figure 6.5. Nucleotide stoichiometry of trapped NBDs. **(A)** Wild-type NBD (250 μ M) was trapped using MgATP (500 μ M) and BeF_x (500 μ M) for 5 minutes at 30 °C in the presence of tracer amounts of either [α -³²P]MgATP (○) or [γ -³²P]-MgATP (●), and separated by size exclusion chromatography (left panel). The nucleotide concentration was determined by β -counting and the protein concentration (straight line) by the BCA assay and OD₂₈₀. The middle panel shows a TLC of the nucleotides incorporated into the dimer. **(B)** E599Q mutant (250 μ M) was trapped with ATP (500 μ M) and tracer amounts of either [α -³²P]ATP (○) or [γ -³²P]ATP (●) in the absence of Mg²⁺ for 5 minutes on ice, and separated by size exclusion chromatography (left panel). The nucleotide and protein concentration was determined as above. The middle panel shows a TLC of the nucleotides incorporated into the dimer. Schemes on the right depict the isolated states. *, the BeF_x-trapped state.

Under the same conditions, incorporation of [α - 32 P]ADP into the dimer was not observed, even in the presence of different concentrations of ATP (data not shown). In experiments with the E599Q mutant, performed at 4 °C and in the absence of Mg^{2+} , the nucleotides coeluted exclusively with the dimer as well. In this experiment, the amount of both [α - 32 P]ATP and [γ - 32 P]ATP bound per dimer was equal and a stoichiometry of two ATP molecules per dimer was obtained (Figure 6.5 B, Table 6.1). TLC analysis demonstrated that ATP and not ADP and P_i were incorporated into the dimer. As mentioned above, incubation with non-hydrolysable ATP analogues did not trigger dimer formation. The data from both the BeF_x -trapped wild-type NBD and the E599Q mutant suggest that at least two different intermediate states can be isolated during the ATP hydrolysis cycle. Importantly, both states contain two nucleotides. In one state, the nucleotides are two ATPs as shown for the E599Q mutant while in the other state both nucleotides have been hydrolysed to ADP and P_i as demonstrated for the trapped wild-type NBD. This suggests that ATP binding on both NBDs induces formation of the dimer and after hydrolysis of both ATP molecules to ADP, the dimeric complex dissociates and ADP is released.

6.1.5 ATP hydrolysis cycle of Mdl1p-NBD

An important remaining question is how the ATPs are hydrolysed during one cycle. Using radiolabelled ATP, it was determined that the E599Q mutant, at 30 °C and in the presence of Mg^{2+} was still able to hydrolyse ATP with a turn-over rate of 0.5 ATP per hour (Janas et al., 2003). Thus the ATPase activity of the E599Q mutant was 3,000-fold reduced compared to the ATPase activity of the wild-type NBD. The amount of released phosphate in the radioactive ATPase assay increased linearly over several hours, indicating that the E599Q mutant can make multiple turn-overs. The strongly reduced turn-over rate was used as a tool to examine the hydrolysis cycle in more detail. When the dimer was incubated with limiting amounts of ATP at 30 °C in the presence of Mg^{2+} in order to allow only one or two ATP hydrolysis turn-overs, the size exclusion chromatography analysis of the E599Q mutant showed that, over time, the amount of dimeric NBD decreases and the amount of monomeric NBD increases (e.g. after 400 min, Figure 6.6 A and B, left panel). The nucleotide composition of the remaining dimer was analysed, and found to contain one ATP and one ADP (Figure 6.6 A., Table 6.1). TLC analysis of the dimer confirmed an intermediate state containing equal amounts of ATP and ADP (Figure 6.6 A, middle panel). The dimers isolated after prolonged incubation times at 30 °C (Figure 6.6 B, left panel) reached a stoichiometry of one ATP and one ADP (6.6 B., right panel), suggesting that this is a stable intermediate state, which can be detected under limiting ATP conditions.

To exclude that the ADP found in the dimer is derived from ADP rebinding from the solution, ADP incorporation was followed under exactly the same conditions using [α - 32 P]ADP as a tracer. Under these conditions no incorporation of [α - 32 P]ADP was detected (Table 6.1). This demonstrated that the dimer-bound ADP is derived from hydrolysis of the first ATP. The in-

intermediate state suggests that the ATP hydrolysis occurs by a sequential mechanism, and that in the E599Q mutant hydrolysis of the second ATP is slower than hydrolysis of the first.

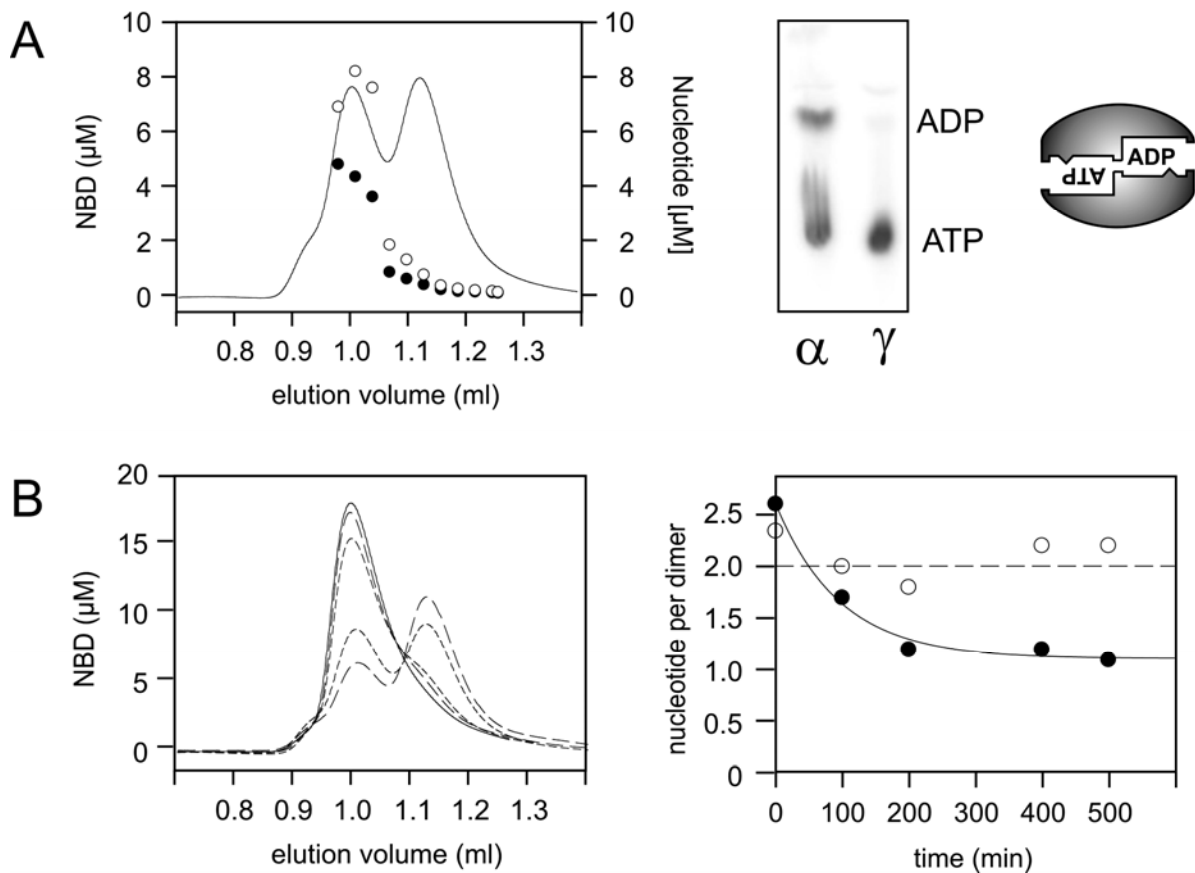


Figure 6.6: Nucleotide stoichiometry of trapped NBDs. **(A)** The E599Q mutant (250 μM) was pre-incubated with ATP (250 μM) and tracer amounts of $[\alpha\text{-}^{32}\text{P}]\text{ATP}$ or $[\gamma\text{-}^{32}\text{P}]\text{ATP}$ at 30 $^{\circ}\text{C}$ for 400 minutes in presence of Mg^{2+} , and isolated by SEC. The nucleotide concentration was determined by β -counting and the protein concentration (straight line) by the BCA assay and OD_{280} . The middle panel shows a TLC of the nucleotides incorporated into the dimer. The scheme on the right depicts the isolated state. **(B)** Dissociation of the E599Q mutant dimer over time (0 min, straight line; 100 min, long dashes; 200 min, intermediate-long dashes; 400 min, intermediate dashes; 500 min, short dashes) monitored by SEC after incubation under ATP-limiting conditions. The right panel shows the ATP/ADP composition of the isolated dimers.

6.2 Characterisation of the full-length ABC transporter Mdl1p

To study the function of Mdl1p, biochemical data and structural information are of key importance. Therefore, the availability of purified and active protein and a stable reconstitution method is required. This part of the work set out to establish high-level over-expression and optimisation of the purification as well as the reconstitution of full-length Mdl1p.

6.2.1 Identification of interaction partners of Mdl1p

The yeast TAP-fusion library is comprised of 4,247 open reading frames tagged with a high-affinity epitope and expressed from its natural chromosomal location (Ghaemmaghani et al., 2003). This library contains a strain with a C-terminal TAP-tagged version of Mdl1p.

Mitochondria prepared from this strain were used for a tandem affinity purification approach to test its capability to obtain highly purified protein and to analyse potential binding partners.

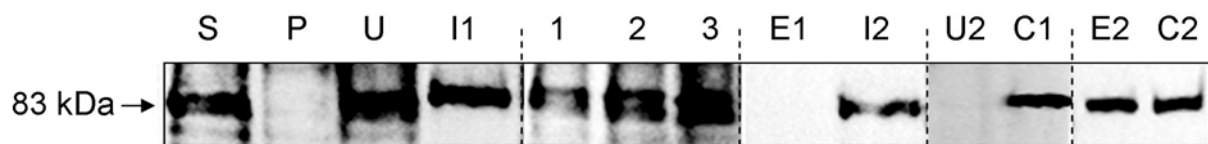


Figure 6.7: Tandem affinity purification of Mdl1p. Immunodetection of Mdl1p after western transfer. Triton X-100 solubilised mitochondria were used for tandem affinity purification of Mdl1p: supernatant after ultracentrifugation (S), pellet after ultracentrifugation (P), supernatant after binding to IgG-sepharose beads (unbound material; U), Mdl1p bound to IgG-beads (I1), TEV cleavage after 1, 2 or 4 hours (1 – 3), supernatant after TEV elution (E1), Mdl1p still bound to IgG-beads after TEV cleavage (I2), supernatant after binding to calmodulin sepharose beads (unbound material; U2), Mdl1p bound to calmodulin beads (C1), supernatant after EGTA elution from calmodulin beads (E2), Mdl1p still bound to calmodulin beads after EGTA elution (C2).

Figure 6.7 shows different steps during a tandem affinity purification. TAP-Mdl1p is almost completely solubilised from mitochondrial membranes (S, P) and protein A was detectable using peroxidase antiperoxidase soluble complex (PAP) in the solubilisate (data not shown). Almost all solubilised TAP-tagged Mdl1p binds to calmodulin sepharose beads (U2, C1) and half of the bound material can be eluted from the beads with EGTA (E2, C2). Up to 50 % of Mdl1p binds to IgG sepharose beads (U, I1). However TEV elution of Mdl1p from IgG sepharose beads was never obtained (1, 2, 3) even after changing cleavage conditions e.g. temperature (4 °C, 30 °C, 37 °C), time (1, 2, 4 hours and overnight), amount of TEV (5, 10, 20 U), or the kind of TEV-protease (TEV, rTEV). In addition, Mdl1p solubilised from mitochondria and directly used for TEV treatment was not cleaved since no shift was detectable on immuno blots. Unfortunately, Mdl1p could not be detected by either Coomassie or in silver staining of gels (data not shown) after TAP-purification. This is probably due to the low expression from the wild-type promoter. Therefore, no binding partners of Mdl1p were identified using this method.

6.2.2 Solubilisation and purification of Mdl1p

Mdl1p is normally expressed at low levels (Ghaemmaghami et al., 2003), and is almost not affected through different stimuli as shown in various array approaches. Quantitative immunoblotting using the purified Mdl1p-NBD as reference demonstrated that Mdl1p is expressed to approximately 0.01 % of total mitochondrial protein. Hence, over-expression was aspired using several approaches. To ease further cloning, the *MDL1*-gene was systematically divided in small cassettes, thus facilitating the exchange between different constructs, and cloned in the *S. cerevisiae* plasmid p426-GPD behind a strong constitutive *GPD*-promoter and into pYES3P_{A2}AAC2 behind a glycerol promoter. Surprisingly, both attempts resulted in protein amounts even lower than the wild-type levels (S. Gompf, Institute of Biochemistry, Goethe-University Frankfurt; personal communication and (Hofacker et al., 2006).

Therefore, also expression of Mdl1p in *E. coli* was investigated. High and low copy number plasmids with different inducible promoters were tested under varying growth conditions and in various hosts. The expression levels were evaluated by quantitative western blotting and immunodetection. To improve the expression chaperones were induced by growth at 42 °C or in 1 M sorbitol, and coexpression with rare tRNAs or the SecY, SecE, SecG and YidC components of the *E. coli* translocase was tested. The different expression conditions did however not strongly affect the level of Mdl1p expression (data not shown), and only low expression levels were obtained (C. Presenti, Institute of Biochemistry, Goethe-University Frankfurt; personal communication and (Hofacker et al., 2006).

Since *L. lactis* has been suggested to be a good host for over-expression of mitochondrial proteins (Kunji et al., 2003) Mdl1p was expressed in *L. lactis*. Expression of Mdl1p from a plasmid with a nisin inducible promoter led to an approximately two fold higher expression level (0.01 % of total membrane protein) compared to *E. coli* but the expression levels were still very low (C. Presenti, Institute of Biochemistry, Goethe-University Frankfurt; personal communication and (Hofacker et al., 2006).

Since only low levels of expression were obtained in both *E. coli* and *L. lactis* it was further tried to over-express Mdl1p in *S. cerevisiae* in an inducible manner. The *MDL1*-gene was cloned into pYES2.1 behind the inducible *GALI*-promoter. Remarkably, over-expression of Mdl1p after induction was time-dependent with an optimum between 8 and 12 hours (S. Gompf, Institute for Biochemistry, Goethe-University Frankfurt; personal communication and (Hofacker et al., 2006).

Mdl1p was over-expressed 100-fold, up to 1 % of total mitochondrial protein. The remarkable optimum in over-expression after induction (Simone), and the reduced levels of Mdl1p expression from a constitutive promoter suggest that high levels of the protein are disfavoured, and results in increased instability or degradation of the protein. The pathway via this degradation occurs is currently unknown. However, using an inducible promoter, and a certain induction time of 12 hours, high levels of Mdl1p suitable for purification were obtained.

To optimise the Mdl1p solubilisation, several detergents were tested at two different ρ -values (Figure 6.8).

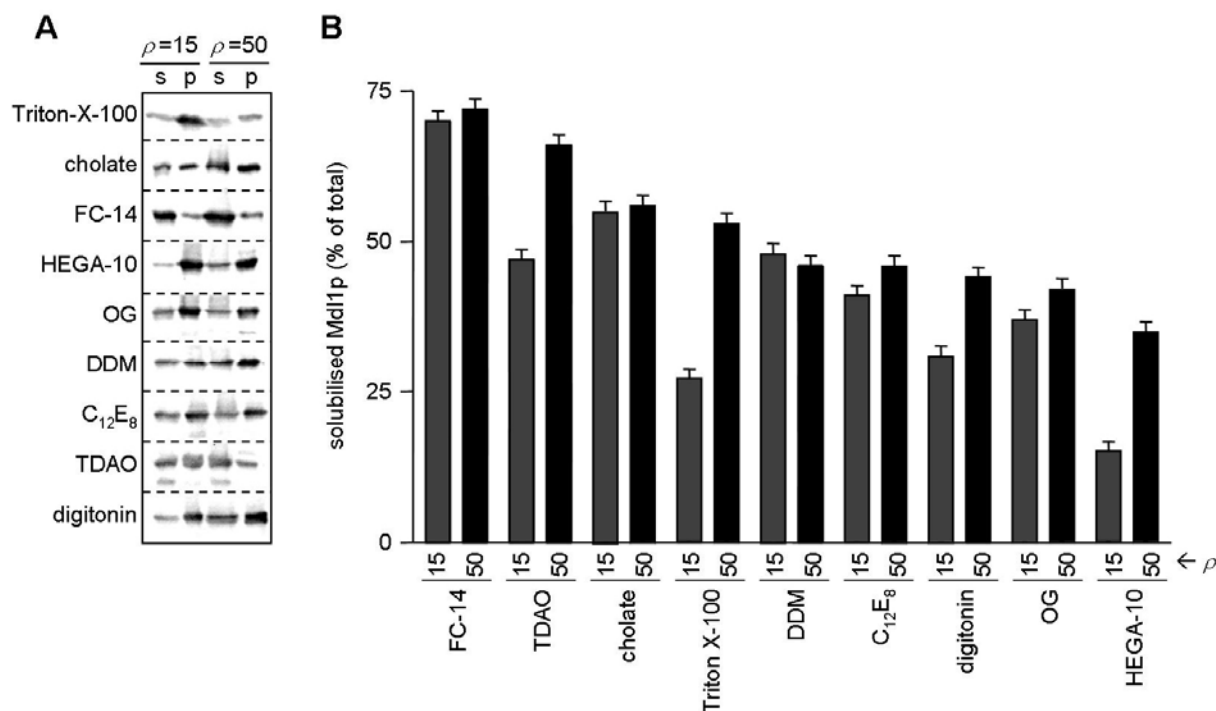


Figure 6.8: Solubilisation of Mdl1p in different detergents. (A) Mitochondria (500 μ g total protein) were resuspended in buffer S whereas digitonin was exchanged for detergents as indicated. Detergent concentrations were used to reach ρ -values of 15 or 50 respectively where ρ is given by: $\rho = [\text{detergent}] \times \text{CMC} / [\text{lipid}]$. The lipid concentration was estimated using an average molecular mass of 875 Da and a lipid to protein ratio of 0.1. Soluble and insoluble fractions were separated by ultracentrifugation. Insoluble material (p) was applied together with the corresponding supernatant (s) to a 10% SDS-PAGE. Mdl1p was detected by chemiluminescence after western transfer. (B) The signals were quantified and a ratio of supernatant vs. supernatant plus pellet (total) was calculated.

The subsequent order was obtained: tetradecylphosphocholine (FC-14) showed by far the highest solubilisation efficiency (> 70 % solubilised Mdl1p) followed by n-tetradecyl-n,n-dimethylamine-n-oxide (TDAO, 66 %), sodium cholate (56 %), Triton X-100 (53 %) and finally dodecylmaltoside (DDM, 48 %), octaethylene glycol monododecyl ether (C₁₂E₈, 46 %), digitonin (44 %), n-octyl- α -d-glucopyranoside (OG, 42 %) and decanoyl-n-hydroxyethylengluamide (HEGA-10, 35 %) (Figure 6.8).

The stability of Mdl1p was next tested by applying the solubilised protein on a blue-native-gel (Figure 6.9). Again, most Mdl1p was obtained after solubilisation with FC-14 and sodium cholate, but Mdl1p appeared on the gel as a smear over almost the complete running distance, indicating that Mdl1p is not very stable in these detergents. Defined bands at a molecular weight of \sim 250 kDa were observed with UDM, DDM and digitonin. Almost no Mdl1p was detectable using TDAO, OG or HEGA-11.

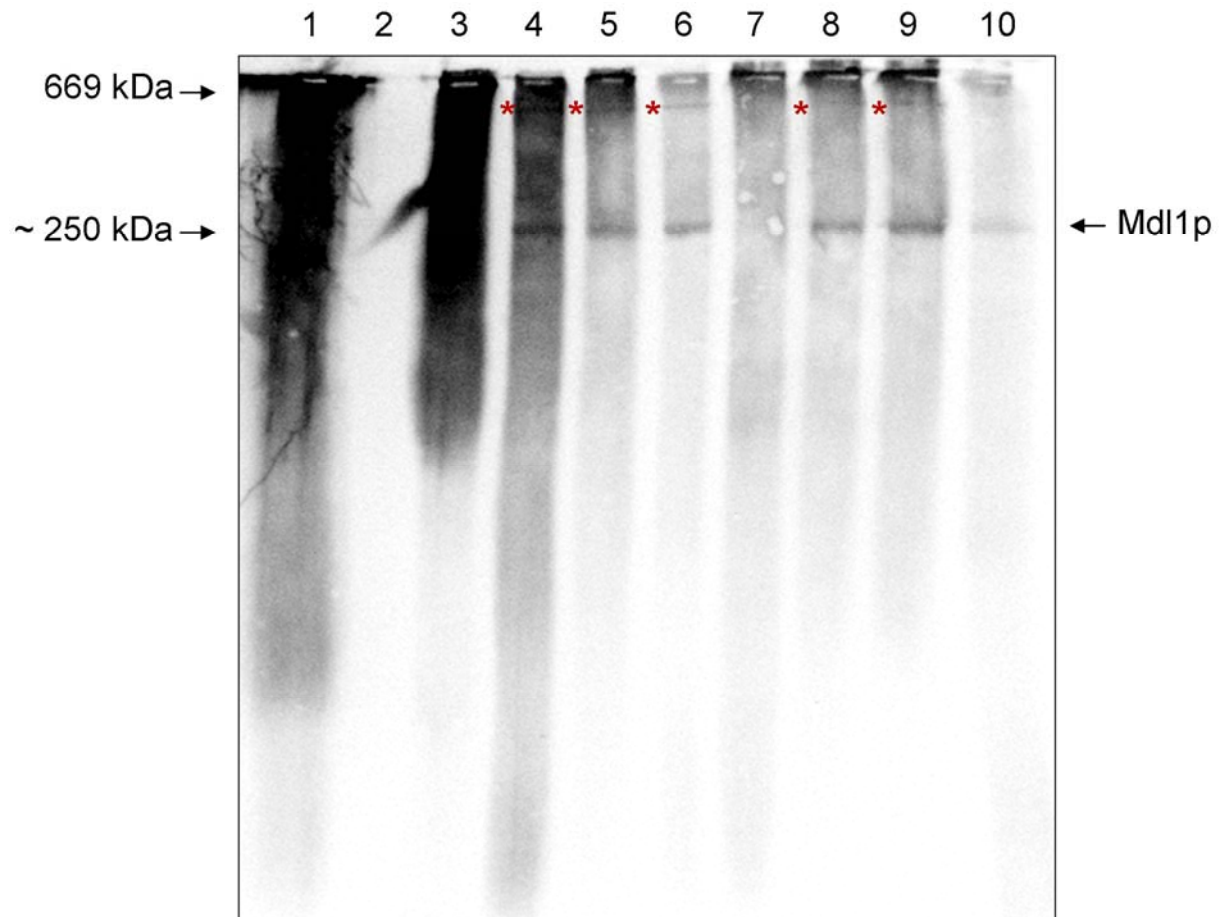


Figure 6.9: Detergent screen using Blue-Native gel electrophoresis and subsequent immunodetection of Mdl1p. Mitochondria (500 μ g) were solubilised in different detergents (1 %; 1: FC-14, 2: TDAO, 3: sodium cholate, 4: Triton X-100, 5: C₁₂E₈, 6: Digitonin, 7: HEGA-10, 8: UDM, 9: DDM, 10: OG) and proteins were separated by Blue-native gel electrophoresis. Mdl1p was detected by immunostaining with an anti-Mdl1p antibody at ~ 250 kDa corresponding to a high molecular weight marker. Red stars indicate a fine band of Mdl1p appearing upon solubilisation in Triton X-100, C₁₂E₈, Digitonin, UDM and DDM showing Mdl1p in a higher oligomeric state.

Three detergents were selected for further analysis: (i) FC-14 as the most efficient detergent (ii) DDM known to preserve active ABC transporters (Margolles et al., 1999) and (iii) digitonin reported to hold fragile membrane protein complexes together (Schägger and Pfeiffer, 2000) and used for purification. Mdl1p was purified using a single Ni-affinity chromatography step. Samples of solubilised mitochondrial membranes, fractions collected at different points of the purification procedure and purified protein were analysed by Coomassie stained SDS-PAGE (digitonin, Figure 6.10, FC-14 and DDM, data not shown).

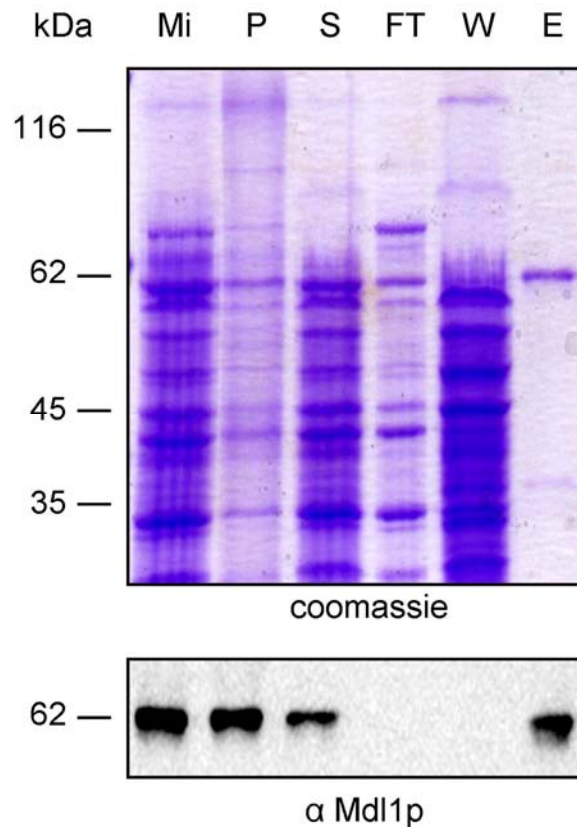


Figure 6.10: Purification of Mdl1p. Different steps in the solubilisation/purification of His-tagged Mdl1p showing the total mitochondrial membrane extract (Mi), the pellet after solubilisation (P), the supernatant after solubilisation with 1 % digitonin (S), the flow through (FT), the wash fraction with 60 mM imidazole (W) and eluted Mdl1p (200 mM imidazole) after Ni^{2+} -chelating affinity purification (E). Identity of the eluted band was confirmed by immunodetection and peptide mass fingerprinting MS analysis (first match Mdl1p (gi | 6323217) with 27 queries matched and a score of 177 (protein scores greater than 75 are significant ($p < 0.05$ %); the next match of a non-homologues protein (gi | 432206) has a score of 44).

Like many integral membrane proteins, Mdl1p migrates at a lower apparent molecular mass than predicted from the deduced amino acid sequence, here 62 kDa instead of 69 kDa. Using FC-14 solubilised Mdl1p approximately 1 mg of Mdl1p of over 95 % purity can be isolated from 1 litre yeast culture whereas in case of DDM and digitonin 0.2 and 0.1 mg respectively were obtained. In addition to immunodetection by the specific antibodies Mdl1p was unified by peptide mass fingerprint.

ATP hydrolysis of the different purifications were measured and showed remarkable differences in ATPase activity (in collaboration with A. Zutz, Institute of Biochemistry, Goethe-University Frankfurt; Figure 6.11). As expected from its instability on the BN-PAGE, the FC-14 solubilised Mdl1p showed only a low ATPase activity. Based on its high ATPase activity, Mdl1p purified in the presence of digitonin was selected for further characterisation.

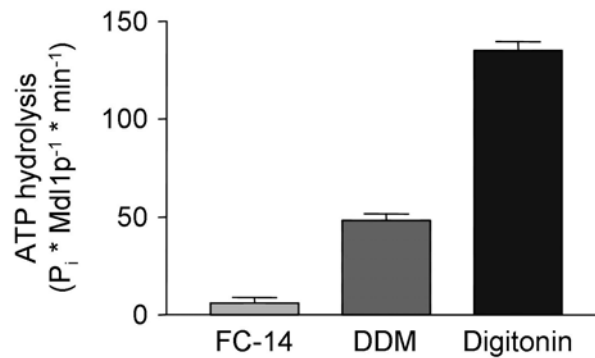


Figure 6.11: ATPase activity of Mdl1p in selected detergents. Mitochondria (5 mg/mL) prepared from *S. cerevisiae* over-expressing Mdl1p were solubilised in different detergents (as indicated) and Mdl1p was purified as described in “Methods”. The ATP hydrolysis of the purified protein was measured at 30 °C in the presence of 5 mM ATP.

At least two ways for targeting of mitochondrial proteins are discussed. One option requires a N-terminal leader sequence of up to 105 amino acids the other signal is encoded by a internal protein fold. To answer the question how Mdl1p is targeted to the inner mitochondrial membrane the purified protein was transferred to a PVDF membrane and analysed by N-terminal Edman degradation. Two result files were obtained. One showed the first eight amino acids with the following sequence: E-S-D-I-A-Q-G-K. Due to background noise a additional sequence was suggested: Q-N-P-N-T-?-Y-?. A second sample where the first six amino acids were analysed gave the following sequence: E-S-D-I-A-Q. The result of this sample was clear and not disturbed by any background signals. Alignment of the obtained sequence with the original Mdl1p-sequence showed that cleavage of the leader sequence occurs after amino acid 59. Why the first amino acid revealed by Edman degradation is a glutamate instead of a glutamine, which is found in the original Mdl1p sequence, is not known.

6.2.3 Mdl1p specifically binds ATP

The purified solubilised full-length Mdl1p was further characterised by 8-azido- $[\alpha\text{-}^{32}\text{P}]\text{ATP}$ photocross-linking experiments. The apparent affinity constant for 8-azido-ATP was 7 μM according to a Langmuir-type (1:1)-binding curve (Figure 6.12). In the presence of 5 μM 8-azido- $[\alpha\text{-}^{32}\text{P}]\text{ATP}$, an IC_{50} value of 0.45 μM was obtained for ATP (Figure 6.13).

Based on the apparent affinity of 8-azido-ATP, an apparent dissociation constant for MgATP of 0.26 μM was calculated.

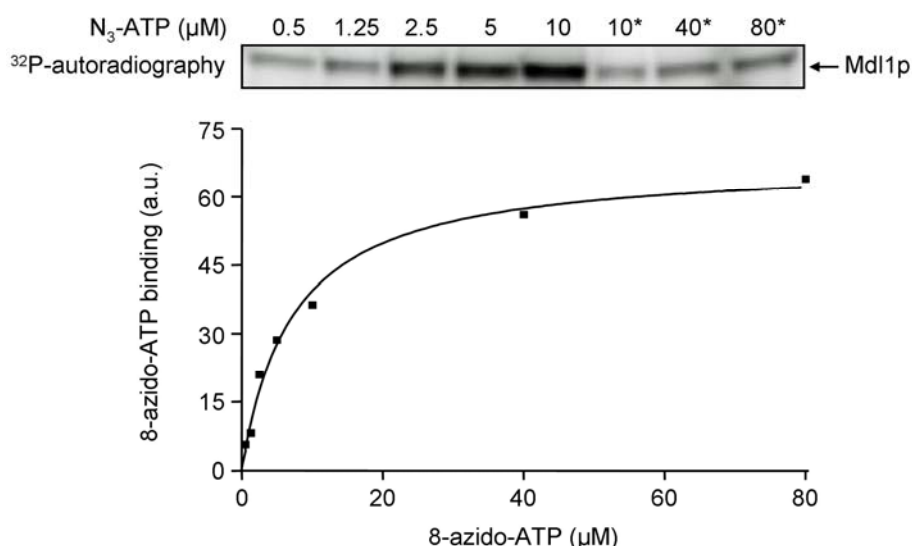


Figure 6.12: ATP competition of 8-azido- $[\alpha\text{-}^{32}\text{P}]\text{ATP}$. Solubilised Mdl1p (0.5 μM) was incubated with 5 μM 8-azido- $[\alpha\text{-}^{32}\text{P}]\text{ATP}$ and increasing concentrations of ATP. The intensities were plotted against the ATP concentration and fitted to an IC_{50} value of 0.45 μM .

ADP, CTP, GTP and UTP (inhibition between 50 % and 85 %, Figure 6.14) showed a similar binding pattern as observed for the isolated NBD. This demonstrated that the isolated solubilised full-length Mdl1p binds nucleotides with a similar affinity as the isolated NBD, suggesting that the TMDs do not affect the nucleotide-binding step.

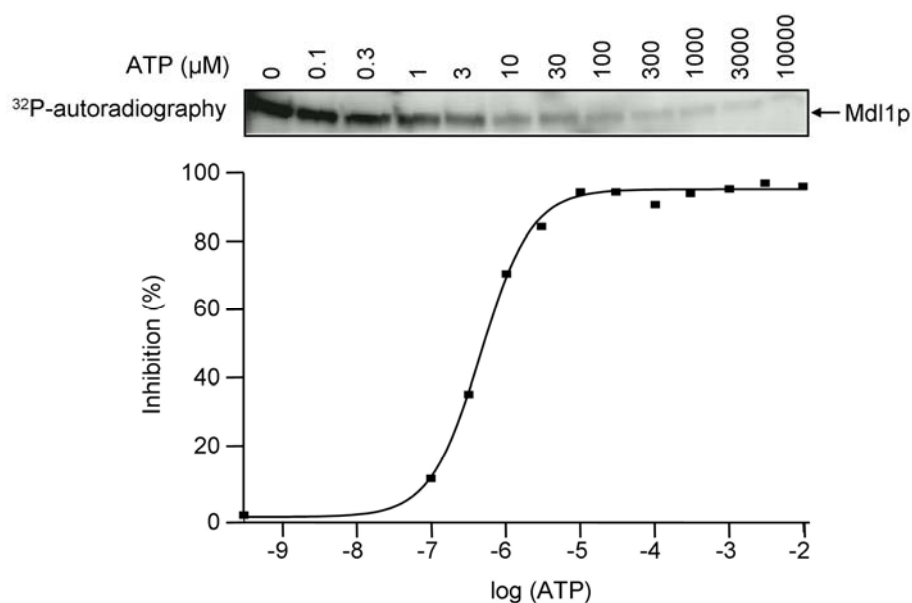


Figure 6.13: 8-azido- $[\alpha\text{-}^{32}\text{P}]\text{ATP}$ titration. Digitonin-solubilised Mdl1p (0.5 μM) was incubated with 8-azido- $[\alpha\text{-}^{32}\text{P}]\text{ATP}$ for 5 minutes at 4 $^{\circ}\text{C}$ and cross-linked by UV-light. For concentrations of 10 μM and above (indicated by stars), 8-azido-ATP was supplemented 1:5 with non-radioactive 8-azido-ATP. The intensities of substituted 8-azido-ATP were adjusted to the non-substituted 8-azido-ATP by comparing the intensities at 10 μM . The intensities were quantified by phosphor-imaging plotted against the 8-azido-ATP concentration and fitted to a Langmuir-type (1:1)-binding curve resulting in an apparent dissociation constant (K_d) of 7 μM .

AMP-PNP, the non-hydrolysable ATP analogue, also bound with a reduced affinity, further demonstrating previous observations, that AMP-PNP does not mimic ATP binding perfectly. Also other studies (Nikaido et al., 1997; Sharma and Davidson, 2000) have seen that AMP-

PNP binds with a reduced affinity, and indeed AMP-PNP can not induce dimerisation of the NBDs. As expected, AMP did not compete with 8-azido-ATP-binding.

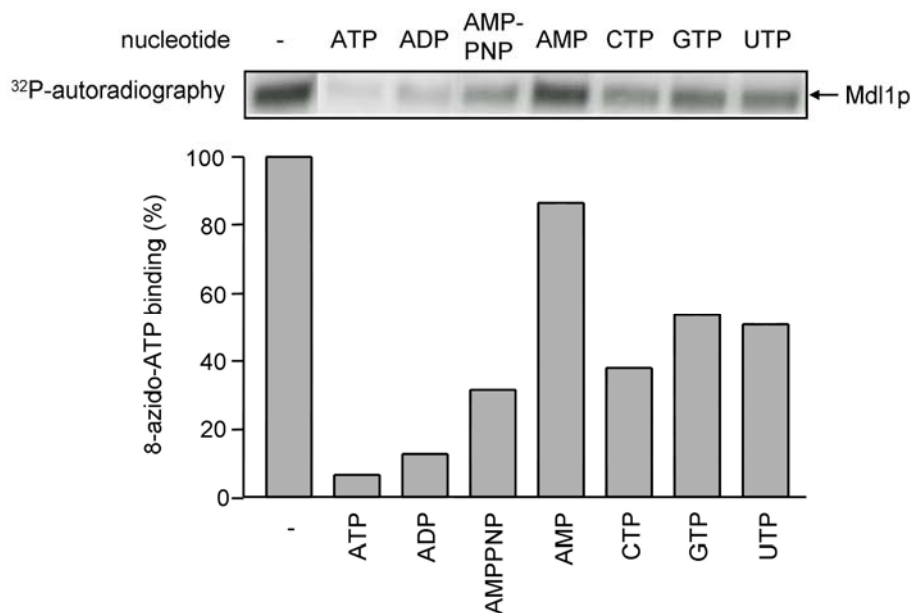


Figure 6.14: Nucleotide-binding specificity of Mdl1p. Digitonin-solubilised Mdl1p (0.5 μ M) was incubated in the presence of 5 μ M 8-azido- $[\alpha\text{-}^{32}\text{P}]\text{ATP}$ together with different other nucleotides at a concentration of 300 μ M each. A sample without competitor nucleotide was set to 100 %. The residual signal in presence of ATP is below 10 % reflecting a high affinity of ATP to Mdl1p. In comparison the AMP signal account for 85 % showing almost no affinity of AMP to Mdl1p.

6.2.4 Mdl1p is active in ATP hydrolysis

To specify the activity of the isolated Mdl1p, ATP hydrolysis was characterised. The solubilised protein showed Michaelis-Menten kinetics (Hill coefficient = 0.98) in ATP hydrolysis with a $K_{M(ATP)}$ of 0.85 mM and a turn over number (k_{cat}) of 2.5 ATP per second (Figure 6.15).

To demonstrate that the ATPase activity observed for the solubilised Mdl1p was derived from the purified protein, and not from a highly active ATPase which copurifies at such low concentrations that it is not observed on Coomassie and silver stained gels, inactive mutants of Mdl1p were used. In recent years, several studies have benefit from mutagenesis of the conserved glutamine one amino acid downstream of the Walker B motif and the histidine in the H-loop, to analyse the dimerisation reaction of the NBDs. After mutagenesis of these residues, the NBDs are trapped in an ATP induced dimeric state, in which the hydrolysis of ATP is either greatly reduced or abolished. Mutagenesis of the glutamine in the NBD of Mdl1p (E599Q) resulted in a 3,000-fold lowered ATPase activity. Mutagenesis of the histidine in the H-loop of HisP (H211) (Shyamala et al., 1991) or MalK (H192) (Davidson and Sharma, 1997) resulted in an ATPase activity below 2 %, and transport was completely abolished (Davidson and Sharma, 1997; Nikaido and Ames, 1999). When the conserved histidine (H662A) of the NBD of HlyB, was mutated, only background levels of ATPase activity (< 0.1%) were detected (Zaitseva et al., 2005c).

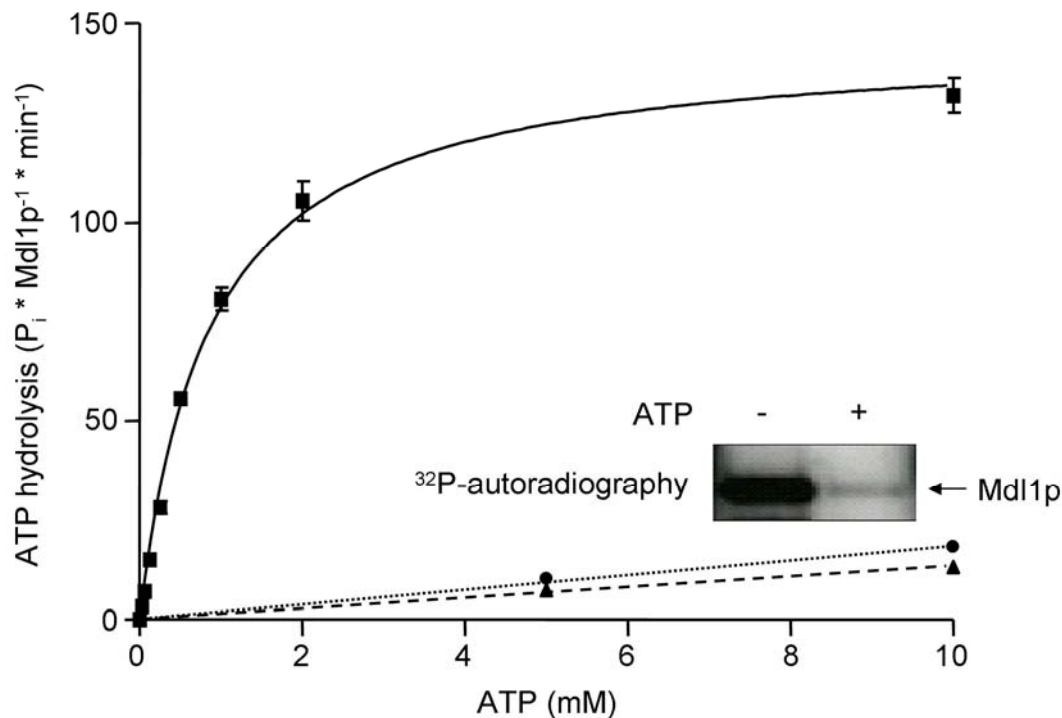


Figure 6.15: ATPase activity of wild-type and mutant Mdl1p. ATPase activity as a function of the ATP concentration was measured at 30 °C with 0.1 μ M Mdl1p. Digitonin solubilised wild-type Mdl1p (■) is active in ATP hydrolysis with a k_{cat} of 2.5 ATP per second and a $K_{M(ATP)}$ of 0.85 mM. The data were fitted to the Hill equation ($y = (ax^n)/(b^n + x^n)$) resulting in a best fit ($R^2 = 0.98$) with a Hill coefficient (n) of 0.98. H631A Mdl1p (▲) binds specifically ATP as shown in 8-azido- $[\alpha\text{-}^{32}\text{P}]$ ATP photocross-linking experiments (see inset) but is deficient in ATP hydrolysis. The same is true for the E599Q mutant (●).

Indeed, both mutants (H631A and E599Q) in full-length Mdl1p showed specific ATP binding in 8-azido-ATP photocross-linking and competition experiments but were defective in ATP hydrolysis (A. Zutz, Institute of Biochemistry, Goethe-University Frankfurt; personal communication and (Hofacker et al., 2006); Figure 6.15). This demonstrated that these mutants behave in a similar manner as in the isolated NBDs, and that the observed ATPase activity resulted from purified Mdl1p. At the protein concentrations at which the experiment was performed, the activity of the full-length protein is much higher than the activity of the isolated NBD at similar concentrations. Remarkably, the activity of the isolated NBD was strongly dependent on the concentration of the NBD (van der Does et al., 2006), and therefore also the activity of the full-length protein as a function of the protein concentration was determined. For the full-length protein the ATP hydrolysis was independent of the protein concentration between 0.01 μ M and 1 μ M. This showed that, contrary to what was observed for the isolated NBD, the association rate of the NBDs is not rate-limiting in the full-length protein. Most likely, this is caused by the fact that in the full-length transporter the NBDs are within once vicinity and therefore are present at high local concentration.

6.2.5 Reconstitution of Mdl1p into lipid vesicles

Mdl1p has been shown to be involved in transport of peptides energised by hydrolysis of ATP. To further study this process, purified Mdl1p was reconstituted into liposomes immedi-

ately after purification by mixing the protein with DDM-stabilised liposomes containing *E. coli* phospholipids. Subsequently, the DDM was removed by absorption to polystyrene beads.

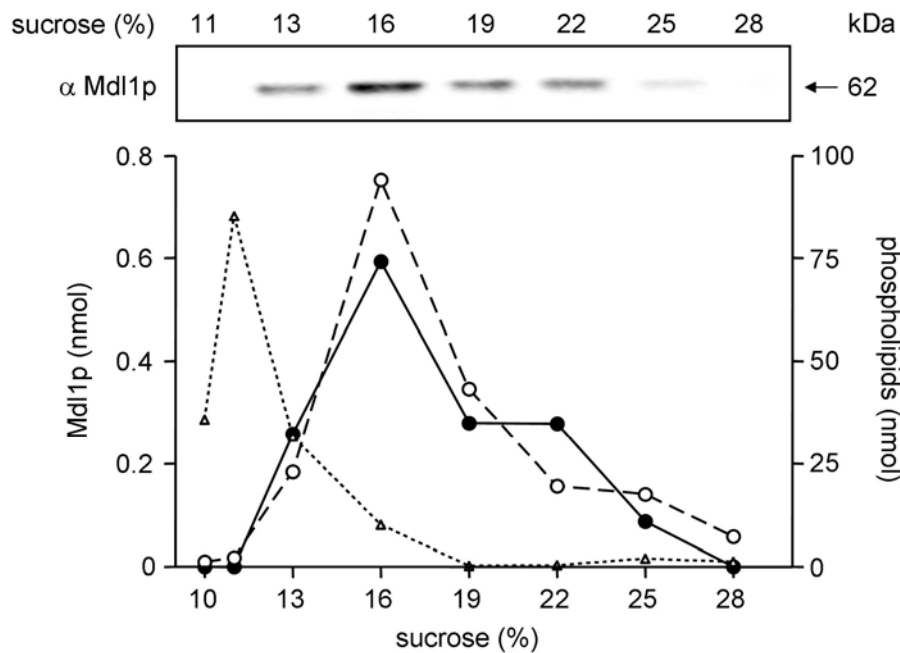


Figure 6.16: Lipid to protein stoichiometry after reconstitution. Lipid vesicles were harvested after reconstitution and applied on top of a discontinuous sucrose gradient (10 – 30 %). Protein was quantified by immunodetection and phospholipids according to chapter 5.2.19. Reconstitution was evident from cocentrifugation of the lipid (dashed line) and the protein fractions (solid line) as both peaks appear at a sucrose concentration of 16 %. The final ratio of phospholipids to protein in the peak fraction was determined to be 160 to 1 (mol/mol). Empty liposomes (dotted line) were detected at 11 % sucrose.

The incorporation of the protein into the liposomes was determined by sucrose gradient centrifugation. Proteoliposomes were applied on top of the gradient and after centrifugation, the position of the liposomes in the sucrose density gradient was determined by measurements of the phosphate content of the collected fractions while the position of Mdl1p in the gradient was determined by Western blotting. Reconstitution of Mdl1p in the liposomes is evident from comigration of Mdl1p and lipids (Figure 6.16).

Empty liposomes were recovered at 11 % sucrose, while the protein containing liposomes were recovered at 16 % sucrose (Figure 6.16). Since no free protein was detected at the bottom of the gradient, all Mdl1p was inserted into liposomes. Additionally, this shows that Mdl1p did not aggregate during the reconstitution procedure. In collaboration with Dr. Haase from the Max-Planck-Institute of Biophysics Frankfurt micrographs of freeze fractured proteoliposomes were analysed and showed well formed lipid vesicles with protein incorporated in the lipid membrane and no evidence of aggregated protein (Figure 6.17).

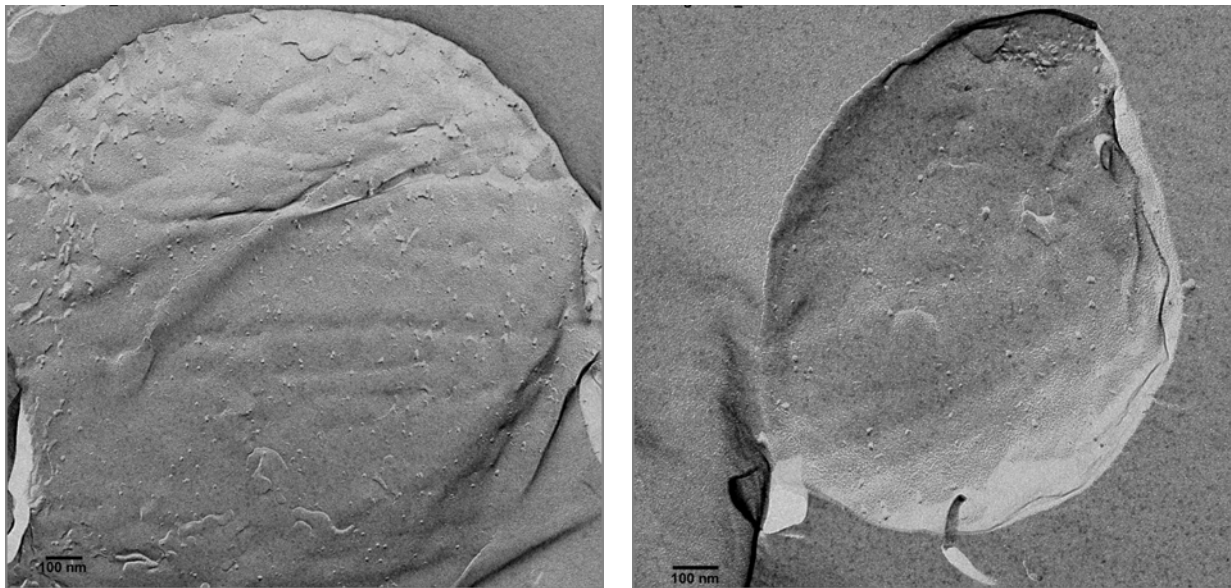


Figure 6.17: Reconstitution of Mdl1p into lipid vesicles. Proteoliposomes with reconstituted Mdl1p were analysed by freeze fracture electron microscopy.

Determination of the protein and lipid content of the proteoliposomes (s. chapter 5.2.19) showed that Mdl1p was reconstituted in a molar Mdl1p to lipid ratio of 1 to 160 lipid molecules. To finally demonstrate that the reconstituted Mdl1p was active, ATP hydrolysis of the proteoliposomes was determined. Indeed 85 % of the ATPase activity as observed for the digitonin-solubilised protein was found (Figure 6.18). In addition, this result indicates that a significant fraction of Mdl1p is reconstituted with the NBDs facing the outside. Under the assumption that the ATPase-activity of Mdl1p did not change in the lipid environment one can conclude that these proteoliposomes contain Mdl1p with the correct inside-out orientation of the NBDs to perform uptake experiments.

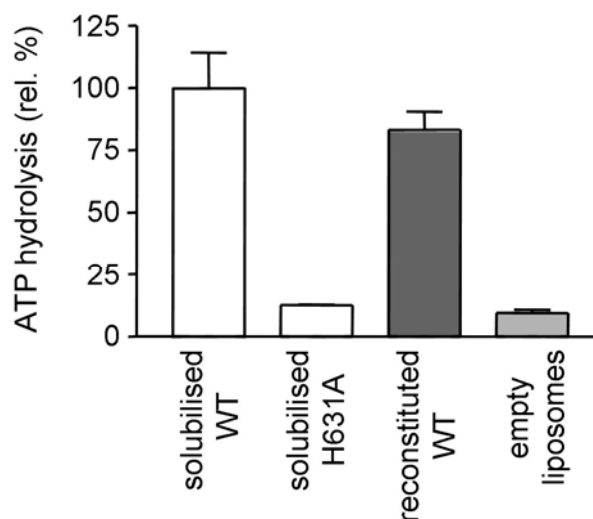


Figure 6.18: ATPase activity of Mdl1p after reconstitution. Functionality of the reconstituted Mdl1p was analysed in respect of ATP hydrolysis after reconstitution. Activity was measured at 30 °C for 10 minutes in presence of 5 mM ATP. Hydrolysis of the wild-type protein was preserved in the lipid bilayer as shown in comparison to the soluble protein.

6.2.6 Transport-assay

Mdl1p was shown to play an important role in the export of peptides between 6 and 20 amino acids in length from the mitochondrial matrix. Combinatorial peptide libraries were shown to be an extremely useful method to characterise substrate and transport specificity of various prokaryotic and eukaryotic transporters (Detmers et al., 2000; Doeven et al., 2004; Uebel et al., 1999). Therefore two peptide libraries $X_{(8)}$ and $X_{(23)}$ (where X represents all 19 amino acids, excluding cysteine, in equimolar distribution) were tested in transport assays using Mdl1p reconstituted into proteoliposomes. The libraries were radiolabelled and initial ATP-dependent transport was followed within 6 minutes. However, only background levels of radioactivity were detected indicating no significant transport of peptides into the liposomes (data not shown).

6.2.7 Single particle analysis of Mdl1p

Single particle analysis (SPA) of Mdl1p and image processing was done in collaboration with/performed by Dr. K. Model from the Max-Planck-Institute of Biophysics Frankfurt.

SPA provides a relatively fast three dimensional reconstruction method for proteins even with low protein concentrations and has been used to investigate the quaternary structure and oligomerisation state of the ABC proteins CFTR (Awayn et al., 2005), TAP1/TAP2 (Velarde et al., 2001), Pdr5p (Ferreira-Pereira et al., 2003), P-glycoprotein (Rosenberg et al., 1997), MRP1 (Rosenberg et al., 2001) and YvcC (Chami et al., 2002): two reports showed data that were interpreted as monomeric particles for P-glycoprotein (Rosenberg et al., 1997) and TAP2 (Velarde et al., 2001), whereas the other four studies reported particles that were identified as dimeric complexes YvcC (Chami et al., 2002), Pdr5p (Ferreira-Pereira et al., 2003), CFTR (Awayn et al., 2005) and MRP1 (Rosenberg et al., 2001). Here, a first three-dimensional reconstruction at low resolution from digitonin-solubilised Mdl1p particles (1404 particles) has been calculated (Figure 6.19 d + e).

Figure 6.19 B shows a representative micrograph of digitonin solubilised Mdl1p particles after negative staining with uranyl acetate (protein density appears white). The picture shows particles of a size range expected for the molecular weight range determined by SEC. Equivalent particles were picked from micrographs of a tilt pair (two different projection views of the same particle) in order to determine the tilt angle and tilt axis. Particles from the zero degree pictures were translationally and rotationally aligned and then classified using the neural network approach (Figure 6.19 C; (Sorzano et al., 2004). First indications of a (pseudo) 2-fold symmetry could be gained from refined classes averages of Mdl1p-particle projections.

A 3D volume was calculated from corresponding particles of the 4 boxed nodes (Figure 6.19 C; red square) enforcing 2-fold symmetry in z-axis perpendicular to the membrane plane (Figure 6.19 D). The dimension of the volume is determined to $125 \times 110 \times 95 \text{ \AA}^3$.

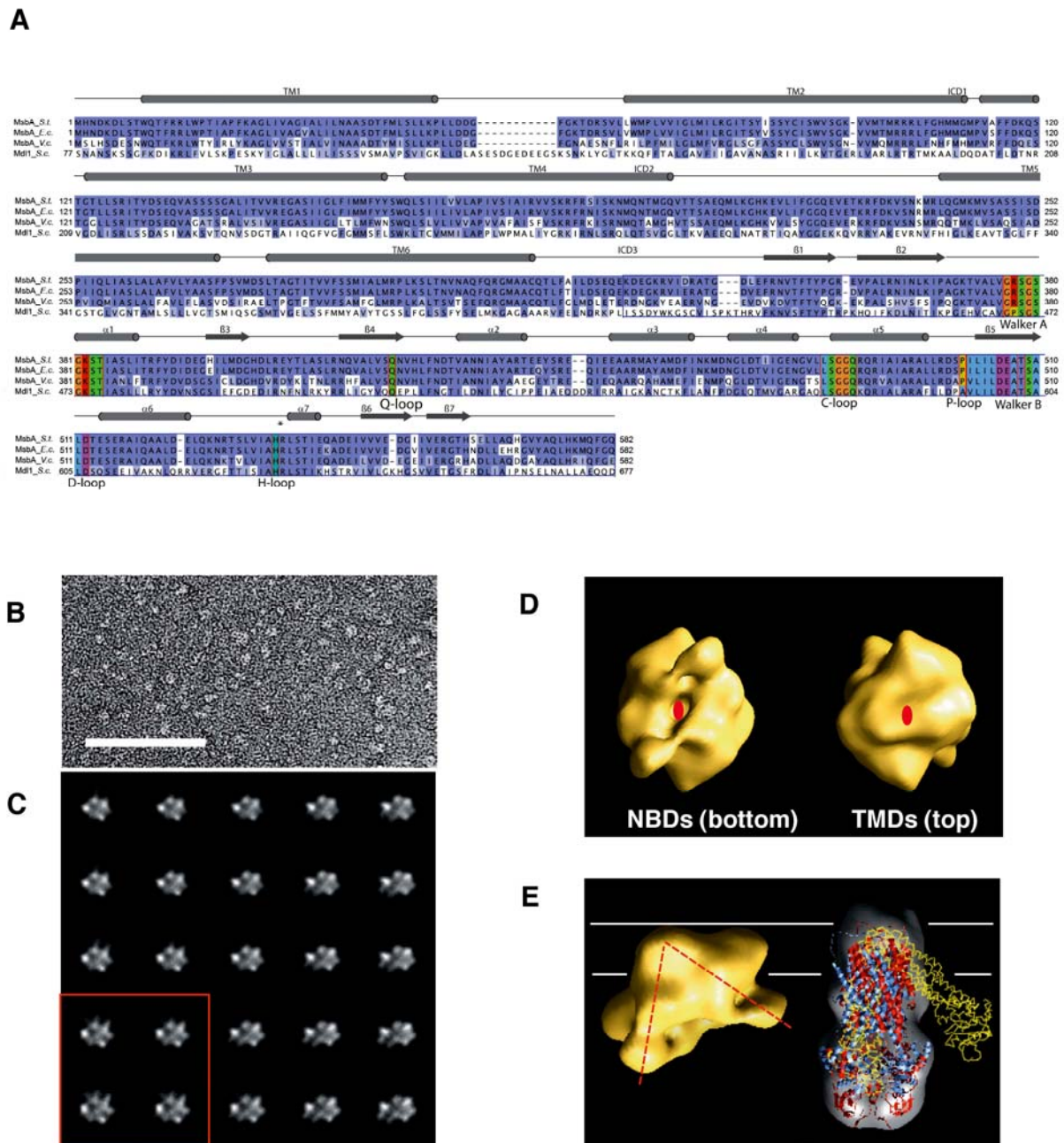


Figure 6.19: Single particle electron microscopy of Mdl1p. (A) Sequence alignment of A-chains from MsbA transporters with PDB accession numbers 1Z2R (closed form; (Reyes and Chang, 2005), 1JSQ (open form; (Chang and Roth, 2001) and 1PF4 (closed form; (Chang, 2003) and Mdl1p. The Walker A and B motifs, the Q-, C-, P-, D- and H-loops are boxed and coloured according to chemical properties of the amino acid residues. The overall colour code results from the BLOSUM62 score. (B) Typical electron micrograph of the negatively stained Mdl1p-SEC fraction. The nodes and corresponding particles used for the subsequent 3D reconstruction are boxed in red. Scale bar 100 nm. (C) Self organising map of 5x5 nodes from the complete data set of untilted particle projections. (D) Surface views of a representative 3D reconstruction of Mdl1p along the two-fold axis marked in red (top and bottom side). (E) Comparison of Mdl1p with different MsbA-crystal structures. The 3D reconstruction of Mdl1p was oriented and compared to the two “arms” of MsbA (1JSQ depicted in yellow). The two main axes are indicated by red dashed lines (left panel). A low-pass filtered volume of a closed MsbA structure was structurally matched and superimposed with all three 3D crystal structures of MsbA (right panel; 1Z2R blue, 1PF4 red and 1JSQ yellow). Membrane dimensions are indicated by white lines.

Figure 6.19 A shows an alignment of three MsbA amino acid sequences and Mdl1p demonstrating their high similarities (51 %). Since 3D structures of the MsbA proteins are available they were compared to Mdl1p single particles. A low-pass filtered volume of a

closed MsbA form was calculated and all three high resolution structures of MsbA were structurally matched and superimposed. Interestingly it was found that the the Mdl1p volume more closely resembles the open form of MsbA rather than the two closed forms (Figure 6.19 E).

The bottom and top views would logically resemble the potential hydrophilic nucleotide binding domains and the transmembrane domains respectively (Figure 6.19 D left and right panel). To date it remains to be verified by further experiments which side is anchored in the membrane and which part contains the nucleotide binding domains. Further refinement of the reconstruction is on the way in order to increase its resolution and perform fitting and docking of subunits into the volume.

6.2.8 *In organello* translation and peptide export assay

It has been shown that Mdl1p is involved in the export of peptides derived from mitochondrial encoded proteins. The exact nature of the transported peptides, and therefore the physiological role remains however uncovered, mostly because the transport function of Mdl1p has not been confirmed using an *in vitro* assay. To identify the substrate and the function of Mdl1p, an *in organello* translation assay was established. Here subunits of the respiratory chain encoded by the mitochondrial genome can be synthesised by isolated mitochondria in the presence of [³⁵S]-methionine (Black-Schaefer et al., 1991; McKee et al., 1984) and subsequently analysed by Tricine-SDS-PAGE (Figure 6.20). Almost no differences in the translation pattern can be detected between different mitochondria preparations.

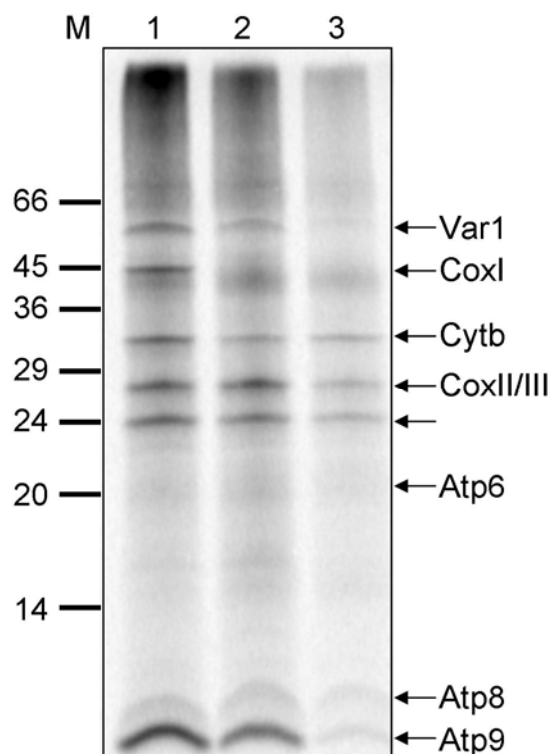


Figure 6.20: *In organello* translation. Tricine-SDS-PAGE of [³⁵S]-methionine labelled mitochondrial encoded proteins after an *in organello* translation assay. Different mitochondria preparations were analysed: 1 wild-type mitochondria grown in YEPD medium, 2 wild-type mitochondria grown in SCD medium, 3 mitochondria lacking Mdl1p and grown in SCD medium, M indicates protein marker in kDa.

Since their nuclear encoded partners are missing these subunits are not correctly assembled and degraded by AAA proteases after prolonged incubation (Arlt et al., 1996). A heterogeneous spectrum of degradation products is thus released from mitochondria. This can be measured as a time dependent accumulation of [^{35}S]-methionine labelled fragments in the supernatant after proteolysis (Figure 6.21).

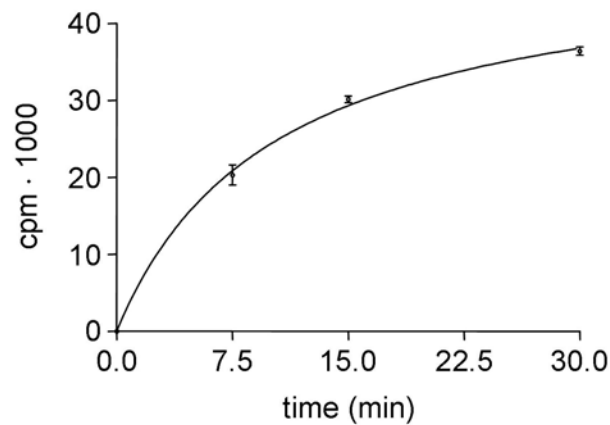


Figure 6.21: Release of [^{35}S]-methionine labelled degradation products from mitochondria of the wild-type *S. cerevisiae* BY4743. Release of a heterogeneous spectrum of peptides and amino acid residues from mitochondria. Supernatants were collected from wild-type mitochondria after 0 min, 7.5 min, 15 min and 30 min at 37 °C.

The supernatants can be further analysed by SEC (Young et al., 2001). Beside full degradation to free amino acids which is reflected by a elution peak of [^{35}S]-methionine two other maxima containing oligopeptides from 600 - 200 Da and 2100 - 600 Da can be distinguished. Mitochondria isolated from wild-type and ΔMDL1 strains were used for labelling of mitochondrial encoded proteins and the release and nature of the degradation products were analysed. The release of long peptides (Fig 6.22, peak I), was reduced by 25 % in ΔMDL1 mitochondria, as revealed by size exclusion chromatography analysis of the supernatant fraction (Figure 6.22) in this particular case. Shorter peptides as well as free methionine accumulated at similar levels in supernatants harvested from wild-type or ΔMDL1 mitochondria.

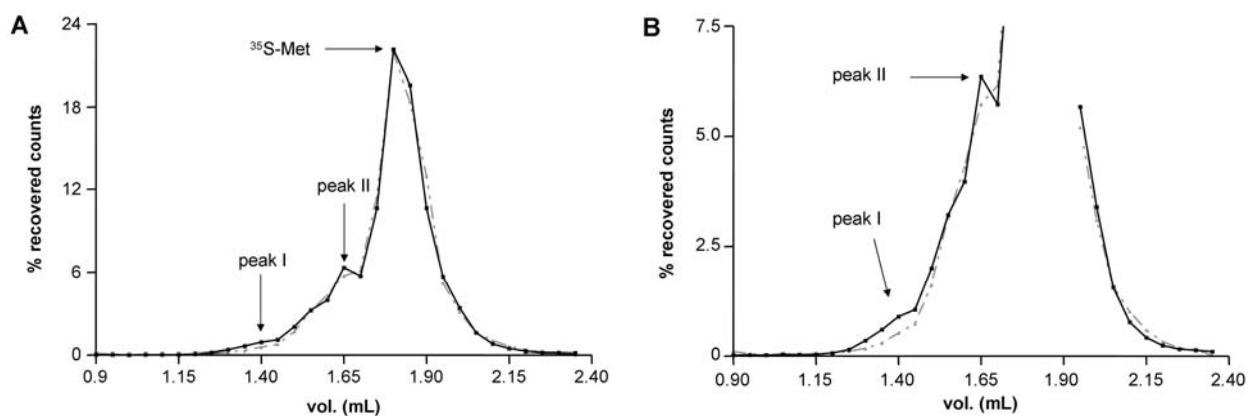


Figure 6.22: Mdl1p mediates peptide export from mitochondria. (A) Mitochondrial supernatants harvested after 30 minutes from wild-type (black solid line), or ΔMDL1 (grey dashed line) strains were fractionated by a Superdex Peptide column and radioactivity in each fraction was determined. Total counts recovered from each column run were set to 100 %. (B) A “zoom in” showing peak I and II in more detail. Representative profiles from single experiments are shown.

However, upon comparison of degradation products generated after *in organello* translation using wild-type and $\Delta MDL1$ mitochondria even after 17 runs no significant differences in peak I or II were detected. This is contrary to the observations of Young and colleagues (Young et al., 2001).

6.2.9 Occluded state in full-length Mdl1p

The isolated NBD of Mdl1p showed intermediate states with different nucleotide compositions generated during the catalytic cycle. Either two ADPs were trapped (wild-type with BeF_x or V_i) or states with two ATPs or one ATP and one ADP occluded in the dimer (E599Q mutant) were isolated (chapter 6.1.2 - 6.1.4). The question arose whether such an intermediate state exists in the full-length transporter to and whether there are differences possibly caused by superimposing effects of the TMDs. Therefore, the hydrolysis deficient mutant (H631A) of full-length Mdl1p was incubated with ATP supplemented with tracer amounts of $[\gamma\text{-}^{32}\text{P}]\text{ATP}$ and applied to a superdex 200 size exclusion chromatography column. Radioactive nucleotides coeluted exclusively with fractions 1 – 4 (Figure 6.23).

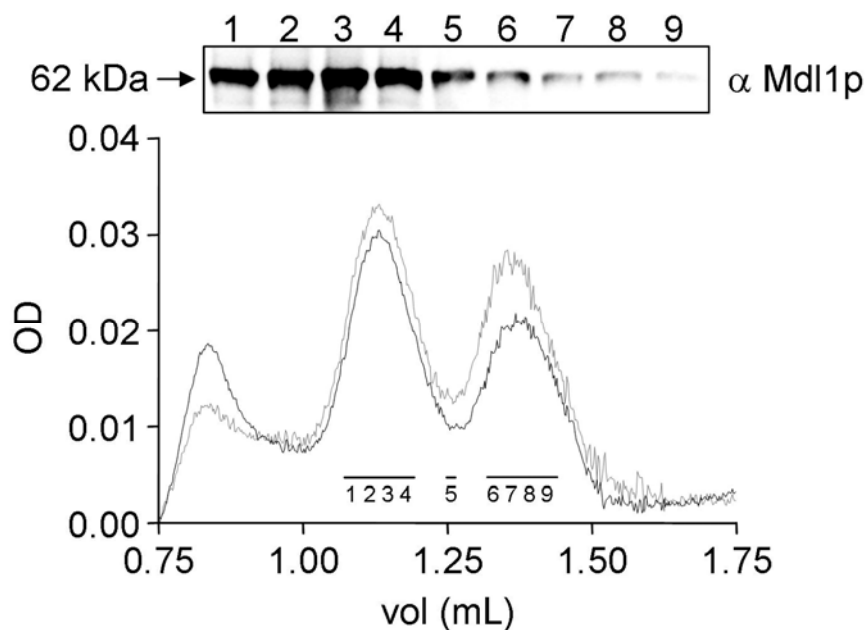


Figure 6.23: ATP to Mdl1p stoichiometry: Gel filtration and corresponding immunodetection. Mutant Mdl1p (H631A; 50 $\mu\text{g}/\text{mL}$) was incubated with 4.82 mM ATP supplemented with 0.062 μM $[\gamma\text{-}^{32}\text{P}]\text{ATP}$ for 5 minutes at 4 $^{\circ}\text{C}$. The Mdl1p peak (OD₂₆₀ grey line, OD₂₈₀ black line) elutes at 1.15 mL and is distributed over 120 μL . The protein amount was determined using the BCA assay whereas ^{32}P was measured by β -counting and the stoichiometry in each fraction was calculated.

All other fractions contained only background levels of radioactivity. The Mdl1p distribution was analysed by immunodetection and the protein concentration of each fraction was determined by the BCA assay. The amount of $[\gamma\text{-}^{32}\text{P}]\text{ATP}$ bound per protein was determined and a stoichiometry was calculated for each of the 4 fractions (Table 6.2).

Fraction	ATP (pmol)	Mdl1p (pmol)	ATP/Mdl1p-monomer
1	2,07	7,79	0,265
2	1,98	24,84	0,080
3	1,56	25,69	0,061
4	1,29	22,02	0,058

Table 6.2: Summary of the ATP to Mdl1p stoichiometry found in different fractions after SEC.

Fraction 1 shows the highest nucleotide content with a value of 26.5 % meaning that only half of a nucleotide is incorporated into one Mdl1p-dimer. This value needs to be considered carefully since a large error in protein determination might occur due to the low protein amount. All other fractions show values below 0.1 ATP per monomeric protein. These data show that however, in full-length Mdl1p no occluded state exists in the time-frame of 45 minutes contrary to the results obtained for the Mdl1p-NBD.

6.2.10 Peptide cross-linking experiments

Mdl1p was reported to play a role in peptide export from the mitochondrial matrix. Therefore, peptide photocross-linking experiments were performed to investigate this function in more detail. For this purpose an approach described in (Uebel et al., 1997) was modified. Besides the peptide R9* used in the study of also other peptides were designed.

N-formylated peptides derived from mitochondrial encoded respiratory chain subunits have been detected as minor antigens in complex with MHC I molecules at the surface of mammalian cells (Fischer Lindahl et al., 1991; Morse et al., 1996) peptides deduced from MHC I-presented sequences e.g. subunit I of cytochrome c oxidase were synthesised containing the photocross-linker benzophenyl-alanine. In addition, the peptides contained a tyrosine, which was used for radiolabelling with Na¹²⁵I. The advantage of the photocross-linking approach is that even transient interactions between substrate and Mdl1p can be detected.

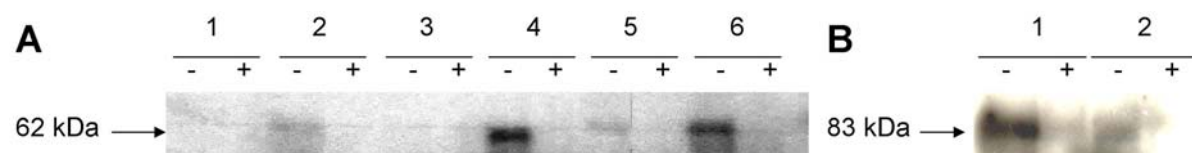


Figure 6.24: (A) Different mitochondria preparations (1: Y24137 ($\Delta MDL1$) in YEPD medium; 2: BY4743 (WT) in YEPD medium; 3: Y24137 + pMdl1p-065 (*gal*-promoter, Mdl1p + His-tag w/o linker) in SCD medium; 4: + pMdl1p-GPD (*gpd*-promoter, Mdl1p + His-tag) in SCD medium; 5: BY4743 + pMdl1-065 in SCD medium; 6: Y24137 + pMdl1-068 (*gal*-promoter, Mdl1p + His-tag + linker) in SCD medium; each 75 μ g) were solubilised with 0.8 % Triton X-100 and incubated with the peptide T10 (f-MYQR-Bpa-LYST-COOH, 4 μ M) for 3 minutes on ice. Cross-linking was performed using UV-light for 10 minutes. Samples were analysed by 10 % SDS-PAGE and autoradiography. Control samples with 100-fold excess of unlabeled peptide are marked with "+". (B) Microsomes (12.5 μ g) with the peptide transporter TAP expressed in Sf9-insect cells were used as reference samples with the peptides T10 (1) and R9* (2; NH₂-R Φ YQ Ψ STEL-COOH; each 4 μ M). Unlabeled competitor peptide (+) was used in an 100-fold excess.

Mitochondria isolated from yeast cells expressing either no Mdl1p or Mdl1p under different conditions were incubated with the cross-linker peptides R9* and T10* after solubilisation. Bound peptide was cross-linked by exposure to UV light. Cross-linking products were sepa-

rated by SDS-PAGE and the gel was exposed to an x-ray film after drying which was developed after 48 hours (Figure 6.24). In order to test the specificity of the reaction cross-linker peptides were competed out by a 100-fold excess of unlabeled peptide. Since the transporter associated with antigen processing TAP was reported to translocate peptides in the range of 8 to 16 amino acids (van Endert et al., 1994) microsomes from insect cells expressing TAP were used as control samples and cross-linking of T10* to TAP was compared with the cross-linking product between TAP and R9* which served as a positive reference. For samples without Mdl1p ($\Delta MDL1$ -cells) and (for unknown reasons) mitochondria from cells expressing Mdl1p plus a His-tag without a spacer in a $\Delta MDL1$ strain no cross-linking products could be obtained whereas all other samples showed cross-linking products running at the expected 62 kDa. The labelled cross-linker peptide can be competed out by an excess of unlabelled peptide in all cases indicating a specific interaction of the peptide with Mdl1p. While changing parameters in subsequent experiments e.g. peptides with different length, cross-linking time and mitochondrial preparations either no cross-linking products were obtained or all samples showed bands in the autoradiography even mitochondria lacking Mdl1p indicating that the peptides are cross-linked to another protein probably mtHsp70 which has a similar mass than Mdl1p.

7 Discussion

7.1 ATP hydrolysis cycle of the Mdl1p-NBD

Several crystal structures showed that the catalytic pocket for ATP hydrolysis is formed only through the cooperation of two NBDs (Hopfner et al., 2000; Locher et al., 2002; Smith et al., 2002) explaining the positive cooperativity in ATPase activity observed for MalFGK₂ and HisQMP₂ (Davidson et al., 1996; Liu et al., 1999; Nikaido and Ames, 1999). The residues involved in ATP binding and subsequent dimerisation of the NBDs have been characterised (Fetsch and Davidson, 2002; Loo et al., 2002; Moody et al., 2002). Although it is widely agreed that the dimer is a functional intermediate, several models have been proposed for the mechanism by which ATP drives the translocation of the substrate. Although it was previously reported that NBDs form dimers (Kennedy and Traxler, 1999), it was not elucidated how dimerisation of the NBDs is coordinated by nucleotides during one catalytic cycle.

Here several different intermediate states in the hydrolysis cycle of the Mdl1p-NBD were isolated and directly analysed in respect of their nucleotide content. Based on these data a new model for the hydrolysis cycle of an ABC transporter was proposed, unifying structural and functional data. Mdl1p has recently been identified as an intracellular homodimeric half-size ABC transporter localised in the inner mitochondrial membrane of *S. cerevisiae* (Young et al., 2001). Focus of this work was to elucidate the mechanism of peptide transport across membranes and how ATP drives this transport in particular. As Mdl1p is proposed to work as a homodimer, the NBD of Mdl1p was chosen as a model.

The C-terminal domain (amino acids D423 – R695) corresponding to the NBD was over-expressed as soluble protein in *E coli* and purified to homogeneity. The purified NBD was active in ATP binding and hydrolysis. The turn-over number of the Mdl1p-NBD (25 ATP/min) is comparable to the values obtained for other isolated NBDs (e.g. MJ0796, 12 ATP/min (Moody et al., 2002) or CFTR 6.7 ATP/min (Annereau et al., 2003)). In general, isolated NBDs show much lower turn-over numbers than the full-length transporters, and no substrate stimulation (Booth et al., 2000). The ATPase activity of the isolated Mdl1p-NBD was observed to be non-linearly dependent on protein concentration, indicating that the active form of Mdl1p is a dimer. Surprisingly, the NBD did not reveal positive cooperativity with increasing ATP concentration. This is in contrast to the behaviour of the isolated MJ0796 NBD, which showed positive cooperativity with a Hill-coefficient of 1.7 (Moody et al., 2002). However, in agreement with our data, other isolated NBDs like HisP and MalK displayed no cooperativity for ATP, while cooperativity in ATPase activity was determined in the fully assembled transporters HisQMP₂ and MalFGK₂ (Davidson et al., 1996; Nikaido et al., 1997). This different behavior of various ABC transporters shows that although dimerisation of the NBDs is proposed for all, there are differences in the cooperativity of the NBDs, which in some cases might be influenced by the TMDs.

The NBD of Mdl1p behaved as a monomer in size exclusion chromatography studies independently of the presence of nucleotides as previously shown for other isolated NBDs (Nikaido et al., 1997). Using either ortho-vanadate or beryllium fluoride the Mdl1p-NBD could be trapped as a dimer. ADP could not replace ATP in the trapping reaction, demonstrating that ATP binding and hydrolysis is essential for dimerisation. Even in the absence of ortho-vanadate or BeF_x , an ATP dependent dimer was obtained by mutation of the conserved glutamate downstream of the Walker B motif of Mdl1p (E599Q). The formation of stable dimers upon ATP binding was described by size exclusion chromatography of mutant archaeal NBDs (MJ0796(E171Q)/MJ1267 (E179Q)) (Moody et al., 2002). These mutants were deficient of steady-state ATPase activity as assayed by standard ATPase assays (P_i or ADP release) as were the equivalent mutants (E552Q/E1197Q or E556Q/E1201Q) of human and mouse P-glycoprotein (Sauna et al., 2002; Urbatsch et al., 2000b). The structures of some ABC transporters have suggested that this conserved glutamate is the most likely candidate to play the role of the catalytic carboxylate (Diederichs et al., 2000; Gaudet and Wiley, 2001; Hopfner et al., 2000; Hung et al., 1998; Karpowich et al., 2001; Smith et al., 2002). On the other hand, this glutamate of human P-glycoprotein was suggested not to function in the cleavage between β - and γ -phosphate but to be part of the switch region of ABC transporters possibly involved in the transmission of interdomain signals from the substrate binding site to NBDs (Sauna et al., 2002).

In this study the nucleotide composition of the trapped states of Mdl1p was analysed in detail by incorporating $[\alpha\text{-}^{32}\text{P}]\text{ATP}$ or $[\gamma\text{-}^{32}\text{P}]\text{ATP}$ into the dimer. After size exclusion chromatography, the nucleotide concentration was analysed by β -counting and correlated to the protein concentration. The nucleotide species were identified by TLC. Radioactive nucleotides were associated exclusively with the dimer. This observation demonstrated that ATP binding to the monomer is transient resulting in either subsequent dimerisation of the NBDs or dissociation of ATP from the monomer. It was shown that non-trapped NBDs have very fast k_{off} rates for nucleotide binding (Urbatsch et al., 1995b). Radioactive ADP in the presence of various concentrations of ATP was not incorporated into the dimer. Based on these results, ATP binding is regarded as essential and sufficient for dimerisation of the mutant.

Interestingly, although AMP-PNP or $\text{ATP}\gamma\text{S}$ binds with similar affinity to the E599Q mutant as ATP, none of these analogues were able to induce ATP dependent dimerisation. This observation is in line with results obtained for mutants from *M. jannaschii* (Moody et al., 2002). Incubation of the wild-type NBD of Mdl1p with an equimolar ratio of unlabeled MgATP and $\text{MgATP}\gamma\text{S}$ under BeF_x trapping conditions did not result in any incorporation of $\text{ATP}\gamma\text{S}$ in the dimer. This suggests that either the dimer interface is disturbed in the presence of $\text{ATP}\gamma\text{S}$ due to sterical hindrance or both nucleotides have to be hydrolysed to obtain the BeF_x trapped intermediate.

Analysis of the dimer always showed two nucleotides bound per dimer. In case of the BeF_x trapped NBD, the nucleotide species was solely ADP (with no P_i in the dimer), while in the E599Q mutant exclusively two ATP molecules were incorporated. These data demonstrated that both NBDs bind ATP during the ATPase cycle. During size exclusion chromatography, which takes 10 – 30 minutes, no nucleotides, but only the phosphate is released from the assembled dimer. Thus, these results demonstrate that both nucleotides have to be bound to both monomers before the stable dimer is formed, and that the two nucleotides then remain associated during the entire hydrolysis cycle.

Surprisingly, incubation of the E599Q mutant with ATP in the presence of Mg^{2+} at 30 °C resulted in slow hydrolysis of ATP, indicating that the E599Q mutant still hydrolyses ATP (but at a 3,000-fold reduced rate compared to the wild-type). This opened up the elegant possibility to explore the nucleotide composition of the mutant E599Q dimer of Mdl1p under single turnover conditions. After prolonged incubation in the presence of limiting amounts of ATP, an intermediate state, which contained one ATP and one ADP was formed. This intermediate state could be isolated for a prolonged period of time under strictly ATP limiting conditions, since in the presence of excess of ATP a state with two ATPs was isolated (data not shown). Such an asymmetric ATP/ADP state can be explained by a hydrolysis-event of the second ATP which is slower than hydrolysis of the first one, and suggests that the ATP hydrolysis occurs by a sequential mechanism.

Mutants in the conserved glutamate in human P-glycoprotein were shown to be able to hydrolyse one ATP molecule but unable to initiate a second ATP hydrolysis (Hrycyna et al., 1999; Sauna et al., 2002; Urbatsch et al., 2000b). However, the E599Q-NBD of Mdl1p catalyses multiple turn-overs. This is probably caused by dimer dissociation of the intermediate state with one ATP and one ADP, and rebinding of ATP by the monomers, starting a new cycle in which again only one ATP is hydrolysed. Indeed under ATP limiting condition this dimer dissociates before it hydrolyses the second ATP. To examine the hydrolysis of the second ATP the fate of the nucleotides after re-isolation of the dimer using size exclusion chromatography was followed. Unfortunately, after dilution by size exclusion chromatography, the association-dissociation kinetics of the equilibrium between the monomeric and dimeric states and the rate of ATP hydrolysis were of the same order ($t_{1/2} = \sim 30$ min), severely complicating the analysis. To examine the coupling of ATP hydrolysis, P_i release and dimer dissociation in detail, either methods with a better time resolution or an E599Q mutant with a faster hydrolysis rate should be used.

Interestingly, an asymmetric state with equimolar amounts of ATP and $\text{ATP}\gamma\text{S}$ was observed after incubation of the E599Q mutant with both of these nucleotides. This resulted in incorporation of one $\text{ATP}\gamma\text{S}$ molecule per dimer (data not shown). The wild-type protein did not incorporate $\text{ATP}\gamma\text{S}$ suggesting that binding of $\text{ATP}\gamma\text{S}$ to the NBD disturbs the dimer-dimer interface. The E599Q mutant seems to retain its ability to form a dimer, if only one $\text{ATP}\gamma\text{S}$ is bound, while the wild-type protein cannot accommodate the $\text{ATP}\gamma\text{S}$ in the dimer. The γ -

phosphate contacts residues in both NBDs, thus stabilising the dimer. Small changes in the NBD around the γ -phosphate thus strongly influence the ability of the NBD to form dimers, and the wild-type protein seems more affected by this than the E599Q mutant.

Published crystal structures of NBDs with a dimeric architecture showed high symmetry of the two monomers and equal occupation of both nucleotide-binding sites (Hopfner et al., 2000; Smith et al., 2002; Zaitseva et al., 2005a) even in the full-length structure of BtuCD (Locher et al., 2002). However, based on ortho-vanadate trapping experiments combined with 8-azido-ATP photolabeling, for P-glycoprotein and homologues a model was proposed in which only one NBD hydrolyses ATP at a time, but in an alternating manner (Senior and Gadsby, 1997; van Veen et al., 2000). Under hydrolysis conditions, it was shown for P-glycoprotein as well as for MalFGK₂ that 8-azido-ATP photolabeling of a BeF_x- or ortho-vanadate-trapped state resulted in approximately one [γ -³²P]ADP bound per dimer (Sankaran et al., 1997; Senior et al., 1995; Sharma and Davidson, 2000; Urbatsch et al., 1995b).

This stoichiometry of the dimer is in contrast to the data presented in this work. For all isolated Mdl1p-NBD dimers two nucleotides were found. Also in the BeF_x-trapped state two [γ -³²P]ADPs per dimer were obtained. This state contradicts the alternating-site model. The biochemical data acquired in this work are supported by observed nucleotide occupancy in different crystal structures. In summary three different intermediate states of the ATP hydrolysis cycle of the Mdl1p-NBD were isolated, containing two ATPs, one ATP and one ADP, or two ADPs.

Based on the experimental data a processive clamp model was proposed, which is depicted in Figure 7.1. As a first step in the ATPase cycle, ATP binds to the monomeric NBD. Since the ATP concentrations in the cell (for Mdl1p, in the mitochondrial matrix) are far above the K_D value determined for ATP binding, almost all of the NBDs would be in the ATP bound state under physiological conditions. Upon ATP binding, the NBDs dimerise. This state is in a dynamic equilibrium between the association, dissociation as well as hydrolysis of the ATP.

In the next step, one ATP is hydrolysed. In the experiments with the E599Q mutant, hydrolysis of the second ATP could not be observed, because in the ATP/ADP or the ADP/ADP bound state, the dimer is unstable and dissociates. In the slow hydrolysis cycle of the E599Q mutant, the dissociated monomers are reloaded with ATP and in a next cycle again one ATP is hydrolysed. Hydrolysis in the wild-type NBD however is 3,000-times faster and here two ADPs can be trapped in the dimer.

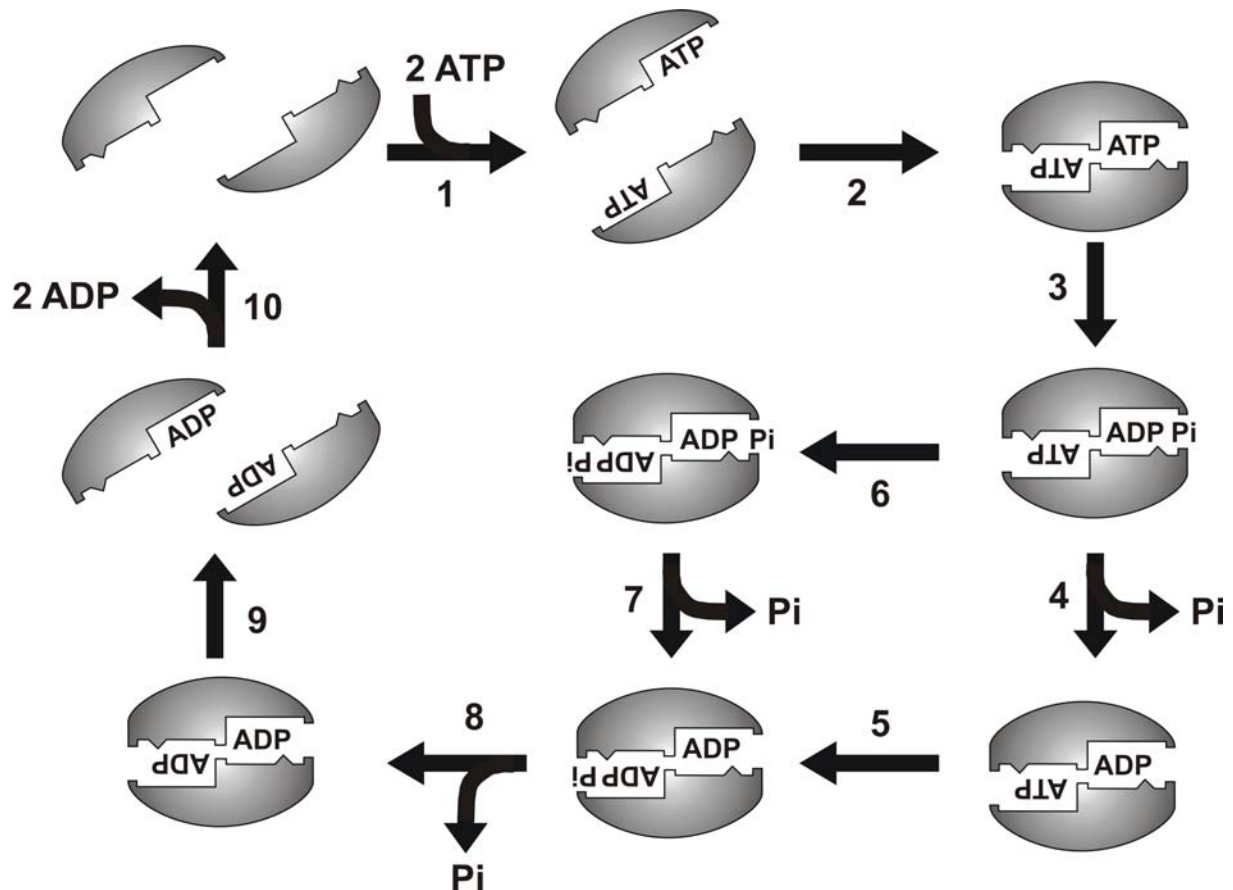


Figure 7.1: A processive clamp model for the ATPase cycle of the NBD from Mdl1p. ATP binding (step 1) on both NBD monomers induces formation of the dimer (step 2). After ATP hydrolysis by the first NBD (step 3), either the P_i is released first (step 4), followed by hydrolysis of the second ATP (step 5) and release of the second P_i (step 8), or the second ATP is hydrolysed first (step 6) and then both phosphates are set free (steps 7 & 8; the resulting ADP-ADP-Dimer is unstable and can only be isolated with the wild-type NDB under trapping conditions). After both ATPs are hydrolysed to ADP and both phosphates are released, the dimeric complex dissociates (step 9) and ADP (step 10) is released. The hydrolysis cycle can then start again with ATP binding. Not depicted in the figure: BeF_x or ortho-vanadate trapped the wild-type NBD in the intermediate state with two bound ADPs. Mutation of the catalytic glutamate resulted in E599Q-NBD, which under non-hydrolysis conditions was trapped with 2 ATPs inside the dimer and under hydrolysis conditions one ADP along with one ATP molecule was incorporated into the dimer.

Based on the much faster kinetics of ATP hydrolysis and the trapping of two ADPs in the wild-type NBD, this work suggests that both ATPs be hydrolysed sequentially in one cycle, in a processive mode. Finally, after both ATPs are hydrolysed, the dimer disassembles and both ADPs are released.

How exactly such a hydrolysis cycle is coupled to transport of the substrate and conformational changes of the TMDs, and whether the TMDs superimpose a regulatory effect on the NBDs remains unknown and requires further investigations. Smith and colleagues (Smith et al., 2002) proposed a possible model for the coupling of ATP hydrolysis to substrate transport. In this model, the TMDs of the non-substrate bound transporter forced the NBDs to remain in their monomeric state. Binding of the substrate to the high affinity site in the TMDs changes the conformation of the TMDs and removes the restraint on the NBD. Only then the ATP-loaded NBDs can form a dimer. Formation of the dimer forces a change on the TMDs and displaces the substrate-binding site, which results in transport of the substrate across the

membrane. Hydrolysis of the ATP and subsequently dissociation of the dimer resets the transporter.

In such a model, which fits to both the crystal structures and the experimental data obtained in this work, the formation of the ATP-bound dimer would be the power stroke. This would also explain how substrate binding induces ATPase activity by transmission of conformational changes between TMDs and NBDs (Chen et al., 2003b; Gorbulev et al., 2001; Neumann et al., 2002; van Veen et al., 2000). The mechanism of the coupling of ATP hydrolysis and substrate transport however requires further investigation.

7.2 Fingerprint of full-length Mdl1p

In order to see whether the Mdl1p transport complex is associated with other proteins in the inner mitochondrial membrane the YLR188W strain expressing Mdl1p fused to the tandem affinity tag (Rigaut et al., 1999) was used in this work. To prevent false positive association of proteins simply because one of them is expressed in high amounts all proteins should be expressed via the intrinsic wild-type promoter. Unfortunately Mdl1p is expressed in such low amounts that it is not visible in Coomassie or silver stained gels. Hence, no interaction partners of Mdl1p could be identified using this method.

ABC transporters residing in the inner mitochondrial membrane are challenging to analyse due to the complex two membrane architecture of mitochondria, the high membrane protein content of all kind of proteins with high affinity to ATP and many different other “transporters”. Hence, to study the structure, function, and mechanism of Mdl1p at molecular level, it is necessary to have the protein in a pure and active form. By systematic screens, the homologous over-expression of Mdl1p was established and the first fingerprint of Mdl1p is presented in this work. The galactose controlled expression system was successfully used to reach 100-fold over-expression of Mdl1p. The transporter was purified to homogeneity via one step affinity chromatography and the expressed protein was functional in respect of ATP hydrolysis. Furthermore, Mdl1p was reconstituted into liposomes preserving its activity.

Two prokaryotes were selected for expression: (i) the gram-negative *E. coli* and (ii) the gram-positive *L. lactis* but in none of them high levels of Mdl1p were reached. It is tantalising to speculate that the different lipid composition in these organisms compared to the inner mitochondrial membrane prevent accurate membrane insertion. Here cardiolipin was pointed out to provide essential function for structural maintenance of inner mitochondrial membrane proteins e.g. the cytochrome *bc*₁ complex (Lange et al., 2001), which is missing in the expression hosts. In addition, improper targeting might play a role since Mdl1p is predicted to have an N-terminal leader sequence, which was deleted in the prokaryotic expression cassettes.

Recently, an approach for heterologous expression of Atm1p – another ABC transporter in the inner mitochondrial membrane of *S. cerevisiae* – was suggested to be a general strategy for the recombinant production of ABC transporters especially for mitochondrial ABC transporters (Kuhnke et al., 2006). In this study a fusion gene containing the sequence of the OmpA signal peptide an octa-His-tag the *ATM1*-gene without the first 26 codons and a C-terminal Strep-tag II was used. Atm1p was expressed in an *E. coli* strain lacking the two major proteases Lon and OmpT. For expression “standard” conditions were used meaning growth at 37 °C in LB-medium. The purified product was processed yielding a protein without the OmpA signal peptide, the His-tag and part of Atm1p. The protein was analysed in regard to ATP hydrolysis both in detergent and reconstituted into proteoliposomes and displayed significant activity. Interestingly the ATPase activity of solubilised Atm1p was stimulated 5-fold upon the addition of cardiolipin emphasising the crucial role of this lipid for proteins of the inner

mitochondrial membrane. According to the authors, a major benefit using this strategy compared to a homologous expression of Atm1p with a Strep-tag II was the amount of protein obtained. In *S. cerevisiae* the yield was 50 µg/L culture where it increased 20-fold to 0.4 – 1 mg/L using *E. coli*. It is interesting whether this approach is sufficient for heterologous expression of Mdl1p and seems to be worth to try.

Another striking observation is the fact that homologous over-expression of Mdl1p is not achieved by using strong constitutive promoters. This is underlined by the observation that even after specifically controlled expression Mdl1p yields decrease drastically after 12 hours of induction. The protein does not seem to be toxic for the cells as growth continues without significant phenotype while Mdl1p is expressed via a *GPD*-promoter. Whether Mdl1p disappears due to transcriptional or translational regulation or due to simple degradation of excess protein is yet unclear. In conclusion, homologous expression only worked by switching from constitutive strong promoters to the inducible *GALI*-system.

Solubilisation of membrane proteins means that they are extracted from their natural surroundings and that the lipid bilayer is exchanged by an artificial environment of the detergent micelle (Poolman and Konings, 1993). The choice of the detergent used for the solubilisation and purification of membrane proteins is critical (Knol et al., 1998; Knol et al., 1996) in particular for proteins from the inner mitochondrial membrane due to its special lipid composition. At least two aspects must be fulfilled by the detergent: (i) reasonable protein amounts must be extractable from the membrane which is best done by tetradecylphosphocholine (FC-14) in the case of Mdl1p. (ii) More important yet is the activity of Mdl1p which is shown to be strongly affected by the type of detergent used. The data of this work show that Mdl1p keeps a significant ATPase activity after purification in 0.1 % digitonin, demonstrating that it remains folded in an active state whereas the zwitter-ionic detergent tetradecylphosphocholine almost destroys the ATPase activity of Mdl1p. The presence of n-dodecyl-β-D-maltoside in the

ATPase experiments drastically decreased ATP hydrolysis of Mdl1p. Strikingly, this detergent was recently reported to preserve the ATPase activity of the ABC transporter Atm1p from the inner mitochondrial membrane of *S. cerevisiae* to a certain extent when stored overnight and compared to n-octyl-β-D-glucoside or Hecameg (digitonin was not tested in this study) (Kuhnke et al., 2006). Digitonin was reported to keep mitochondrial protein formations and its higher oligomers e.g. complexes III, IV and V of the respiratory chain in a stable and active form (Schägger and Pfeiffer, 2000). Hence, digitonin is the detergent of choice for protein electrophoresis under native conditions. Since ATPase activity of Mdl1p was preserved in digitonin, it was used in the following experiments.

In order to determine the apparent binding constant of ATP for Mdl1p, 8-azido[α-³²P]ATP photocross-linking experiments were performed, in which 8-azido[α-³²P]ATP is a competitive substrate for ATP with a similar specificity constant (k_{cat}/K_M) as ATP. Remarkably, the apparent dissociation constant of MgATP of 0.26 µM for Mdl1p was obtained. This value is 2 to 3

orders lower than that of other ABC transporters (Horn et al., 2003; Lapinski et al., 2003; Qu et al., 2003; Wolters et al., 2005). Since the ATP concentration inside the matrix is in the lower millimolar range (1 – 5 mM; Prof. U. Brandt, Medical School, Goethe-University Frankfurt, personal communication) Mdl1p is always “loaded” with ATP. The $K_{M(ATP)}$ of 850 μM , which is more than 3,000 times higher than $K_{D(ATP)}$ implies that ATP-binding and ATP-hydrolysis are different steps which are independent from each other. It is possible that hydrolysis is triggered by an external signal e.g. substrate binding.

As shown in this work on the isolated NBD of Mdl1p, ATP binding induces a conformational change of the NBD enabling the dimerisation of the catalytic domain, which is the first step in ATP hydrolysis and substrate transport. In competition assays with 8-azido[α - ^{32}P]ATP, using solubilised full-length Mdl1p, the nucleotide specificity was alighted and the following order was obtained: ATP as the physiological substrate shows the highest affinity for Mdl1p whereas ADP, AMP-PNP, CTP, UTP and GTP have an intermediate affinity. This demonstrated that the isolated solubilised full-length Mdl1p binds nucleotides with a similar affinity as the isolated NBD, suggesting that the TMDs do not affect the nucleotide-binding step. AMP-PNP, the non-hydrolysable ATP analogue, also bound with a reduced affinity, further demonstrating previous observations, that AMP-PNP does not mimick ATP binding perfectly. Other studies (Nikaido et al., 1997; Sharma and Davidson, 2000) as well have demonstrated that AMP-PNP binds with a reduced affinity, and indeed AMP-PNP can not induce dimerisation of the NBDs.

AMP displays a very low affinity as expected and did not compete with 8-azido-ATP-binding. This is important in view of publications which showed that CFTR has an adenylate kinase activity (Gross et al., 2006). Since Mdl1p does not bind AMP, it is clear that this is not a general property of ABC proteins.

In summary, Mdl1p can be energised by different nucleoside triphosphates. This broad specificity is also found for other ABC transporters (al-Shawi and Senior, 1993; Meyer et al., 1994; Müller et al., 1994) and results only from a π - π interaction between the base of the nucleotide with the NBD (Hung et al., 1998).

Purified Mdl1p shows a high ATPase activity ($2.1 \mu\text{mol} * \text{min}^{-1} * \text{mg}^{-1}$). To proof that the observed activity was derived from the purified protein and not from another ATPase which was copurified in very low amounts two ATPase deficient mutants were used. The E599Q mutant of the conserved glutamine one amino acid downstream of the Walker B motif showed already in the soluble NBD a 3,000-fold lowered ATP hydrolysis activity. The mutation of the histidine in the H-loop of different ABC transporter NBDs (Davidson and Sharma, 1997; Nikaido and Ames, 1999; Shyamala et al., 1991; Zaitseva et al., 2005c) led to proteins that showed almost no ATPase or transport activities.

The E599Q and H631A mutant of full-length Mdl1p were able to bind ATP but were defective in ATP hydrolysis. This demonstrated that these mutants behave in a similar manner as in

the isolated NBDs, and that the above observed ATPase activity resulted from purified Mdl1p. The activity of the full-length protein is much higher than the activity of the isolated NBD at similar concentrations. Remarkably, the activity of the isolated NBD was strongly dependent on the NBD concentration where it was independent of the concentration in the full-length protein. This showed that the association rate of the NBDs is not rate-limiting in the full-length protein most likely because of the high local concentration of the NBDs in the full-length transporter due to their close vicinity.

In vivo complementation studies described by Chloupková and colleagues (Chloupková et al., 2003) were used to further analyse the E599Q and H631A mutant in a more natural environment. *ΔATMI* cells show a strong growth defect that can be overcome by over-expression of Mdl1p. Since the influence of different yeast strains and selection markers should be excluded the same strains and plasmids applied in the report above were used (kindly provided by M. Chloupková, Portland OR). The only change was made by introducing the point mutations in the *MDL1*-gene. No rescue of the *ΔATMI* phenotype was achieved with the E599Q and H631A mutant of Mdl1p (S. Gompf, Institute of Biochemistry, Goethe-University Frankfurt; personal communication). This is in line with the observation that an ATPase deficient ABC transporter *in vitro* leads to a non-functional transporter *in vivo*.

The observed activity of Mdl1p is higher than activities reported for the majority of ABC transporters e.g. MRP ($0.46 \mu\text{mol} \cdot \text{min}^{-1} \cdot \text{mg}^{-1}$, (Chang et al., 1997), MsbA ($0.04 - 0.15 \mu\text{mol} \cdot \text{min}^{-1} \cdot \text{mg}^{-1}$, (Doerrler and Raetz, 2002) or BmrA ($1.2 \mu\text{mol} \cdot \text{min}^{-1} \cdot \text{mg}^{-1}$, (Ravaud et al., 2006). Only Atm1p which like Mdl1p is an ABC transporter of the inner mitochondrial membrane showed a similar turn over of $127 \cdot \text{min}^{-1}$ ($1.9 \mu\text{mol} \cdot \text{min}^{-1} \cdot \text{mg}^{-1}$) (Kuhnke et al., 2006) compared to $150 \cdot \text{min}^{-1}$ in case of Mdl1p. It is possible that the high activity of Mdl1p is caused by a stimulating factor e.g. the substrate or a certain lipid e.g. cardiolipin (s. above) that is bound to the protein during purification and still present in the ATPase assay.

The ATPase activity of Mdl1p was measured in the presence of DTT. DTT, glutathione and β -mercapthoethanol slightly stimulate the ATPase activity of Mdl1p about 1.3-fold (Ariane Zutz, Institute of Biochemistry, Goethe-University Frankfurt, personal communication). A similar stimulation of the ATPase activity by DTT was seen in P-glycoprotein (MDR1/ABCB1) (Urbatsch et al., 2000a; Urbatsch et al., 2000b). Mdl1p has five non-conserved cysteines: one in the putative targeting sequence, which is cleaved off in the functional transport complex, one in TMH 4 and three in non-conserved regions of the NBD. Whether the stimulatory effect of DTT is due to reduced cysteines and opened disulphide bridge(s) in Mdl1p is not yet clear.

In a recent report the influence of different thiolgroup-containing compounds on the ATPase activity of Atm1p was investigated in more detail (Kuhnke et al., 2006). At millimolar concentrations of glutathione, cysteine, cysteinyl-glycine and DTT stimulated the ATP hydrolysis 3.5 to 5-fold. The oxidised forms of the chemicals did not increase the ATPase activity. Cys-

teine thiol groups in peptides already increased the ATPase activity at micromolar concentrations suggesting that in addition to the thiol groups Atm1p recognises the peptide backbone. Since Mdl1p is a high copy suppressor of the Atm1p knock-out phenotype it would be interesting whether these substrates influence the ATPase activity of Mdl1p.

Surprisingly, no occluded state with two nucleotides (2 ATPs, 1 ATP and 1 ADP or 2 ADPs) trapped inside Mdl1p could be isolated using the H631A full-length Mdl1p mutant as it was found for the isolated E599Q mutant NBD. Since ATP binding is not changed in the full-length transporter this observation can be explained by a much faster off-kinetic in case of full-length Mdl1p meaning that the nucleotides are lost on the way through the gel filtration column (45 – 60 min).

In this work purified Mdl1p was used for structural analysis via single particle electron microscopy. Single particle analysis has successfully been applied to other ABC transporters demonstrating the power of this method already for particles below 750 kDa. The Mdl1p preparation method uses digitonin to extract the protein from the membrane, affinity purification, and a step via size exclusion in order to obtain a monodisperse preparation. This procedure yields suitable Mdl1p particles ready for a first structure determined via SPA.

Although conformation by fitting and further analysis of the present data needs to be done in the single particle analysis Mdl1p appears to be in a dimeric state in digitonin since the dimensions of the particle of $125 \times 110 \times 95 \text{ \AA}^3$ are most likely to small for a dimer and to large for a monomer. Since the protein is active in ATP hydrolysis in this detergent the minimal functional unit of Mdl1p is a dimer as it was already concluded from the Mdl1p-NBD data. Interestingly, there are different particles obtained for different ABC transporters. The full-size transporters MRP1, Pdr5p and CFTR gave particle dimensions which fit to (homo) dimers whereas in particles of P-glycoprotein which is a full-size transporter only a monomer can be imagined. Similar sizes were obtained for the half-size transport complex TAP1/TAP2 and YvcC implicating heterodimeric or homodimeric structures respectively.

In a further step it would be interesting to see whether a modified preparation for SPA adding lipids and a subsequent detergent removal step with Bio-beads leads already towards 2D crystallisation (refer to chapter of reconstitution). Possibly this method would result in Mdl1p-lipid patches like it was shown for YvcC. Therefore, this work shows a first glimpse of a mitochondrial ABC transporter and understands it self as a step towards high resolution 3D structure determination giving not only insights to the mode of action of Mdl1p but in addition uncovers its natural substrate.

Mdl1p was reconstituted into DDM destabilised proteoliposomes prepared from *E. coli* lipids. The method has been successfully used for the functional reconstitution of a variety of transporters (Driessen et al., 1988; Knol et al., 1996; Patzlaff et al., 2003; Poolman et al., 2005).

Reconstituted Mdl1p shows 85 % of the ATPase activity as observed for the digitonin solubilised protein confirming that Mdl1p is stable during the reconstitution procedure. In addition,

this result indicates that a significant fraction of Mdl1p is reconstituted with the NBDs facing to the outside. Under the assumption that the ATPase-activity of Mdl1p did not change in the lipid environment a inside-out orientation of most of the protein can be implied which makes the proteoliposomes suitable for uptake experiments.

Strikingly, no transport activities for peptides included in combinatorial $X_{(8)}$ or $X_{(23)}$ peptide libraries could be detected with this system. Either this is due to the fact that Mdl1p has rather high substrate specificity and this explicit peptide(s) is/are underrepresented in the peptide pool of the libraries and hence not detectable in the uptake studies. Alternatively, the substrate of Mdl1p is not only a set of peptides but also more complex. This speculation would fit into the context that for example ABC-me a homologue of Mdl1p in mice erythrocytes is up regulated upon increased heme biosynthesis (Shirihai et al., 2000). In this case, the peptide serves as a kind of chaperone for a potential intermediate in the course of heme biosynthesis and Mdl1p would function as a linker between the two compartments of heme synthesis namely the mitochondrial matrix and the cytosol.

Another explanation for the negative result in the transport assay with purified reconstituted protein might be the C-terminal manipulation of Mdl1p by the octa-His-tag. *In vitro* assays performed in this study clearly showed Mdl1p to be active in ATP hydrolysis. Complementation assays where Mdl1p is used to overcome the phenotype of a *Atm1p* knock-out indicate that only the wild-type but not the His-tagged version is able to substitute *Atm1p* (S. Gompf, Institute of Biochemistry, Goethe-University Frankfurt; personal communication). Both results indicate that ATP hydrolysis is a very robust property of ABC transporters conserved *in vitro* but the whole transport process might be much more fragile. This is in line with the observation that already subtle changes at the C-terminal end of the ABC transporter TAP lead to transport deficient mutants (Ehse et al., 2005).

In this context another remark needs to be considered. Mdl1p was suggested to be a peptide transport using a rather indirect method. Different supernatants were compared in respect of [^{35}S]-methionine labelled peptides exported from mitochondria. Since Mdl1p resides in the inner membrane one can imagine a processing of the substrate transported by Mdl1p in the inter membrane space. Hence, the identified peptides outside in the supernatant can be dramatically misleading especially concerning the length of the peptide.

In order to decrease the complexity of a whole transport event in a reconstituted system another experiment was used to approach the substrate specificity of Mdl1p. Solubilised Mdl1p was tried to be cross-linked with UV-light activated peptides. The advantage of the photocross-linking approach is that even transient interactions between substrate and Mdl1p can be detected and an accumulation of this product is achieved. Unfortunately promising results where a 9mer peptide mimicking the C-terminal end of *Cox1p* was specifically cross-linked to Mdl1p were not reproducible. Peptides of a *Cox1p* homolog in mouse were found on cell surfaces presented by MHC class I molecules (Fischer Lindahl et al., 1991) meaning that these minor antigens need to be transported from the mitochondrial matrix to the ER lumen. There-

fore, it was speculated that a similar pathway might exist using Mdl1p even so that *S. cerevisiae* lacks an immune system.

Finally, the peptide export experiments based on a *in organello* translation set-up did not show significant differences between Mdl1p containing mitochondria and organelles lacking the ABC-transporter. This is in contrast to data published by Young and colleagues (Young et al., 2001). Here differences in culturing the cells e.g. harvesting the cells at different ODs and therefore at different timepoints in the cell life cycle or subtle differences during assay handling might account for this discrepancy since the reported effects in *AMD1* cells are tiny.

Several computational analysis predicted Mdl1p to contain a presequence for mitochondrial targeting and inner membrane insertion (Claros and Vincens, 1996). Based on these data two constructs lacking the first 59 and 68 amino acids respectively were generated in order to test the ability to switch the insertion of Mdl1p from the inner mitochondrial membrane to the endoplasmatic reticulum or the plasma membrane. Immuno-gold labelling experiments confirmed the localisation of Mdl1p in the ER membrane (Gompf et al., 2006). This approach is based on the idea to analyse the transport activity of Mdl1p in simpler environment compared to the situation inside the mitochondrion.

Microsomes prepared from wildtype BY4743, $\Delta Y11048c$ and $\Delta Y11048c$ cells expressing $\Delta 68Mdl1p$ were used for uptake experiments (a modified assay is described in chapter 5.2.23). Various radiolabelled peptide libraries containing 5 to 23 amino acid residues, and the peptide R9LQK, which is a model peptide for the TAP transporter were used but no Mdl1p specific accumulation was detected indicating that no transport occurred. As a further remark these libraries did also not stimulate ATP hydrolysis of digitonin solubilised Mdl1p later on (A. Zutz, Institute of Biochemistry, Goethe-University Frankfurt; personal communication). The same was true for the 6, 9 and 12 amino acid residues long peptides T8, T9, T10 whose sequences were deduced from findings that formylated peptides were found in complex with class I major histocompatibility molecules at the surface of mammalian cells as minor antigens derived from mitochondrial encoded respiratory chain subunits (Fischer Lindahl et al., 1991) e.g. subunit I of cytochrome c oxidase. To test the possibility that Mdl1p is involved in the heme-biosynthesis pathway shuttling intermediate products from the matrix to the cytosol [^{14}C]aminolevulinic acid was used in transport experiments using microsomes with $\Delta 68Mdl1p$, but again no transport was observed (S. Gompf, Institute of Biochemistry, Goethe-University Frankfurt; personal communication).

As mentioned above mitochondrial targeting is often mediated through N-terminal leader sequences consisting of up to 105 residues highly enriched in basic, hydrophobic and hydroxylated amino acids (Graf et al., 2004; Neupert, 1997). Also much less is known about sequence and structure of internal mitochondrial targeting signals such internal leader sequences have been observed e.g. for the ATP/ADP carrier or the oxoglutarate carrier (Kubrich et al., 1998; Palmisano et al., 1998). In addition, such a internal signal for targeting was discussed for

Mdl1p in a recent report (Janas, 2002). To answer the question of the targeting sequence purified Mdl1p was analysed by N-terminal sequencing (Edman degradation) in this work. The sequence, which was obtained by this approach, continued on position 60 of the original Mdl1p sequence meaning that the protein is cleaved after amino acid 59. In combination with the immuno-gold labelling results of yeast cells expressing a $\Delta 59$ version of Mdl1p that is found in the endoplasmatic reticulum (Gompf et al., 2006) a N-terminal targeting sequence of 59 amino acids can be assumed for Mdl1p. In two out of three sequences the first amino acid revealed by Edman degradation is a glutamate instead of a glutamine which is found in the original Mdl1p sequence at position 60. So far, no modification by the cleavage enzyme in the mitochondrion turning a carbonyl function to an amine group is described so far. However, there is a chance caused by the sequencing procedure itself that in each step approximately 10 % of glutamine turns into glutamate (Prof. H. Schagger, Medical School, Goethe-University Frankfurt, personal communication)

The *in organello* translation assay established in this work was used to synthesise the substrate of Mdl1p by its natural source. The supernatant after such an assay and subsequent proteolysis was used for uptake assays using proteoliposomes and inverted membrane vesicles (IMVs) generated from mitochondria. The IMVs were shown to contain Mdl1p with the NBDs facing to the outside serving the basis for import studies (S. Gompf, Institute of Biochemistry, Goethe-University Frankfurt; personal communication). Again no significant transport of the [³⁵S]-methionine-labelled peptides were measured.

To summarise all experiments (which are: peptide cross-linking, stimulated ATP hydrolysis, peptide transport assays with proteoliposomes and microsomes containing an Mdl1p variant and IMVs plus substrate generated by *in organello* synthesis) performed in order to reveal the potential substrate of Mdl1p and to illuminate its physiological role as a peptide transporter somehow missed a clear positive answer.

More drastically the peptide export assay described by Young and colleagues (Young et al., 2001) (that pointed Mdl1p out be a peptide exporter) established in this work did however not confirm the differences in the pattern of exported peptides between mitochondria containing Mdl1p and mitochondria lacking the transporter. Therefore, the role of Mdl1p as a “simple” peptide exporter from the mitochondrial matrix to the intermembrane space should be reconsidered. A complex situation like the one which is found for Mdl1p potentially bares a complex substrate.

7.3 Outlook

To current knowledge, the expression of a mitochondrial ABC transporter to a level as high as 1 % of total membrane protein, as obtained in this study, has not been reported so far. Additionally this study provides an efficient procedure to obtain highly purified Mdl1p, functionally reconstituted into liposomes prepared from *E. coli* lipids. The availability of straightforward methods for over-expression and purification of Mdl1p, and the ease of DNA manipulation due to the gene cassette approach provide the basis for future studies on structure and function of Mdl1p.

It is now feasible to resolve the transport function and substrate specificity of the protein complex *in vitro* and to investigate the molecular mechanism by which ATP binding and ATP hydrolysis drive solute translocation.

Furthermore, the chemo-mechanical coupling between the two motor domains and the transmembrane domains can now be studied by different biochemical and biophysical methods.

Finally, the reported expression and purification procedure is a basis to determine the structural organisation of the homodimeric Mdl1p complex including its membrane topology, the architecture of the translocation pore and potential substrate-binding sites.

To identify the substrate specificity and transport function of Mdl1p, an *in organello* translation assay with isolated mitochondria was established. Here, the mitochondria-encoded genes are translated and labelled with [³⁵S]-methionine. These translation products are degraded by AAA proteases. The export of radiolabelled fragments from mitochondria isolated from *ΔMDL1*, wild-type and Mdl1p over-expressing strains can now be examined in more detail especially by mass spectrometry. In parallel, the accumulation of degradation products in Mdl1p positive and negative mitochondria can be compared.

Furthermore *in organello* translation provides an elegant way of synthesising the potential substrate of Mdl1p in an already labelled way. This way the substrate can be exported from Mdl1p-containing mitochondria after *in organello* translation into the supernatant and recovered from there or it is kept inside the matrix of mitochondria lacking Mdl1p.

To test the alternative hypothesis if Mdl1p is involved in transport function related to iron homeostasis or heme biosynthesis mitochondria can be exposed through various radioactive compounds e.g. iron or organic precursors and the trace can be followed throughout the exported material. Comparison of mitochondria isolated from *ΔMDL1*, wild-type and Mdl1p over-expressing strains may shed light on the physiological role of Mdl1p.

Another technique to identify compounds transported by Mdl1p might be a test for stimulated ATPase activity like it was shown for several ABC transporters (Borths et al., 2005; Gorbulev et al., 2001). This setup uses the circumstances that ABC transports display a much higher turn-over rate of ATP hydrolysis in the presence of the (bound) substrate. This approach can

be applied to reconstituted Mdl1p as well as to solubilised protein in a simpler design. Basically a whole catalogue of (hydrophobic) substances can be screened this way.

As depicted above, ATP binding induces dimer formation of the NBDs. By means of site-directed mutagenesis of catalytic residues (e.g. E599Q) or trapping reagents (BeF_x or orthovanadate), a dimer with two nucleotides bound can be arrested. Since it turned out to be more complicated to transfer this experiment to the full-length protein monitoring of catalytic processes upon ATP binding needs a different attempt. One possibility is site-specific labelling of the transporter by fluorescent adaptors. The fluorophores bind to the C-terminus of each nucleotide-binding domain via Ni^{2+} -NTA-groups (van der Does et al., 2006), which, based on biochemical and structural data of other ABC transporters, undergo large conformational changes during the transport cycle. Thus, ATP-induced dimer formation also in the homodimeric Mdl1p complex reconstituted into liposomes should be followed by homo-FRET or fluorescence quenching.

One of the key questions concerning primary transporters is how the energy of binding and hydrolysis of ATP is transferred to substrate translocation. Based on structural and biochemical similarities with secondary transporters, it was proposed that ABC transporters function via an alternating access model, where formation of an ATP-sandwiched dimer of the NBDs results in transfer of the substrate across the membrane (van der Does and Tampé, 2004). To validate this model, conformational changes within the TMDs dependent on ATP binding or hydrolysis need to be identified. Guided by the MsbA structure from *Vibrio cholera* (Chang, 2003) or *S. typhimurium* (Reyes and Chang, 2005) cysteines will be introduced in TM2 and TM5 of Mdl1p, which are possibly located on the dimer interface. A cysteine-less Mdl1p has already been created by replacing all five cysteines to alanines or serines. After expression of single-cysteine mutants, a screen for disulphide cross-linked Mdl1p monomers after addition of copper o-phenanthroline or thiol-specific cross-linkers with different spacer lengths can be performed. Furthermore, it can be determine how ATP binding, dimer formation, or possibly substrate binding in wild-type and mutant Mdl1p (E599Q, H631A, etc.) modulates the identified contacts with the transmembrane domains. The accessibility of single-cysteine residues toward thiol-specific reagents at different stages of the translocation cycle will be examined. These studies will provide important information regarding to conformational changes within the transporter and help to identify the step where the energy stored in the NBD is transferred to the TMDs. In order to study the interaction between the NBDs and the TMDs, cysteine-scanning mutagenesis will be applied. Based on homology modelling, cysteines will be inserted on the transmission interface of the NBDs, which will be able to form disulphide cross-links after oxidation with copper o-phenanthroline or thiol-specific cross-linkers. Again, whether these cross-links are modulated by different transport conditions will be investigated.

The reconstitution of Mdl1p was optimised, and 85 % of the protein is oriented with the NBD facing the outside according to the ATP hydrolysis data assuming that no activity of Mdl1p is lost or stimulated in the liposomes. However, a direct proof of the orientation is still waiting.

To answer this question one can use protease protection assays in which the His-tag is cleaved off by Factor X_a (a cleavage-site lies between the C-terminal end of Mdl1p and the His-tag). Exact quantification can be achieved by taking fully solubilised proteoliposomes as background and non-cleaved proteoliposomes as a 100 % value. To optimise reconstitution, the effect of different lipids on the ATPase activity can be systematically analysed.

Single particle EM pictures already made the entry into structure determination of Mdl1p. For higher resolution, attempts will be made to reconstitute Mdl1p at high protein-to-lipid ratios, to thus obtain 2D crystals. These 2D crystals will also be studied by negative stain and cryo electron microscopy. After optimising the over-expression and purification, sufficient protein amounts are available to start the study of the 3D structure of the Mdl1p complex. A long-term objective might be structure determination of the transport complex Mdl1p by x-ray analysis. Within the last years, significant achievements have been made in the structural analysis of various bacterial transporters. However, eukaryotic transporters, in particular expressed at low levels, are still a challenge in structural biology. A necessary step here is to scale up the expression to high volume fermentation. Also the solubilisation and purification procedure might need to be further adapted for this purpose.

A last proposal in order to reveal the physiological role of Mdl1p includes the fact that yeast mitochondria contain a non-proteinaceous pool of copper in the matrix (Cobine et al., 2004) and serve as copper storehouse. Copper is essential for several enzymes but excess accumulation of copper results in toxicity since it is used as fungicide, molluscicide and algicide. Balancing of copper in different cell compartments must be attained to minimise deleterious effects. Moreover, copper distribution must be very flexible to adapt the cell to different environmental influences. In yeast copper ions are required for at least three key enzymes: the cytosolic superoxide dismutase Sod1p, the plasma membrane enzyme ferroxidase Fet3p and the mitochondrial inner membrane enzyme cytochrome *c* oxidase. Therefore, it is obvious that exchange of copper between the cytosol and the matrix and vice versa must occur. How copper is exported from the matrix is unknown so far. To prevent free copper ions it is likely that it is chelated e.g. by a peptide with a coordination site composed of several cysteines. It is alluring to speculate whether Mdl1p can be the pathway for such a copper chelater complex. This would be an elegant way to combine the following observations: (i) Mdl1p is involved in the export of peptides between 6 and 20 amino acids from the mitochondrial matrix, (ii) Mdl1p can substitute Atm1p function, (iii) Mdl1p plays a role in resistance to oxidative stress and (iv) Atm1p is stimulated by cysteine (thiol group) containing peptides in the area of 16 amino acids.

8 Abbreviations

ABC	ATP binding cassette
AAA	ATPases associated with a variety of cellular activities
ABCA	ABC transporter subfamily A
ABCB	ABC transporter subfamily B
ABCC	ABC transporter subfamily C
ABCD	ABC transporter subfamily D
ADP	Adenosine diphosphate
ALDP	Adrenoleukodystrophy
AMP	Adenosine monophosphate
APS	Ammonium peroxodisulphate
Atm1p	IMM ABC transporter exports precursors of Fe/S-clusters
ATP	Adenosine triphosphate
BCA	Bicinchonic acid
BSA	Bovine serum albumin
BtuCD	Vitamin B ₁₂ import system permease
C ₁₂ E ₈	Octaethylene glycol monododecyl ether
CFTR	Cystic fibrosis transmembrane conductance regulator
CMC	Critical micelle concentration
Cox	Subunit of cytochrome c oxidase
Cta1	Catalase A
CTP	Cytosine triphosphate
CysA	Sulphate transport ATP-binding ABC transporter protein
Da	Dalton
DDM	n-Dodecyl-β-D-maltoside
DMF	Dimethylformamide
DMSO	Dimethylsulfoxide
DNA	Deoxyribonucleic acid
Dpp	Dipeptide ATP binding/permease complex
DtpT	Di-/tripeptide transporter
DTT	1,4-Dithio-DL-threitol
<i>E. coli</i>	<i>Escherichia coli</i>
EDTA	1-(4-Isothiocyanatobenzyl)ethylenediamine-N,N,N',N'-tetraacetic acid
EGTA	Ethylene glycol-bis(2-aminoethylether)-N,N,N',N'-tetraacetic acid
ER	Endoplasmic reticulum
ERp57	Protein disulphide isomerase-associated 3
FC-14	Tetradecylphosphocholine
Fhu	Ferrichrome ATP transport complex
FtsY	Cell division protein
g	Gram or gravity constant
GIP	General import pore
GlcSTUV ₂	Glucose transport ABC complex
GTP	Guanosine triphosphate
h	hour
H ₍₁₀₎	deca-His-tag
H ₍₆₎	hexa-His-tag
HEGA-10	Decanoyl-n-hydroxyethylglucamide

HEPES	<i>N</i> -(2-hydroxyethylpiperazine)- <i>N'</i> -2-ethanesulfonic acid
HisQMP ₂	Histidine transport ABC complex
HlyA/B	α -Hemolysin/translocation ATP permease
HPLC	High performance liquid chromatography
IDA	Iminodiacetic acid
IMAC	Immobilised metal affinity chromatography
IMM	Inner mitochondrial membrane
IMS	Intermembrane space
IPTG	Isopropyl β -D-thiogalactopyranoside
kb	kilo base
k_{cat}	Catalytic constant
K_D	Dissociation constant
K_M	Michaelis-Menten constant
L	liter
<i>L. lactis</i>	<i>Lactococcus lactis</i>
LB	Luria-Bertani
Leu1p	Isopropylmalate isomerase
LiAc	Lithium acetate
LmrA	Multidrug ABC exporter (<i>Lactococcus lactis</i>)
LPS	Lipopolysaccharide
m	meter
M	mol/L
MALDI	Matrix-assisted laser desorption/ionization
MalFGK ₂	Maltose transport ABC complex
Mdl1p	Multi-drug resistance like protein 1
MDR	Multidrug resistance
MHC	Major histocompatibility complex
min	minute
MOPS	3-(<i>N</i> -Morpholino)propanesulfonic acid
MRP	Multi-drug resistant protein
MS	Mass spectrometry
MsbA	Lipid A export ATP binding/permease protein
mt	mitochondrial
NBD	Nucleotide-binding domain
o/n	overnight
OD	Optical Density
OG	<i>n</i> -Octyl- α -D-glucopyranoside
OMM	Outer mitochondrial membrane
Opp	Oligopeptide ATP binding/permease complex
PAGE	Polyacrylamide gel electrophoresis
PAM	Presequence translocase associated motor
PBS	Phosphate buffered saline
PCR	Polymerase chain reaction
PDR	Pleiotropic drug resistance
PEG	Poly(ethylene glycole)
pH	Potentia hydrogenii
P _i	Inorganic phosphate
PMF	Proton motive force
PMSF	Phenylmethanesulfonyl fluoride

Rad50	DNA double-strand break repair ATPase
RbsA	Ribose transport ATP-binding protein
Rli	RNase L inhibitor
RNA	Ribonucleic acids
RNC	Ribosome nascent chain complex
rpm	Rounds per minute
RT	room temperature
s	second
<i>S. cerevisiae</i>	<i>Saccharomyces cerevisiae</i>
SAM	Sorting and assembly machinery
SBP	Substrate binding protein
SC(D)	Synthetic complete (dextrone)/ sodium cholat
SDS	Sodium dodecyl sulphate
Sec/SEC	Membraneprotein "secretion" system/ Size exclusion chromatography
SPA	Single particle analysis
SRP	Signal recognition particle
Ste6	Mating factor A secretion protein
TAP	Transporter associated with antigen processing
Tat	Twin arginin translocation complex
TBS(T)	Tris buffered saline (Tween)
TCA/TFA	Trichloroacetic acid/ Trifluoroacetic acid
TDAO	n-Tetradecyl-N,N-dimethylamine-N-oxide
TEMED	N,N,N'N'-Tetramethylethylenediamine
TIM/TOM	Translocase of inner/outer membrane
TMD	Transmembrane domain
TMH	Transmembrane helix
TOF	Time of flight
ToIC	Type I secretion channel of the outer membrane
Tris	Tris-(hydroxymethyl)-aminomethane
Tween 20	Polyoxyethylenesorbitan monolaurate
UTP	Uridine triphosphate
UV	Ultraviolet
V	Volt
Var1	Mitochondrial ribosomal protein of the small subunit
V _i	Inorganic vanadate
v_{max}	Maximum reaction velocity
W	Watt
wt	wild-type
YEPD	Yeast peptone dextrone
Yme1	Subunit of the mitochondrial inner membrane i-AAA protease
Yta10	Component of the mitochondrial inner membrane m-AAA protease

9 References

- Abele, R. and Tampé, R. (2004) The ABCs of immunology: structure and function of TAP, the transporter associated with antigen processing. *Physiology (Bethesda)*, **19**, 216-224.
- Abou-Sleiman, P.M., Muqit, M.M. and Wood, N.W. (2006) Expanding insights of mitochondrial dysfunction in Parkinson's disease. *Nat Rev Neurosci*, **7**, 207-219.
- Adam, Z., Adamska, I., Nakabayashi, K., Ostersetzer, O., Haussuhl, K., Manuell, A., Zheng, B., Vallon, O., Rodermeil, S.R., Shinozaki, K. and Clarke, A.K. (2001) Chloroplast and mitochondrial proteases in Arabidopsis. A proposed nomenclature. *Plant Physiol*, **125**, 1912-1918.
- al-Shawi, M.K. and Senior, A.E. (1993) Characterization of the adenosine triphosphatase activity of Chinese hamster P-glycoprotein. *J Biol Chem*, **268**, 4197-4206.
- Annereau, J.P., Ko, Y.H. and Pedersen, P.L. (2003) Cystic fibrosis transmembrane conductance regulator: the NBF1+R (nucleotide-binding fold 1 and regulatory domain) segment acting alone catalyses a $\text{Co}^{2+}/\text{Mn}^{2+}/\text{Mg}^{2+}$ -ATPase activity markedly inhibited by both Cd^{2+} and the transition-state analogue orthovanadate. *Biochem J*, **371**, 451-462.
- Arlt, H., Tauer, R., Feldmann, H., Neupert, W. and Langer, T. (1996) The YTA10-12 complex, an AAA protease with chaperone-like activity in the inner membrane of mitochondria. *Cell*, **85**, 875-885.
- Arnold, I. and Langer, T. (2002) Membrane protein degradation by AAA proteases in mitochondria. *Biochim Biophys Acta*, **1592**, 89-96.
- Augustin, S., Nolden, M., Muller, S., Hardt, O., Arnold, I. and Langer, T. (2005) Characterization of peptides released from mitochondria: evidence for constant proteolysis and peptide efflux. *J Biol Chem*, **280**, 2691-2699.
- Awayn, N.H., Rosenberg, M.F., Kamis, A.B., Aleksandrov, L.A., Riordan, J.R. and Ford, R.C. (2005) Crystallographic and single-particle analyses of native- and nucleotide-bound forms of the cystic fibrosis transmembrane conductance regulator (CFTR) protein. *Biochem Soc Trans*, **33**, 996-999.
- Black-Schaefer, C.L., McCourt, J.D., Poyton, R.O. and McKee, E.E. (1991) Mitochondrial gene expression in *Saccharomyces cerevisiae*. Proteolysis of nascent chains in isolated yeast mitochondria optimized for protein synthesis. *Biochem J*, **274**, 199-205.
- Booth, C.L., Pulaski, L., Gottesman, M.M. and Pastan, I. (2000) Analysis of the properties of the N-terminal nucleotide-binding domain of human P-glycoprotein. *Biochemistry*, **39**, 5518-5526.

- Borths, E.L., Poolman, B., Hvorup, R.N., Locher, K.P. and Rees, D.C. (2005) In vitro functional characterization of BtuCD-F, the Escherichia coli ABC transporter for vitamin B12 uptake. *Biochemistry*, **44**, 16301-16309.
- Bouabe, H. and Knittler, M.R. (2003) The distinct nucleotide binding states of the transporter associated with antigen processing (TAP) are regulated by the non-homologous C-terminal tails of TAP1 and TAP2. *Eur J Biochem*, **270**, 4531-4546.
- Brachmann, C.B., Davies, A., Cost, G.J., Caputo, E., Li, J., Hieter, P. and Boeke, J.D. (1998) Designer deletion strains derived from Saccharomyces cerevisiae S288C: a useful set of strains and plasmids for PCR-mediated gene disruption and other applications. *Yeast*, **14**, 115-132.
- Chabi, B., Adihetty, P.J., Ljubivic, V. and Hood, D.A. (2005) How is mitochondrial biogenesis affected in mitochondrial disease? *Med Sci Sports Exerc*, **37**, 2102-2110.
- Chami, M., Steinfels, E., Orelle, C., Jault, J.M., Di Pietro, A., Rigaud, J.L. and Marco, S. (2002) Three-dimensional structure by cryo-electron microscopy of YvcC, an homodimeric ATP-binding cassette transporter from Bacillus subtilis. *J Mol Biol*, **315**, 1075-1085.
- Chang, G. (2003) Structure of MsbA from Vibrio cholera: a multidrug resistance ABC transporter homolog in a closed conformation. *J Mol Biol*, **330**, 419-430.
- Chang, G. and Roth, C.B. (2001) Structure of MsbA from E. coli: a homolog of the multidrug resistance ATP binding cassette (ABC) transporters. *Science*, **293**, 1793-1800.
- Chang, X.B., Hou, Y.X. and Riordan, J.R. (1997) ATPase activity of purified multidrug resistance-associated protein. *J Biol Chem*, **272**, 30962-30968.
- Chen, J., Lu, G., Lin, J., Davidson, A.L. and Quioco, F.A. (2003a) A tweezers-like motion of the ATP-binding cassette dimer in an ABC transport cycle. *Mol Cell*, **12**, 651-661.
- Chen, M., Abele, R. and Tampé, R. (2003b) Peptides induce ATP hydrolysis at both subunits of the transporter associated with antigen processing. *J Biol Chem*, **278**, 29686-29692.
- Chen, M., Abele, R. and Tampé, R. (2004) Functional non-equivalence of ATP-binding cassette signature motifs in the transporter associated with antigen processing (TAP). *J Biol Chem*, **279**, 46073-46081.
- Chen, P.S., Toribara, T.Y. and Warner, H. (1956) Microdetermination of Phosphorus. *Anal Chem*, **28**, 1756-1758.
- Cheng, Y. and Prusoff, W.H. (1973) Relationship between the inhibition constant (K₁) and the concentration of inhibitor which causes 50 per cent inhibition (I₅₀) of an enzymatic reaction. *Biochem Pharmacol*, **22**, 3099-3108.

- Chloupková, M., LeBard, L.S. and Koeller, D.M. (2003) MDL1 is a high copy suppressor of ATM1: evidence for a role in resistance to oxidative stress. *J Mol Biol*, **331**, 155-165.
- Claros, M.G. and Vincens, P. (1996) Computational method to predict mitochondrially imported proteins and their targeting sequences. *Eur J Biochem*, **241**, 779-786.
- Cobine, P.A., Ojeda, L.D., Rigby, K.M. and Winge, D.R. (2004) Yeast contain a non-proteinaceous pool of copper in the mitochondrial matrix. *J Biol Chem*, **279**, 14447-14455.
- Davidson, A.L., Laghaeian, S.S. and Mannering, D.E. (1996) The maltose transport system of *Escherichia coli* displays positive cooperativity in ATP hydrolysis. *J Biol Chem*, **271**, 4858-4863.
- Davidson, A.L. and Sharma, S. (1997) Mutation of a single MalK subunit severely impairs maltose transport activity in *Escherichia coli*. *J Bacteriol*, **179**, 5458-5464.
- Dean, M., Allikmets, R., Gerrard, B., Stewart, C., Kistler, A., Shafer, B., Michaelis, S. and Strathern, J. (1994) Mapping and sequencing of two yeast genes belonging to the ATP-binding cassette superfamily. *Yeast*, **10**, 377-383.
- Decottignies, A. and Goffeau, A. (1997) Complete inventory of the yeast ABC proteins. *Nat Genet*, **15**, 137-145.
- Detmers, F.J., Lanfermeijer, F.C., Abele, R., Jack, R.W., Tampé, R., Konings, W.N. and Poolman, B. (2000) Combinatorial peptide libraries reveal the ligand-binding mechanism of the oligopeptide receptor OppA of *Lactococcus lactis*. *Proc Natl Acad Sci U S A*, **97**, 12487-12492.
- Diederichs, K., Diez, J., Grellner, G., Müller, C., Breed, J., Schnell, C., Vorrhein, C., Boos, W. and Welte, W. (2000) Crystal structure of MalK, the ATPase subunit of the trehalose/maltose ABC transporter of the archaeon *Thermococcus litoralis*. *EMBO J*, **19**, 5951-5961.
- Doerrler, W.T. and Raetz, C.R. (2002) ATPase activity of the MsbA lipid flippase of *Escherichia coli*. *J Biol Chem*, **277**, 36697-36705.
- Doeven, M.K., Abele, R., Tampé, R. and Poolman, B. (2004) The binding specificity of OppA determines the selectivity of the oligopeptide ATP-binding cassette transporter. *J Biol Chem*, **279**, 32301-32307.
- Driessen, A.J., Manting, E.H. and van der Does, C. (2001) The structural basis of protein targeting and translocation in bacteria. *Nat Struct Biol*, **8**, 492-498.
- Driessen, A.J., Zheng, T., In't Veld, G., Op den Kamp, J.A. and Konings, W.N. (1988) Lipid requirement of the branched-chain amino acid transport system of *Streptococcus cremoris*. *Biochemistry*, **27**, 865-872.

- Ehse, S., Leonhardt, R.M., Hansen, G. and Knittler, M.R. (2005) Functional role of C-terminal sequence elements in the transporter associated with antigen processing. *J Immunol*, **174**, 328-339.
- Ferreira-Pereira, A., Marco, S., Decottignies, A., Nader, J., Goffeau, A. and Rigaud, J.L. (2003) Three-dimensional reconstruction of the *Saccharomyces cerevisiae* multidrug resistance protein Pdr5p. *J Biol Chem*, **278**, 11995-11999.
- Fetsch, E.E. and Davidson, A.L. (2002) Vanadate-catalyzed photocleavage of the signature motif of an ATP-binding cassette (ABC) transporter. *Proc Natl Acad Sci U S A*, **99**, 9685-9690.
- Fischer Lindahl, K., Hermel, E., Loveland, B.E. and Wang, C.R. (1991) Maternally transmitted antigen of mice: a model transplantation antigen. *Annu Rev Immunol*, **9**, 351-372.
- Fisher, A.J., Smith, C.A., Thoden, J.B., Smith, R., Sutoh, K., Holden, H.M. and Rayment, I. (1995) X-ray structures of the myosin motor domain of *Dictyostelium discoideum* complexed with MgADP.BeFx and MgADP.AIF4. *Biochemistry*, **34**, 8960-8972.
- Foucaud, C., Kunji, E.R., Hagting, A., Richard, J., Konings, W.N., Desmazeaud, M. and Poolman, B. (1995) Specificity of peptide transport systems in *Lactococcus lactis*: evidence for a third system which transports hydrophobic di- and tripeptides. *J Bacteriol*, **177**, 4652-4657.
- Frank, J., Radermacher, M., Penczek, P., Zhu, J., Li, Y., Ladjadj, M. and Leith, A. (1996) SPIDER and WEB: processing and visualization of images in 3D electron microscopy and related fields. *J Struct Biol*, **116**, 190-199.
- Gaudet, R. and Wiley, D.C. (2001) Structure of the ABC ATPase domain of human TAP1, the transporter associated with antigen processing. *EMBO J*, **20**, 4964-4972.
- Ghaemmaghami, S., Huh, W.K., Bower, K., Howson, R.W., Belle, A., Dephoure, N., O'Shea, E.K. and Weissman, J.S. (2003) Global analysis of protein expression in yeast. *Nature*, **425**, 737-741.
- Gompf, S., Hofacker, M., Presenti, C., Haase, W., van der Does, C. and Tampé, R. (2006) Switching of the transporter Mdl1p from posttranslational mitochondrial import to co-translationally ER insertion. *In preparation*.
- Gorbulev, S., Abele, R. and Tampé, R. (2001) Allosteric crosstalk between peptide-binding, transport, and ATP hydrolysis of the ABC transporter TAP. *Proc Natl Acad Sci U S A*, **98**, 3732-3737.
- Graf, S.A., Haigh, S.E., Corson, E.D. and Shirihai, O.S. (2004) Targeting, import, and dimerization of a mammalian mitochondrial ATP binding cassette (ABC) transporter, ABCB10 (ABC-me). *J Biol Chem*, **279**, 42954-42963.

- Gross, C.H., Abdul-Manan, N., Fulghum, J., Lippke, J., Liu, X., Prabhakar, P., Brennan, D., Willis, M.S., Faerman, C., Connelly, P., Raybuck, S. and Moore, J. (2006) Nucleotide-binding domains of cystic fibrosis transmembrane conductance regulator, an ABC transporter, catalyze adenylate kinase activity but not ATP hydrolysis. *J Biol Chem*, **281**, 4058-4068.
- Hagting, A., Kunji, E.R., Leenhouts, K.J., Poolman, B. and Konings, W.N. (1994) The di- and tripeptide transport protein of *Lactococcus lactis*. A new type of bacterial peptide transporter. *J Biol Chem*, **269**, 11391-11399.
- Higgins, C.F. (1992) ABC transporters: from microorganisms to man. *Annu Rev Cell Biol*, **8**, 67-113.
- Higgins, C.F. and Gottesman, M.M. (1992) Is the multidrug transporter a flippase? *Trends Biochem Sci*, **17**, 18-21.
- Higgins, C.F., Haag, P.D., Nikaido, K., Ardeshir, F., Garcia, G. and Ames, G.F. (1982) Complete nucleotide sequence and identification of membrane components of the histidine transport operon of *S. typhimurium*. *Nature*, **298**, 723-727.
- Higgins, C.F. and Linton, K.J. (2004) The ATP switch model for ABC transporters. *Nat Struct Mol Biol*, **11**, 918-926.
- Hofacker, M., Gompf, S., Zutz, A., Presenti, C., Model, K., Haase, W., van der Does, C. and Tampé, R. (2006) Fingerprint of the mitochondrial ABC transporter Mdl1 from *Saccharomyces cerevisiae*. *In preparation*.
- Holland, I.B., Schmitt, L. and Young, J. (2005) Type 1 protein secretion in bacteria, the ABC-transporter dependent pathway (review). *Mol Membr Biol*, **22**, 29-39.
- Hopfner, K.P., Karcher, A., Shin, D.S., Craig, L., Arthur, L.M., Carney, J.P. and Tainer, J.A. (2000) Structural biology of Rad50 ATPase: ATP-driven conformational control in DNA double-strand break repair and the ABC-ATPase superfamily. *Cell*, **101**, 789-800.
- Horn, C., Bremer, E. and Schmitt, L. (2003) Nucleotide dependent monomer/dimer equilibrium of OpuAA, the nucleotide-binding protein of the osmotically regulated ABC transporter OpuA from *Bacillus subtilis*. *J Mol Biol*, **334**, 403-419.
- Hrycyna, C.A., Ramachandra, M., Germann, U.A., Cheng, P.W., Pastan, I. and Gottesman, M.M. (1999) Both ATP sites of human P-glycoprotein are essential but not symmetric. *Biochemistry*, **38**, 13887-13899.
- Hung, L.W., Wang, I.X., Nikaido, K., Liu, P.Q., Ames, G.F. and Kim, S.H. (1998) Crystal structure of the ATP-binding subunit of an ABC transporter. *Nature*, **396**, 703-707.
- Hunter, W.M. and Greenwood, F.C. (1964) A radio-immunoelectrophoretic assay for human growth hormone. *Biochem J*, **91**, 43-56.

- Janas, E. (2002) Intracellular Peptide Trafficking in Yeast. *Phd thesis, Institute of Biochemistry, Goethe-University Frankfurt.*
- Janas, E., Hofacker, M., Chen, M., Gompf, S., van der Does, C. and Tampé, R. (2003) The ATP hydrolysis cycle of the nucleotide-binding domain of the mitochondrial ATP-binding cassette transporter Mdl1p. *J Biol Chem*, **278**, 26862-26869.
- Jarchau, T., Chakraborty, T., Garcia, F. and Goebel, W. (1994) Selection for transport competence of C-terminal polypeptides derived from Escherichia coli hemolysin: the shortest peptide capable of autonomous HlyB/HlyD-dependent secretion comprises the C-terminal 62 amino acids of HlyA. *Mol Gen Genet*, **245**, 53-60.
- Juhola, M.K., Shah, Z.H., Grivell, L.A. and Jacobs, H.T. (2000) The mitochondrial inner membrane AAA metalloprotease family in metazoans. *FEBS Lett*, **481**, 91-95.
- Karpowich, N., Martsinkevich, O., Millen, L., Yuan, Y.R., Dai, P.L., MacVey, K., Thomas, P.J. and Hunt, J.F. (2001) Crystal structures of the MJ1267 ATP binding cassette reveal an induced-fit effect at the ATPase active site of an ABC transporter. *Structure*, **9**, 571-586.
- Kennedy, K.A. and Traxler, B. (1999) MalK forms a dimer independent of its assembly into the MalFGK2 ATP-binding cassette transporter of Escherichia coli. *J Biol Chem*, **274**, 6259-6264.
- Kenny, B., Chervaux, C. and Holland, I.B. (1994) Evidence that residues -15 to -46 of the haemolysin secretion signal are involved in early steps in secretion, leading to recognition of the translocator. *Mol Microbiol*, **11**, 99-109.
- Kerr, I.D. (2002) Structure and association of ATP-binding cassette transporter nucleotide-binding domains. *Biochim Biophys Acta*, **1561**, 47-64.
- Kispal, G., Csere, P., Guiard, B. and Lill, R. (1997) The ABC transporter Atm1p is required for mitochondrial iron homeostasis. *FEBS Lett*, **418**, 346-350.
- Kispal, G., Csere, P., Prohl, C. and Lill, R. (1999) The mitochondrial proteins Atm1p and Nfs1p are essential for biogenesis of cytosolic Fe/S proteins. *EMBO J*, **18**, 3981-3989.
- Klanner, C., Prokisch, H. and Langer, T. (2001) MAP-1 and IAP-1, two novel AAA proteases with catalytic sites on opposite membrane surfaces in mitochondrial inner membrane of Neurospora crassa. *Mol Biol Cell*, **12**, 2858-2869.
- Knol, J., Sjollem, K. and Poolman, B. (1998) Detergent-mediated reconstitution of membrane proteins. *Biochemistry*, **37**, 16410-16415.
- Knol, J., Veenhoff, L., Liang, W.J., Henderson, P.J., Leblanc, G. and Poolman, B. (1996) Unidirectional reconstitution into detergent-destabilized liposomes of the purified lactose transport system of Streptococcus thermophilus. *J Biol Chem*, **271**, 15358-15366.

- Koch, J., Guntrum, R., Heintke, S., Kyritsis, C. and Tampé, R. (2004) Functional dissection of the transmembrane domains of the transporter associated with antigen processing (TAP). *J Biol Chem*, **279**, 10142-10147.
- Koch, J., Guntrum, R. and Tampé, R. (2005) Exploring the minimal functional unit of the transporter associated with antigen processing. *FEBS Lett*, **579**, 4413-4416.
- Kohlhaw, G.B. (1988) Beta-isopropylmalate dehydrogenase from yeast. *Methods Enzymol*, **166**, 429-435.
- Kubrich, M., Rassow, J., Voos, W., Pfanner, N. and Honlinger, A. (1998) The import route of ADP/ATP carrier into mitochondria separates from the general import pathway of cleavable preproteins at the trans side of the outer membrane. *J Biol Chem*, **273**, 16374-16381.
- Kuchler, K., Dohlman, H.G. and Thorner, J. (1993) The a-factor transporter (STE6 gene product) and cell polarity in the yeast *Saccharomyces cerevisiae*. *J Cell Biol*, **120**, 1203-1215.
- Kuchler, K., Sterne, R.E. and Thorner, J. (1989) *Saccharomyces cerevisiae* STE6 gene product: a novel pathway for protein export in eukaryotic cells. *EMBO J*, **8**, 3973-3984.
- Kuhnke, G., Neumann, K., Muhlenhoff, U. and Lill, R. (2006) Stimulation of the ATPase activity of the yeast mitochondrial ABC transporter Atm1p by thiol compounds. *Mol Membr Biol*, **23**, 173-184.
- Kunji, E.R., Fang, G., Jeronimus-Stratingh, C.M., Bruins, A.P., Poolman, B. and Konings, W.N. (1998) Reconstruction of the proteolytic pathway for use of beta-casein by *Lactococcus lactis*. *Mol Microbiol*, **27**, 1107-1118.
- Kunji, E.R., Slotboom, D.J. and Poolman, B. (2003) *Lactococcus lactis* as host for overproduction of functional membrane proteins. *Biochim Biophys Acta*, **1610**, 97-108.
- Kurjan, J. (1992) Pheromone response in yeast. *Annu Rev Biochem*, **61**, 1097-1129.
- Lange, C., Nett, J.H., Trumpower, B.L. and Hunte, C. (2001) Specific roles of protein-phospholipid interactions in the yeast cytochrome bc1 complex structure. *EMBO J*, **20**, 6591-6600.
- Langer, T. (2000) AAA proteases: cellular machines for degrading membrane proteins. *Trends Biochem Sci*, **25**, 247-251.
- Lapinski, P.E., Raghuraman, G. and Raghavan, M. (2003) Nucleotide interactions with membrane-bound transporter associated with antigen processing proteins. *J Biol Chem*, **278**, 8229-8237.

- Leighton, J. and Schatz, G. (1995) An ABC transporter in the mitochondrial inner membrane is required for normal growth of yeast. *EMBO J*, **14**, 188-195.
- Lewis, H.A., Buchanan, S.G., Burley, S.K., Conners, K., Dickey, M., Dorwart, M., Fowler, R., Gao, X., Guggino, W.B., Hendrickson, W.A., Hunt, J.F., Kearins, M.C., Lorimer, D., Maloney, P.C., Post, K.W., Rajashankar, K.R., Rutter, M.E., Sauder, J.M., Shriver, S., Thibodeau, P.H., Thomas, P.J., Zhang, M., Zhao, X. and Emtage, S. (2004) Structure of nucleotide-binding domain 1 of the cystic fibrosis transmembrane conductance regulator. *EMBO J*, **23**, 282-293.
- Liu, P.Q., Liu, C.E. and Ames, G.F. (1999) Modulation of ATPase activity by physical disengagement of the ATP-binding domains of an ABC transporter, the histidine permease. *J Biol Chem*, **274**, 18310-18318.
- Liu, R. and Sharom, F.J. (1997) Fluorescence studies on the nucleotide binding domains of the P-glycoprotein multidrug transporter. *Biochemistry*, **36**, 2836-2843.
- Liu, Z.J., Shah, A.K., Habel, J.E., Ng, J.D., Kataeva, I., Xu, H., Horanyi, P., Yang, H., Chang, J., Zhao, M., Huang, L., Chang, S., Tempel, W., Chen, L., Zhou, W., Lee, D., Lin, D., Zhang, H., Newton, M.G., Rose, J. and Wang, B.C. (2005) Salvaging Pyrococcus furiosus protein targets at SECSG. *J Struct Funct Genomics*, **6**, 121-127.
- Locher, K.P., Lee, A.T. and Rees, D.C. (2002) The E. coli BtuCD structure: a framework for ABC transporter architecture and mechanism. *Science*, **296**, 1091-1098.
- Loo, T.W., Bartlett, M.C. and Clarke, D.M. (2002) The "LSGGQ" motif in each nucleotide-binding domain of human P-glycoprotein is adjacent to the opposing walker A sequence. *J Biol Chem*, **277**, 41303-41306.
- Margolles, A., Putman, M., van Veen, H.W. and Konings, W.N. (1999) The purified and functionally reconstituted multidrug transporter LmrA of Lactococcus lactis mediates the transbilayer movement of specific fluorescent phospholipids. *Biochemistry*, **38**, 16298-16306.
- McGrath, J.P. and Varshavsky, A. (1989) The yeast STE6 gene encodes a homologue of the mammalian multidrug resistance P-glycoprotein. *Nature*, **340**, 400-404.
- McKee, E.E., McEwen, J.E. and Poyton, R.O. (1984) Mitochondrial gene expression in Saccharomyces cerevisiae. II. Fidelity of translation in isolated mitochondria from wild type and respiratory-deficient mutant cells. *J Biol Chem*, **259**, 9332-9338.
- Meisinger, C., Sommer, T. and Pfanner, N. (2000) Purification of Saccharomyces cerevisiae mitochondria devoid of microsomal and cytosolic contaminations. *Anal Biochem*, **287**, 339-342.
- Meyer, T.H., van Endert, P.M., Uebel, S., Ehring, B. and Tampé, R. (1994) Functional expression and purification of the ABC transporter complex associated with antigen processing (TAP) in insect cells. *FEBS Lett*, **351**, 443-447.

- Moody, J.E., Millen, L., Binns, D., Hunt, J.F. and Thomas, P.J. (2002) Cooperative, ATP-dependent association of the nucleotide binding cassettes during the catalytic cycle of ATP-binding cassette transporters. *J Biol Chem*, **277**, 21111-21114.
- Morse, M.C., Bleau, G., Dabhi, V.M., Hetu, F., Drobetsky, E.A., Lindahl, K.F. and Perreault, C. (1996) The COI mitochondrial gene encodes a minor histocompatibility antigen presented by H2-M3. *J Immunol*, **156**, 3301-3307.
- Mourez, M., Hofnung, M. and Dassa, E. (1997) Subunit interactions in ABC transporters: a conserved sequence in hydrophobic membrane proteins of periplasmic permeases defines an important site of interaction with the ATPase subunits. *EMBO J*, **16**, 3066-3077.
- Müller, K.M., Ebensperger, C. and Tampé, R. (1994) Nucleotide binding to the hydrophilic C-terminal domain of the transporter associated with antigen processing (TAP). *J Biol Chem*, **269**, 14032-14037.
- Neumann, L., Abele, R. and Tampé, R. (2002) Thermodynamics of peptide binding to the transporter associated with antigen processing (TAP). *J Mol Biol*, **324**, 965-973.
- Neupert, W. (1997) Protein import into mitochondria. *Annu Rev Biochem*, **66**, 863-917.
- Nijenhuis, M. and Hammerling, G.J. (1996) Multiple regions of the transporter associated with antigen processing (TAP) contribute to its peptide binding site. *J Immunol*, **157**, 5467-5477.
- Nikaido, H. (2002) How are the ABC transporters energized? *Proc Natl Acad Sci U S A*, **99**, 9609-9610.
- Nikaido, K. and Ames, G.F. (1999) One intact ATP-binding subunit is sufficient to support ATP hydrolysis and translocation in an ABC transporter, the histidine permease. *J Biol Chem*, **274**, 26727-26735.
- Nikaido, K., Liu, P.Q. and Ames, G.F. (1997) Purification and characterization of HisP, the ATP-binding subunit of a traffic ATPase (ABC transporter), the histidine permease of *Salmonella typhimurium*. Solubility, dimerization, and ATPase activity. *J Biol Chem*, **272**, 27745-27752.
- Ogura, T. and Wilkinson, A.J. (2001) AAA+ superfamily ATPases: common structure--diverse function. *Genes Cells*, **6**, 575-597.
- Oshima, T. and Takano, I. (1980) Duplicated genes producing transposable controlling elements for the mating-type differentiation in *Saccharomyces cerevisiae*. *Genetics*, **94**, 859-870.
- Palmisano, A., Zara, V., Honlinger, A., Voza, A., Dekker, P.J., Pfanner, N. and Palmieri, F. (1998) Targeting and assembly of the oxoglutarate carrier: general principles for bio-

- genesis of carrier proteins of the mitochondrial inner membrane. *Biochem J*, **333** (Pt 1), 151-158.
- Patzlaff, J.S., van der Heide, T. and Poolman, B. (2003) The ATP/substrate stoichiometry of the ATP-binding cassette (ABC) transporter OpuA. *J Biol Chem*, **278**, 29546-29551.
- Pettersen, E.F., Goddard, T.D., Huang, C.C., Couch, G.S., Greenblatt, D.M., Meng, E.C. and Ferrin, T.E. (2004) UCSF Chimera--a visualization system for exploratory research and analysis. *J Comput Chem*, **25**, 1605-1612.
- Pfanner, N., Wiedemann, N., Meisinger, C. and Lithgow, T. (2004) Assembling the mitochondrial outer membrane. *Nat Struct Mol Biol*, **11**, 1044-1048.
- Poolman, B., Doeven, M.K., Geertsma, E.R., Biemans-Oldehinkel, E., Konings, W.N. and Rees, D.C. (2005) Functional analysis of detergent-solubilized and membrane-reconstituted ATP-binding cassette transporters. *Methods Enzymol*, **400**, 429-459.
- Poolman, B. and Konings, W.N. (1993) Secondary solute transport in bacteria. *Biochim Biophys Acta*, **1183**, 5-39.
- Powis, S.J., Townsend, A.R., Deverson, E.V., Bastin, J., Butcher, G.W. and Howard, J.C. (1991) Restoration of antigen presentation to the mutant cell line RMA-S by an MHC-linked transporter. *Nature*, **354**, 528-531.
- Qu, Q., Russell, P.L. and Sharom, F.J. (2003) Stoichiometry and affinity of nucleotide binding to P-glycoprotein during the catalytic cycle. *Biochemistry*, **42**, 1170-1177.
- Radermacher, M., Wagenknecht, T., Verschoor, A. and Frank, J. (1987) Three-dimensional reconstruction from a single-exposure, random conical tilt series applied to the 50S ribosomal subunit of Escherichia coli. *J Microsc*, **146** (Pt 2), 113-136.
- Ravaud, S., Do Cao, M.A., Jidenko, M., Ebel, C., Le Maire, M., Jault, J.M., Di Pietro, A., Haser, R. and Aghajari, N. (2006) The ABC transporter BmrA from Bacillus subtilis is a functional dimer when in a detergent-solubilized state. *Biochem J*, **395**, 345-353.
- Renart, J., Reiser, J. and Stark, G.R. (1979) Transfer of proteins from gels to diazobenzylloxymethyl-paper and detection with antisera: a method for studying antibody specificity and antigen structure. *Proc Natl Acad Sci U S A*, **76**, 3116-3120.
- Reuter, G., Janvilisri, T., Venter, H., Shahi, S., Balakrishnan, L. and van Veen, H.W. (2003) The ATP binding cassette multidrug transporter LmrA and lipid transporter MsbA have overlapping substrate specificities. *J Biol Chem*, **278**, 35193-35198.
- Reyes, C.L. and Chang, G. (2005) Structure of the ABC transporter MsbA in complex with ADP.vanadate and lipopolysaccharide. *Science*, **308**, 1028-1031.

- Rigaut, G., Shevchenko, A., Rutz, B., Wilm, M., Mann, M. and Seraphin, B. (1999) A generic protein purification method for protein complex characterization and proteome exploration. *Nat Biotechnol*, **17**, 1030-1032.
- Rosenberg, M.F., Callaghan, R., Ford, R.C. and Higgins, C.F. (1997) Structure of the multidrug resistance P-glycoprotein to 2.5 nm resolution determined by electron microscopy and image analysis. *J Biol Chem*, **272**, 10685-10694.
- Rosenberg, M.F., Mao, Q., Holzenburg, A., Ford, R.C., Deeley, R.G. and Cole, S.P. (2001) The structure of the multidrug resistance protein 1 (MRP1/ABCC1). crystallization and single-particle analysis. *J Biol Chem*, **276**, 16076-16082.
- Sankaran, B., Bhagat, S. and Senior, A.E. (1997) Inhibition of P-glycoprotein ATPase activity by beryllium fluoride. *Biochemistry*, **36**, 6847-6853.
- Santini, C.L., Ize, B., Chanal, A., Muller, M., Giordano, G. and Wu, L.F. (1998) A novel sec-independent periplasmic protein translocation pathway in Escherichia coli. *EMBO J*, **17**, 101-112.
- Sanz, Y., Lanfermeijer, F.C., Renault, P., Bolotin, A., Konings, W.N. and Poolman, B. (2001) Genetic and functional characterization of dpp genes encoding a dipeptide transport system in Lactococcus lactis. *Arch Microbiol*, **175**, 334-343.
- Sauna, Z.E., Muller, M., Peng, X.H. and Ambudkar, S.V. (2002) Importance of the conserved Walker B glutamate residues, 556 and 1201, for the completion of the catalytic cycle of ATP hydrolysis by human P-glycoprotein (ABCB1). *Biochemistry*, **41**, 13989-14000.
- Schägger, H. and Pfeiffer, K. (2000) Supercomplexes in the respiratory chains of yeast and mammalian mitochondria. *EMBO J*, **19**, 1777-1783.
- Scheffel, F., Demmer, U., Warkentin, E., Hulsmann, A., Schneider, E. and Ermler, U. (2005) Structure of the ATPase subunit CysA of the putative sulphate ATP-binding cassette (ABC) transporter from Alicyclobacillus acidocaldarius. *FEBS Lett*, **579**, 2953-2958.
- Scheffers, D.J., den Blaauwen, T. and Driessen, A.J. (2000) Non-hydrolysable GTP-gamma-S stabilizes the FtsZ polymer in a GDP-bound state. *Mol Microbiol*, **35**, 1211-1219.
- Schmidt, M., Lupas, A.N. and Finley, D. (1999) Structure and mechanism of ATP-dependent proteases. *Curr Opin Chem Biol*, **3**, 584-591.
- Schmitt, L., Benabdelhak, H., Blight, M.A., Holland, I.B. and Stubbs, M.T. (2003) Crystal structure of the nucleotide-binding domain of the ABC-transporter haemolysin B: identification of a variable region within ABC helical domains. *J Mol Biol*, **330**, 333-342.
- Schmitt, L. and Tampé, R. (2000) Affinity, specificity, diversity: a challenge for the ABC transporter TAP in cellular immunity. *Chembiochem*, **1**, 16-35.

- Schmitt, L. and Tampé, R. (2002) Structure and mechanism of ABC transporters. *Curr Opin Struct Biol*, **12**, 754-760.
- Schrodt, S., Koch, J. and Tampé, R. (2006) Membrane topology of the transporter associated with antigen processing (TAP1) within an assembled functional peptide-loading complex. *J Biol Chem*, **281**, 6455-6462.
- Senbongi, H., Ling, F. and Shibata, T. (1999) A mutation in a mitochondrial ABC transporter results in mitochondrial dysfunction through oxidative damage of mitochondrial DNA. *Mol Gen Genet*, **262**, 426-436.
- Senior, A.E., al-Shawi, M.K. and Urbatsch, I.L. (1995) The catalytic cycle of P-glycoprotein. *FEBS Lett*, **377**, 285-289.
- Senior, A.E. and Gadsby, D.C. (1997) ATP hydrolysis cycles and mechanism in P-glycoprotein and CFTR. *Semin Cancer Biol*, **8**, 143-150.
- Shah, Z.H., Hakkaart, G.A., Arku, B., de Jong, L., van der Spek, H., Grivell, L.A. and Jacobs, H.T. (2000) The human homologue of the yeast mitochondrial AAA metalloprotease Yme1p complements a yeast yme1 disruptant. *FEBS Lett*, **478**, 267-270.
- Sharma, S. and Davidson, A.L. (2000) Vanadate-induced trapping of nucleotides by purified maltose transport complex requires ATP hydrolysis. *J Bacteriol*, **182**, 6570-6576.
- Sherman, F. (1991) Getting started with yeast. *Methods Enzymol*, **194**, 3-21.
- Shirihai, O.S., Gregory, T., Yu, C., Orkin, S.H. and Weiss, M.J. (2000) ABC-me: a novel mitochondrial transporter induced by GATA-1 during erythroid differentiation. *EMBO J*, **19**, 2492-2502.
- Shyamala, V., Baichwal, V., Beall, E. and Ames, G.F. (1991) Structure-function analysis of the histidine permease and comparison with cystic fibrosis mutations. *J Biol Chem*, **266**, 18714-18719.
- Sickmann, A., Reinders, J., Wagner, Y., Joppich, C., Zahedi, R., Meyer, H.E., Schonfisch, B., Perschil, I., Chacinska, A., Guiard, B., Rehling, P., Pfanner, N. and Meisinger, C. (2003) The proteome of *Saccharomyces cerevisiae* mitochondria. *Proc Natl Acad Sci U S A*, **100**, 13207-13212.
- Smith, C.A. and Rayment, I. (1996) X-ray structure of the magnesium(II).ADP.vanadate complex of the *Dictyostelium discoideum* myosin motor domain to 1.9 Å resolution. *Biochemistry*, **35**, 5404-5417.
- Smith, P.C., Karpowich, N., Millen, L., Moody, J.E., Rosen, J., Thomas, P.J. and Hunt, J.F. (2002) ATP binding to the motor domain from an ABC transporter drives formation of a nucleotide sandwich dimer. *Mol Cell*, **10**, 139-149.

- Sorzano, C.O., Marabini, R., Velazquez-Muriel, J., Bilbao-Castro, J.R., Scheres, S.H., Carazo, J.M. and Pascual-Montano, A. (2004) XMIPP: a new generation of an open-source image processing package for electron microscopy. *J Struct Biol*, **148**, 194-204.
- Spies, T. and DeMars, R. (1991) Restored expression of major histocompatibility class I molecules by gene transfer of a putative peptide transporter. *Nature*, **351**, 323-324.
- Taglicht, D. and Michaelis, S. (1998) *Saccharomyces cerevisiae* ABC proteins and their relevance to human health and disease. *Methods Enzymol*, **292**, 130-162.
- Thomas, B.J. and Rothstein, R. (1989) Elevated recombination rates in transcriptionally active DNA. *Cell*, **56**, 619-630.
- Towbin, H., Staehelin, T. and Gordon, J. (1979) Electrophoretic transfer of proteins from polyacrylamide gels to nitrocellulose sheets: procedure and some applications. *Proc Natl Acad Sci U S A*, **76**, 4350-4354.
- Tynkkynen, S., Buist, G., Kunji, E., Kok, J., Poolman, B., Venema, G. and Haandrikman, A. (1993) Genetic and biochemical characterization of the oligopeptide transport system of *Lactococcus lactis*. *J Bacteriol*, **175**, 7523-7532.
- Uebel, S., Meyer, T.H., Kraas, W., Kienle, S., Jung, G., Wiesmuller, K.H. and Tampé, R. (1995) Requirements for peptide binding to the human transporter associated with antigen processing revealed by peptide scans and complex peptide libraries. *J Biol Chem*, **270**, 18512-18516.
- Uebel, S., Plantinga, T., Weber, P.J., Beck-Sickinger, A.G. and Tampé, R. (1997) Peptide binding and photocross-linking to detergent solubilized and to reconstituted transporter associated with antigen processing (TAP). *FEBS Lett*, **416**, 359-363.
- Uebel, S., Wiesmuller, K.H., Jung, G. and Tampé, R. (1999) Peptide libraries in cellular immune recognition. *Curr Top Microbiol Immunol*, **243**, 1-21.
- Urbatsch, I.L., Gimi, K., Wilke-Mounts, S. and Senior, A.E. (2000a) Investigation of the role of glutamine-471 and glutamine-1114 in the two catalytic sites of P-glycoprotein. *Biochemistry*, **39**, 11921-11927.
- Urbatsch, I.L., Julien, M., Carrier, I., Rousseau, M.E., Cayrol, R. and Gros, P. (2000b) Mutational analysis of conserved carboxylate residues in the nucleotide binding sites of P-glycoprotein. *Biochemistry*, **39**, 14138-14149.
- Urbatsch, I.L., Sankaran, B., Bhagat, S. and Senior, A.E. (1995a) Both P-glycoprotein nucleotide-binding sites are catalytically active. *J Biol Chem*, **270**, 26956-26961.
- Urbatsch, I.L., Sankaran, B., Weber, J. and Senior, A.E. (1995b) P-glycoprotein is stably inhibited by vanadate-induced trapping of nucleotide at a single catalytic site. *J Biol Chem*, **270**, 19383-19390.

- van der Does, C., Presenti, C., Schulze, K., Dinkelaker, S. and Tampé, R. (2006) Kinetics of the ATP Hydrolysis Cycle of the Nucleotide-binding Domain of Mdl1 Studied by a Novel Site-specific Labeling Technique. *J Biol Chem*, **281**, 5694-5701.
- van der Does, C. and Tampé, R. (2004) How do ABC transporters drive transport? *Biol Chem*, **385**, 927-933.
- van Endert, P.M., Tampé, R., Meyer, T.H., Tisch, R., Bach, J.F. and McDevitt, H.O. (1994) A sequential model for peptide binding and transport by the transporters associated with antigen processing. *Immunity*, **1**, 491-500.
- van Veen, H.W., Margolles, A., Muller, M., Higgins, C.F. and Konings, W.N. (2000) The homodimeric ATP-binding cassette transporter LmrA mediates multidrug transport by an alternating two-site (two-cylinder engine) mechanism. *EMBO J*, **19**, 2503-2514.
- Velarde, G., Ford, R.C., Rosenberg, M.F. and Powis, S.J. (2001) Three-dimensional structure of transporter associated with antigen processing (TAP) obtained by single Particle image analysis. *J Biol Chem*, **276**, 46054-46063.
- Verdon, G., Albers, S.V., Dijkstra, B.W., Driessen, A.J. and Thunnissen, A.M. (2003a) Crystal structures of the ATPase subunit of the glucose ABC transporter from *Sulfolobus solfataricus*: nucleotide-free and nucleotide-bound conformations. *J Mol Biol*, **330**, 343-358.
- Verdon, G., Albers, S.V., van Oosterwijk, N., Dijkstra, B.W., Driessen, A.J. and Thunnissen, A.M. (2003b) Formation of the productive ATP-Mg²⁺-bound dimer of GlcV, an ABC-ATPase from *Sulfolobus solfataricus*. *J Mol Biol*, **334**, 255-267.
- Walker, J.E., Saraste, M., Runswick, M.J. and Gay, N.J. (1982) Distantly related sequences in the alpha- and beta-subunits of ATP synthase, myosin, kinases and other ATP-requiring enzymes and a common nucleotide binding fold. *EMBO J*, **1**, 945-951.
- Wickner, S., Maurizi, M.R. and Gottesman, S. (1999) Posttranslational quality control: folding, refolding, and degrading proteins. *Science*, **286**, 1888-1893.
- Wilson, K.L. and Herskowitz, I. (1984) Negative regulation of STE6 gene expression by the alpha 2 product of *Saccharomyces cerevisiae*. *Mol Cell Biol*, **4**, 2420-2427.
- Wilson, K.L. and Herskowitz, I. (1987) STE16, a new gene required for pheromone production by a cells of *Saccharomyces cerevisiae*. *Genetics*, **115**, 441-449.
- Wolters, J.C., Abele, R. and Tampé, R. (2005) Selective and ATP-dependent translocation of peptides by the homodimeric ATP binding cassette transporter TAP-like (ABCB9). *J Biol Chem*, **280**, 23631-23636.
- Young, L., Leonhard, K., Tatsuta, T., Trowsdale, J. and Langer, T. (2001) Role of the ABC transporter Mdl1 in peptide export from mitochondria. *Science*, **291**, 2135-2138.

- Yuan, Y.R., Blecker, S., Martsinkevich, O., Millen, L., Thomas, P.J. and Hunt, J.F. (2001) The crystal structure of the MJ0796 ATP-binding cassette. Implications for the structural consequences of ATP hydrolysis in the active site of an ABC transporter. *J Biol Chem*, **276**, 32313-32321.
- Zaitseva, J., Jenewein, S., Jumpertz, T., Holland, I.B. and Schmitt, L. (2005a) H662 is the linchpin of ATP hydrolysis in the nucleotide-binding domain of the ABC transporter HlyB. *EMBO J*, **24**, 1901-1910.
- Zaitseva, J., Jenewein, S., Oswald, C., Jumpertz, T., Holland, I.B. and Schmitt, L. (2005b) A molecular understanding of the catalytic cycle of the nucleotide-binding domain of the ABC transporter HlyB. *Biochem Soc Trans*, **33**, 990-995.
- Zaitseva, J., Jenewein, S., Wiedenmann, A., Benabdelhak, H., Holland, I.B. and Schmitt, L. (2005c) Functional characterization and ATP-induced dimerization of the isolated ABC-domain of the haemolysin B transporter. *Biochemistry*, **44**, 9680-9690.
- Zhang, F., Zhang, W., Liu, L., Fisher, C.L., Hui, D., Childs, S., Dorovini-Zis, K. and Ling, V. (2000) Characterization of ABCB9, an ATP binding cassette protein associated with lysosomes. *J Biol Chem*, **275**, 23287-23294.
- Zhao, C., Tampé, R. and Abele, R. (2006) TAP and TAP-like - Brothers in arms? *Naunyn Schmiedebergs Arch Pharmacol*, **372**, 444-450.

10 Publications

Results of this work were published in these articles:

Hofacker, M., Gompf, S., Zutz, A., Presenti, C., Model, K., Haase, W., van der Does, C. and Tampé, R. (2006) Fingerprint of the mitochondrial ABC transporter Mdl1p from *Saccharomyces cerevisiae*. In preparation.

Gompf, S., **Hofacker, M.**, Presenti, C., Haase, W., van der Does, C. & Tampé, R. (2006) Switching of the transporter Mdl1p from posttranslational mitochondrial import to cotranslationally ER insertion. In preparation.

Janas, E., **Hofacker, M.**, Chen, M., Gompf, S., van der Does, C. and Tampe, R. (2003) The ATP hydrolysis cycle of the nucleotide-binding domain of the mitochondrial ATP-binding cassette transporter Mdl1p. *J. Biol. Chem.*, **278**, 26862-26869.

Danksagung

Mein erster Dank geht an Herrn Prof. Dr. Robert Tampé für die Möglichkeit, die er mir geboten hat, diese Arbeit im Institut für Biochemie anzufertigen. Lieber Robert, ich danke Dir für Deine Unterstützung über all die Jahre.

Herrn Prof. Dr. Bernd Ludwig danke ich für die Übernahme des Zweitgutachtens. Danke, dass Du Dir Zeit genommen hast.

Mijn bijzonder dank gaat naar Dr. Chris van der Does voor zijn supervisie en leiden van het Mdl1-projekt ook over tijd- en landesgrenzen heen. Chris, je bent voor mij zowel wetenschappelijk maar ook als persoon een voorbeeld.

Als nächstes möchte ich mich bedanken bei Prof. Dr. Alexander Gottschalk, Prof. Dr. Lutz Schmitt, Dr. Rupert Abele, Dr. Joachim Koch und Dr. Jacob Piehler für Ihr immer offenes Ohr bei allen erdenklichen Fragen. Von Euch konnte ich lernen wie viel Begeisterung von Forschung und Wissenschaft ausgeht.

Ganz herzlich bedanken möchte ich mich bei Stephanie Dinkelaker, Krzysztof Dobrynin, Simone Gompf, Eva Janas, Chiara Presenti und Ariane Zutz für Ihre Zusammenarbeit und Hilfe auf dem Mdl1p-Projekt. Ohne Euch wäre es nicht gegangen!

Daran anschließen möchte ich den Dank an alle Kolleginnen und Kollegen des Institutes für Biochemie für die freundschaftliche Atmosphäre. Auch Eure Hilfsbereitschaft war unentbehrlich.

Bei Christina Fischer, Nils Hanekop, Peter Lamken, Tanja Mittag, Susanne Schrodte und Katharina Strube, möchte ich mich für die gemeinsame Studien- und Promotionszeit herzlich bedanken. Ich würde mir wünschen, dass diese Freundschaft noch lange hält.

Mein Dank für die Zusammenarbeit auf dem Projekt der Einzelpartikelanalyse geht an Dr. Kirstin Model. Danke für Deinen großen zeitlichen Einsatz.

Bei Prof. Dr. Peter Rehling, Dr. Ann Frazier und Inge Perschil möchte ich mich für die freundliche Aufnahme in Freiburg bedanken. Danke Peter und Inge für die Hilfe bei der Mitochondrienpräparation, thank you Peter and Ann for telling me the secrets of the „*in organello translation*“.

Bei Prof. Dr. Thomas Langer und Steffen Augustin möchte ich mich für die freundliche Hilfe in Köln bezüglich des Peptidexports aus Mitochondrien bedanken. Euer Angebot war nicht selbstverständlich.

Bei Ute Hellmich möchte ich mich für die vielen Tipps zu Fragen der Rekonstitution sowie das Lesen der Arbeit bedanken. Das war wirklich hilfreich.

Forschung, wie ich sie kennen gelernt habe, lebt von Kommunikation – ist ohne die Bereitschaft sich auszutauschen nicht möglich. Viele Menschen sind mir auf dem Weg der Doktorarbeit begegnet von denen ich viel gelernt habe. Bei diesen Menschen – sind sie auch namentlich nicht genannt – möchte ich mich herzlich bedanken.

Schließlich möchte ich mich bei meinen Eltern und Geschwistern sowie meiner Freundin Eva aus ganzem Herzen bedanken. Ohne Eure Geduld, Liebe und Unterstützung wäre meine Arbeit nicht möglich gewesen.

Lebenslauf

Persönliche Informationen

Geburtsdatum: 25. Februar 1976
Geburtsort: Langen (Hessen)
Familienstand: Ledig
Nationalität: Deutsch



Naturwissenschaftliche Ausbildung

Promotion

seit 07/2001

Promotion am Institut für Biochemie der Johann Wolfgang Goethe-Universität Frankfurt am Main (Arbeitsgruppe Prof. Dr. Robert Tampé) in Kooperation mit dem Max-Planck-Institut für Biophysik Frankfurt am Main (Arbeitsgruppe Prof. Dr. Werner Kühlbrandt/Dr. Kirstin Model).
Thema: Expression und funktionale Analyse des mitochondrialen ABC-Transporters Mdl1p aus *Saccharomyces cerevisiae*

Studium

04/2001

Abschluss: Diplom-Biochemiker an der Johann Wolfgang Goethe-Universität Frankfurt am Main, Note 1.0 mit Auszeichnung

09/2000 – 04/2001

Externe **Diplomarbeit** am Max-Planck-Institut für Biophysik Frankfurt am Main (Prof. Dr. Hartmut Michel/Dr. Roy Lancaster) in Zusammenarbeit mit dem Institut für Genetik der Universität Frankfurt (Prof. Dr. Bernd Ludwig)

08/1998

Vordiplom in Biochemie, Note 1.0

10/1996 – 08/2000

Studium der Biochemie an der Johann Wolfgang Goethe-Universität Frankfurt am Main

Schule und Zivildienst

08/1995 – 08/1996

Zivildienst im Ortsverband Langen der Arbeiter Wohlfahrt

07/1995

Abitur, Note 1.8

08/1988 – 07/1995

Gymnasium (Dreieichschule Langen)

Praktika

03/2005

2-tägiger Workshop "**Chemie, Pharmazie und Entwicklung der Statine**", Johann Wolfgang Goethe-Universität Frankfurt am Main (Prof. Dr. Günther Wess)

03/2002

"**International Workshop on Lipid-Peptide/Lipid-Protein Interactions**", Gomadingen (Deutsche Gesellschaft für Biophysik)

03/2000

Blockpraktikum Biologische Kristallographie, Max-Planck-Institut für Biophysik (Prof. Dr. Michel)

09/1997

Paul-Ehrlich-Institut, Langen (4 Wochen)

„Untersuchung des Mechanismus der HIV-Pathogenese“ (Dr. Joachim Denner)

Auszeichnungen und Konferenzen

06/2005	[i]lab award “Grants for greater mobility” der Sanofi-Aventis Group
09/2003	„Young Investigator Award“ , Internationale Sommerschule Hirschegg 2003, Österreich
03/2003	„FEBS Youth Travel Award” der Federation of Biochemical Societies
06/2005	Gordon Research Conference: “Mechanisms of Membrane Transport” (Posterpräsentation), Tilton (NH)
05/2005	5th Transport Colloquium – Castle Rauischholzhausen, Germany
05/2003	4th Transport Colloquium – Castle Rauischholzhausen, Germany
03/2003	4th FEBS Advanced Lecture Course: “ATP-Binding Cassette (ABC) Proteins: From Genetic Disease to Multidrug Resistance” , (Posterpräsentation), Gosau Austria
05/2001	3th Transport Colloquium – Castle Rauischholzhausen, Germany
seit 06/2000	Mitglied der “Gesellschaft für Biochemie und Molekularbiologie e. V. (GBM)“

Publikationen

Matthias Hofacker, Simone Gompf, Kirstin Model, Ariane Zutz, Chiara Presenti, Winfried Haase, Chris van der Does and Robert Tampé
Fingerprint of the mitochondrial ABC transporter Mdl1 from *Saccharomyces cerevisiae*.
In Preparation.

Simone Gompf, **Matthias Hofacker**, Chiara Presenti, Winfried Haase, Chris van der Does and Robert Tampé
Switching of the transporter Mdl1p from posttranslational mitochondrial import to cotranslationally ER insertion. In Preparation.

Eva Janas, **Matthias Hofacker**, Min Chen, Simone Gompf, Chris van der Does and Robert Tampé
The ATP Hydrolysis Cycle of the Nucleotide-binding Domain of the Mitochondrial ATP-binding Cassette Transporter Mdl1p
The Journal of Biological Chemistry, JBC (2003), Vol. 278, No. 29, p. 26862-26869